

# General Rank Transmit Beamforming Methods for Multicasting Networks

vom Fachbereich Elektrotechnik und Informationstechnik  
der Technischen Universität Darmstadt  
zur Erlangung des akademischen Grades eines  
Doktor-Ingenieurs (Dr.-Ing.)  
genehmigte Dissertation  
von

Dipl.-Ing./M.Sc. Dima Taleb

Referent:	Prof. Dr.-Ing. Marius Pesavento
Korreferent:	Prof. Dr.-Ing. Martin Haardt
Tag der Einreichung:	19.03.2023
Tag der mündlichen Prüfung:	24.07.2023

Darmstadt 2023

Dima Taleb: *General Rank Transmit Beamforming Methods for Multicasting Networks*  
Darmstadt, Technische Universität Darmstadt  
Jahr der Veröffentlichung der Dissertation auf TUprints: 2023  
Tag der mündlichen Prüfung: 24.07.2023

Veröffentlicht unter CC BY-SA 4.0 International  
<https://creativecommons.org/licenses/>

# Acknowledgments

I would like to express my deepest appreciation to my advisor Prof. Dr.-Ing. Marius Pesavento. His relentless support and insightful thoughts have enriched my experience. I am proud to be one of his students and feel very lucky to know him as a teacher, professor and a person.

I am also grateful to all my colleagues in the communication systems group for the valuable discussions, life time of memories and the enjoyable moments. I would deeply thank my colleagues Christina Steffen, Florian Bahlke, Ganapati Hegde, David Scheck, Fabio Nikolay, Oscar Ramos for the careful review of this dissertation and insightful thoughts. Special thanks to Marlis Gorecki for all the help in the administrative and organizational matters.

To my loving father, who passed away so early. May his soul rest in peace. I am deeply indebted to him, my mother, sister and brother for their support and love.

Finally, I would also like to extend my deepest gratitude to my husband Salah. His support and encouragement cannot be overestimated.



---

## Kurzfassung

In den letzten Jahren haben sich die Kommunikationsnetze in Bezug auf Datenrate, Kapazität und Dienstqualität erheblich weiterentwickelt. Ein breites Spektrum moderner Anwendungen wie Videokonferenzen und Live-Streams, zieht immer mehr Nutzer an. Mit steigender Zahl von Mobilfunknutzern werden Frequenzressourcen zunehmend knapper. Aus diesem Grund wurden spektral effiziente Methoden in den letzten Jahren intensiv untersucht. Sendestrahlförmung (Transmit Beamforming) kann bei Systemen mit mehreren Antennen eingesetzt werden, um mehrere Nutzer gleichzeitig auf denselben Frequenzressourcen zu bedienen. Bei der klassischen Rang-eins Beamforming für Multicasting-Netzwerke wird ein einzelner Beamformer verwendet, um eine einzelne Gruppe von Benutzern zu bedienen. Allerdings verschlechtert sich die Leistung herkömmlicher Rang-Eins Beamformingmethoden erheblich, wenn die Anzahl der Netzwerknutzer zunimmt. Das Alamouti-basierte Beamformingverfahren kombiniert die Raum-Zeit-Blockcodes (STBCs) mit dem Beamforming. Dabei werden zwei Beamformer eingesetzt, um die Informationen an die Nutzer zu senden, wodurch sich die Freiheitsgrade im Beamformerentwurf im Vergleich zum klassischen Rang-Eins-Ansatz verdoppeln. Das Rang-Zwei Beamformerentwurfverfahren erreicht nachweislich eine optimale Leistung, wenn die Anzahl der Nutzer einen bestimmten Schwellenwert nicht überschreitet.

Der Alamouti Code ist der einzige STBC, der Orthogonalität, volle Rate und Diversitätsgewinn bietet. In dieser Arbeit werden jedoch mehrere STBCs-basierte Ansätze vorgestellt, um alternative, effiziente Methoden zu liefern und den auf Rang-Zwei basierenden Beamformerentwurfsansatz zu übertreffen.

In dieser Arbeit werden verschiedene allgemeine Beamformertechniken, nämlich Raum-Zeit-Trellis-Codes (STTCs), Orthogonale Raum-Zeit-Blockcodes (OSTBCs), Realwert-OSTBCs und STBCs-basierte Beamforming für das Szenario einzelner Gruppen-Multicasting Netzwerke vorgestellt. Verschiedene STBC-basierte Beamformermethoden werden bereitgestellt, um die Freiheitsgrade zu erhöhen und somit mehr Nutzer im Vergleich zum Rang-Zwei Beamformerentwurf zu bedienen, ohne die Optimalität zu beeinträchtigen. Allgemeine Beamformerentwürfe verbessern die Gesamtsystemleistung in Bezug auf Zuverlässigkeit, Kapazität und Übertragungsleistung.

STTCs sind leistungsfähige Fehlerkorrekturcodes, die Diversität und Kodierungsgewinn bieten und damit die OSTBCs übertreffen. Die auf STTCs basierende Beamformerentwurfsmethode bietet einen optimalen allgemeinen Rang, bei dem mehrere

Beamformer gleichzeitig in die gewünschte Richtung der Netzteilnehmer gelenkt werden. Dadurch erhöhen sich die Freiheitsgrade, und es können mehr Benutzer bedient werden, ohne dass die Systemleistung beeinträchtigt wird. STTCs leiden jedoch unter einer hohen Dekodierungskomplexität im Vergleich zur einfachen Symbol-für-Symbol-Erkennung von OSTBCs.

OSTBCs höherer Ordnung ( $> 2$ ) haben nicht die volle Übertragungsrate. Im OSTBCs-basierten Beamformerentwurfsansatz wird der Ratenverlust entweder durch ein hohes Modulationsschema oder eine höhere Kanalkodiertrate kompensiert. Der OSTBCs-basierte Beamformerentwurfsansatz bietet optimale Lösungen für Multicasting-Netzwerke mit einer größeren Anzahl von Nutzer im Vergleich zum Rang-Zwei Beamformerentwurf und einfachen Symbol-für Symbol Dekodierungsmethoden auf der Nutzerseite. Allerdings stellt der verfolgte Ansatz greifbare Beschränkungen auf entweder das Modulationsschema oder den verwendeten Kanalkode.

Reellwertige OSTBCs-basierte Beamformerentwürfe mit voller Rate bieten Beamformerlösungen von allgemeinem Rang. Sie erlauben einfache Dekodierungsverfahren an den Empfängern, allerdings mit erhöhter Bitfehlerrate im Vergleich zu einem auf Rang-Zwei basierenden Beamformerentwurf. Grund dafür ist die Optimalität der Beamformerlösungen für Szenarien mit einer größeren Anzahl von Nutzern, oberhalb des spezifizierten Schwellwerts, wie zuvor erwähnt. Obwohl bei diesem Ansatz die volle Coderate erreicht wird, weisen reellwertige Modulationsverfahren im Vergleich zu den komplexwertigen Methoden eine höhere Fehlerrate auf.

Beim STBCs-basierten Beamformerentwurf wird die Orthogonalitätseigenschaft des OSTBCs-basierten Beamformerentwurf geopfert und stattdessen STBCs mit voller Rate verwendet. Der Beamformerentwurf mit dem traditionellen, weit verbreiteten Optimierungsproblem ist nicht mehr möglich. Die ungünstigste paarweise Fehlerwahrscheinlichkeit wird minimiert, um die Leistung des Gesamtsystems zu verbessern. Quasi-Orthogonale OSTBCs (QOSTBCs) werden als Beispiel für nicht-orthogonale STBCs zur Bewertung der Leistung des Mutlicasting-Systems verwendet. Das nicht-konvexe Optimierungsproblem wird durch die Taylor-Reihenentwicklung erster Ordnung approximiert, und ein iterativer Algorithmus wird eingesetzt, um die Beamformerlösung zu erhalten. Der größte Nachteil dieses Ansatzes ist die erhöhte Komplexität auf der Empfängerseite im Vergleich zur einfachen Symbol-für-Symbol Kodierungsmethode von OSTBCs.

Ein weiterer wichtiger Beitrag dieser Dissertation ist das Verfahren der Rangregulierung der Beamformerlösung. Eine stetige Annäherung der Rangfunktion wird verwendet

und mittels der Taylor-Reihenentwicklung erster Ordnung linearisiert. Ein zweistufiger iterativer Algorithmus wird entwickelt, um den Rang sequentiell zu reduzieren, und dann später zu einem einstufigen Algorithmus vereinfacht. Um einen Vergleich mit dem Stand der Technik zu ermöglichen, werden verschiedene, aktuelle Verfahren verallgemeinert und mit den vorgeschlagenen Verfahren verglichen. Wie aus den Simulationsergebnissen hervorgeht, übertreffen all vorgeschlagenen Ansätze den Stand der Technik.





---

# Abstract

Recent wireless communication networks have experienced major developments in data rate, capacity and quality of service. A wide range of modern applications like video conferences and live streams are constantly attracting more users. With the growth of number of mobile subscribers, the frequency resources are becoming more and more scarce and occupied. To deal with this frequency scarcity, spectrally efficient methods were intensively studied in the past few years. Transmit beamforming can be applied in multi-antenna systems to simultaneously serve multi-users on the same frequency resources by exploiting spatial diversity. In classical rank one transmit beamforming for multicasting networks, a single beamformer is used to serve a group of users. However, the performance of conventional rank one beamforming methods degrade severely as the number of network users increases. The Alamouti based beamforming procedure combines space-time block codes (STBCs) with transmit beamforming. Hence, two beamformers are employed to send the information to the users, which doubles the degrees of freedom in the beamformer design compared with the classical rank one design. The rank two beamforming approach can be shown to achieve optimal performance if the number of users does not exceed a certain threshold.

The Alamouti code is the only STBC, which provides orthogonality, full rate and diversity gain. However, several advanced STBCs based beamforming approaches are presented through this thesis to deliver alternative, efficient methods and outperform the rank two based beamforming approach.

In this thesis, various general rank beamforming techniques, namely Space-time trellis codes (STTC)s, orthogonal space-time codes (OSTBCs), real-valued OSTBCs and STBCs based beamforming, are presented for the scenario of single group multicasting networks. Several novel STBCs based beamforming methods are provided to increase the degrees of freedom, thus serving more users compared to rank two beamforming design; nevertheless, maintaining the optimality. General rank beamforming designs enhance the overall system performance in terms of reliability, capacity and transmit power.

STTCs are powerful error correcting codes, which provide diversity and coding gain, thus outperform the OSTBCs. The novel STTCs based beamforming method offers an optimal general rank, where multiple beamformers are steered towards the desired direction of network users simultaneously, thus, increasing the degrees of freedom and the number of served users with tangible system performance improvement. However,

STTCs suffer from high decoding complexity compared with the simple symbol-by-symbol detection of OSTBCs.

Higher order ( $> 2$ ) OSTBCs do not enjoy full transmission rate. In OSTBCs based beamforming design, the rate loss is compensated either by using higher modulation scheme or a higher channel code rate. The innovative OSTBCs based beamforming approach provides optimal solutions for multicasting networks with a larger number of users compared with the rank two beamforming design, enhances the system performance in terms of the bit-error rate (BER) and allows for simple symbol-by-symbol decoding method at the users' side. However, the followed approach poses tangible restrictions on either the modulation scheme or the used channel code.

The developed Real-valued full rate OSTBCs based beamforming design offers general rank beamforming solutions. It admits a simple decoding scheme at the receivers, with improved BER performance compared with the rank two based beamforming design due to the optimality of the beamforming solutions for scenarios with larger number of users above the specified threshold as mentioned before. Although the full code rate is achieved in this approach, real-valued modulation schemes are associated with a higher error rate compared to the complex-valued methods.

In the unique STBCs based beamforming design, the orthogonality property of OSTBCs based beamforming design is sacrificed and full rate STBCs is utilized instead. Due to the utilization of the non-orthogonal OSTBCs, the beamformer design using the traditional widely spread optimization problems is no more possible. Instead, the worst user pairwise error probability (PEP) is minimized as a novel way to enhance the overall system performance. Quasi-orthogonal OSTBCs (QOSTBCs) as an example of non-orthogonal STBCs are used to evaluate the performance of the multicasting system. The non-convex optimization problem is approximated using the first order Taylor approximation and an iterative algorithm is employed to obtain the beamforming solutions. The newly developed optimization problem delivers a superior performance in terms of BER compared with the OSTBCs, real-valued OSTBCs, rank two and rank one based beamforming. The major drawback of this approach is the increased complexity at the receivers' side compared with the simple symbol-by-symbol decoding method of OSTBCs.

A further contribution of this dissertation is the procedure of the rank regularization of the beamforming solutions. A smooth approximation of the rank function is employed and then linearized using the first order Taylor approximation method. A two scale iterative algorithm is devised to reduce the rank sequentially and later simplified to a

one scale algorithm. A generalization of several state-of-the-art procedures is provided, which ensures a fair comparison between all designs.

As depicted in the simulation results, all the proposed approaches outperforms the state-of-the-art designs.



# Contents

<b>1</b>	<b>Introduction</b>	<b>1</b>
1.1	Background . . . . .	2
1.1.1	Space-time Coding . . . . .	4
1.1.2	Transmit Beamforming . . . . .	6
1.1.3	Rank Reduction Techniques . . . . .	7
1.2	Contributions and Thesis Overview . . . . .	8
<b>2</b>	<b>State of the art</b>	<b>13</b>
2.1	Introduction . . . . .	13
2.2	Space-time Block Codes . . . . .	14
2.2.1	Alamouti Space-time Block Code . . . . .	14
2.2.2	Higher Order OSTBCs . . . . .	15
2.2.3	Space-time Trellis Codes . . . . .	16
2.2.3.1	STTCs Encoding . . . . .	16
2.2.3.2	Decoding . . . . .	19
2.3	Rank One Transmit Beamforming For Single Group Multicasting . . . . .	21
2.3.1	System Model . . . . .	21
2.3.2	QoS Optimization Problem . . . . .	22
2.3.3	MMF Optimization Problem . . . . .	23
2.4	Rank Two Transmit Beamforming Technique . . . . .	25
2.4.1	Optimization Problem . . . . .	27
<b>3</b>	<b>General Rank Transmit Beamforming</b>	<b>31</b>
3.1	STTCs Based Transmit Beamforming . . . . .	31
3.1.1	Optimization Problem . . . . .	33
3.1.2	Simulation Results . . . . .	34
3.2	High Order OSTBCs Based Beamforming . . . . .	37
3.2.1	Optimization Problem . . . . .	40
3.2.2	Randomization Procedure . . . . .	41
3.2.3	Simulation Results . . . . .	42
3.3	Real-valued OSTBCs Based Beamforming . . . . .	45
3.3.1	Optimization Problem . . . . .	46
3.4	Detection Method . . . . .	47
3.5	Simulation results . . . . .	48
3.6	STBCs Based Beamforming . . . . .	51
3.6.1	Optimization Problem . . . . .	53
3.6.2	Theoretically Upper Bound . . . . .	55

---

3.6.3	Convex Approximation Technique . . . . .	56
3.6.4	QOSTBC Encoding and Decoding . . . . .	59
3.6.5	Simulation Results . . . . .	61
3.7	Summary . . . . .	65
<b>4</b>	<b>Rank Regularized Beamforming</b>	<b>69</b>
4.1	Motivation and Background . . . . .	71
4.2	Rank Reduction Approach . . . . .	72
4.3	Computational Complexity of Algorithm 5 . . . . .	77
4.4	Simulation Results . . . . .	77
4.4.1	A Generalization of the MU Algorithm . . . . .	77
4.4.2	A Generalization of the ADMM Algorithm . . . . .	78
4.4.3	A Generalization of the SLA procedure . . . . .	78
4.5	Summary . . . . .	89
<b>5</b>	<b>Conclusion and Outlook</b>	<b>95</b>
	<b>List of Acronyms</b>	<b>99</b>
	<b>List of Symbols</b>	<b>103</b>
	<b>List of Notations</b>	<b>105</b>
	<b>List of Figures</b>	<b>107</b>
	<b>List of Tables</b>	<b>110</b>
	<b>Bibliography</b>	<b>111</b>
	<b>Lebenslauf</b>	<b>121</b>

# Chapter 1

## Introduction

Wireless communication is a term used to describe transmit and receive systems, which use electromagnetic waves to carry the information signals with the complete absence of wired connections. With its wide range of technologies such as mobile communications, wireless local area networks (WLAN), global positioning system (GPS) and many others, wireless communications changed the mankind life and introduced incredible applications such as internet of things (IoT), vehicle to everything (V2X) communication and even health monitoring devices.

One major issue of the practical wireless channels is the fluctuations in time, frequency and space. These fluctuations are resulting from multi-path propagation and known as fading. They affect the overall system performance in terms of reliability and capacity.

To reduce the fading effect, multiple-input multiple-output (MIMO) and multiple-input single-output (MISO) systems were developed to increase the diversity gain by using multiple transmit and receive antennas. As the receiver is provided with multiple copies of the same information, where each copy is transmitted via a different antenna experiencing different fading, the probability that all channels fade simultaneously is very small, which in turn improves the performance by reducing the error rate [BC17].

Beamforming techniques can also be utilized to eliminate the fading effects. Coherent processing is applied to constructively and destructively superimpose the signal waves transmitted from each antenna at the location of the desired and undesired co-channel users, respectively, with the objective to enhance the signal strength and suppress the interference.

In this dissertation, several novel general beamforming designs based on space-time block coding (STBC)s are presented, MISO systems are considered, where the transmitter has multiple transmit antennas and the receiver has a single receive antenna. The utilization of MISO system along with the beamforming techniques provides diversity gain and spatial multiplexing, which improves the system performance in terms of throughput and reliability. The combination of beamforming techniques with STBCs has the purpose of providing additional degrees of freedom in the beamforming design, and it is fundamentally different from the conventional use of STBC techniques, which generally do not use beamforming and do not require channel state information.

## 1.1 Background

Cellular communications is one of the most widespread wireless communication scenarios. The first-generation (1G) of mobile communication systems was developed in 1980s and was based on merely analog technology. It provided mainly a voice service [Mol11]. A new digital communications era began with the deployment of the second-generation (2G) mobile networks by the early 1990s. 2G overcame many of 1G issues, e.g., security and reliability and provided higher data rate, more capacity and better voice quality, by using time division multiple access (TDMA) or code division multiple access (CDMA) techniques. Moreover, 2G has provided new services such as short messaging, caller ID and most importantly roaming, which enabled the users to move across the cell boundaries seamlessly [MP92]. The use of 2G phones spread over the whole world, in the meanwhile the demands for more data connections like internet access, were also increasing. Global systems for mobile communications (GSM) is the most widely used standard for 2G networks. The 2.5G was developed with the improvements of GSM technology, facilitating higher data rates and providing voice with data using the general packet radio service (GPRS) and enhanced data rates for GSM evolution (EDGE) technologies. The 3rd generation partnership project (3GPP) was formed in December 1998 as a standardization body with the goals of the development of third-generation (3G) mobile communication systems, which was deeply influenced by the 2G TDMA-based GSM specifications. 3GPP supported a revolutionary change, which accompanied the introduction of third-generation (3G) early 2000, where the 3G systems evolved to data centric systems rather than voice centric systems. Moreover, wide code division multiple access (WCDMA) using 5 MHz bandwidth was developed and provided a data rate up to 2 Mbps, hence allowed various networks services, e.g., voice and video streaming, internet surfing and online games [Kor03, HT04]. Specifications for the fourth-generation (4G) mobile communications were employed in 2011. In addition to orthogonal frequency-division multiplexing (OFDM), 4G employed many technologies, e.g., MIMO and pure packet switching networks. The users were offered wide broadband connections and high data rates, which vary from 100 Mbps to 1 Gbps depending on mobility. The most bandwidth-intensive applications, such as video conferencing, cloud computing, and high definition (HD) mobile television, were supported by both 3G and 4G services [DPS01, AMH22]. However, the data traffic has increased dramatically, due to the widespread use of smart mobile phones, tablets and other devices, which support all the 4G offered services. To accommodate these huge changes, the fifth-generation (5G) of mobile communications was standardized and deployed by 2019 [VT17].

Via the use of millimeter wave (mmWave) communications, 5G offers data rates



more than 10 Gbps. Furthermore, it offers machine-to-machine (M2M) connections and improves the performance of 4G. Moreover, 5G delivers high reliability and real-time latency of just a few milliseconds, two of the technology's key advantages [VT17, Rod15, Dik22]. Due to the high data throughput and low time latency of 5G networks, the industrial IoT specifically experienced an acceleration in growth. A growing number of applications, like augmented reality, 3D video, and the internet of everything, are straining the capabilities of 5G and are the primary driving force behind the development of the sixth-generation 6G mobile communications, which is anticipated to happen in the upcoming years [Dik22].

The second widespread wireless technology is WLAN. IEEE initiated a project called 802 in 1980 [KL15]. However, the first WLAN standard 802.11 appeared in 1997. It supported a data rate of 1 or 2 Mbps and operated at frequency of 2.4 GHz [OP05]. The 802.11 standard was expanded in 1999 to 801.11b and 802.11a at 2.4 GHz and 5 GHz frequency bands, respectively. 802.11b supported a data rate up to 11 Mbps using the complementary code key (CCK) [WMB06], while 802.11a supported a data rate up to 54 Mbps by employing OFDM [AZ11]. The high cost of radio frequency implementation in year 2000 prevented the deployment of 802.11a at the 5 GHz frequency band. However, the demand for higher data rate beyond 11 Mbps was increasing. Adopting the same physical layer and media access control (MAC) specifications allowed the development of 802.11g, which provided a data rate up to 54 Mbps using the 2.4 GHz band [KL15]. The continuous growth of demand of internet access and its multimedia content pushed towards developing 802.11n in 2009, which offered a throughput of 100 Mbps. 802.11n employed MIMO technology, spatial-division multiplexing (SDM) up to four streams, transmit beamforming, and STBC. Adding more technologies such as downlink multi-user MIMO (MU-MIMO) allowed to develop the 802.11ac standard, which offered a network data rate up to 160 MHz and up to 8 streams instead of 4 streams as in 802.11n [KL15].

A report of CISCO [CIS20] predicted that WLAN connection will be used by more than 66% of the global population in 2023. Moreover, more than 70% of the population worldwide will be connected via mobile devices, where 5G will represent 10% of the mobile connections. Currently, the wireless telecommunication networks account for two to three percent of the global energy consumption, but it will grow to over 10% by 2030 [BDFS22]. Hence, efficient techniques such as Multi-antenna technologies are intensively studied to utilize the frequency resources to serve more users and achieve more capacity while reducing the energy consumption per bit.

Multi-antenna systems use the same spectral resources to simultaneously serve multiple users to enhance the overall system performance in terms of increased throughput and

reliability, while maintaining the transmit power objectives [Jan04]. Two widely known techniques are utilized in Multi-antenna systems, namely space-time codes (STC) and transmit beamforming technique.

### 1.1.1 Space-time Coding

A signal transmitted from a base station (BS) to a receiver can experience multi-path effects. Multiple copies of the same signal reach the destination through different paths. The received signal components can add constructively, enhancing the signal power, or destructively, causing the received signal-to-interference-plus-noise ratio (SINR) to decrease deeply.

Several copies of the same signal are sent using transmit diversity techniques over multiple time slots, frequency bands, or antennas. Each copy of the signal experiences different phase shifts, hence constructive or destructive superposition. If the number of copies send over the independent transmission paths is large, then the probability of the simultaneous drop of all received signal copies is rather small [Jaf05]. Figure 1.1 provides an illustration of the transmit diversity technique using multiple antennas at the transmitter.

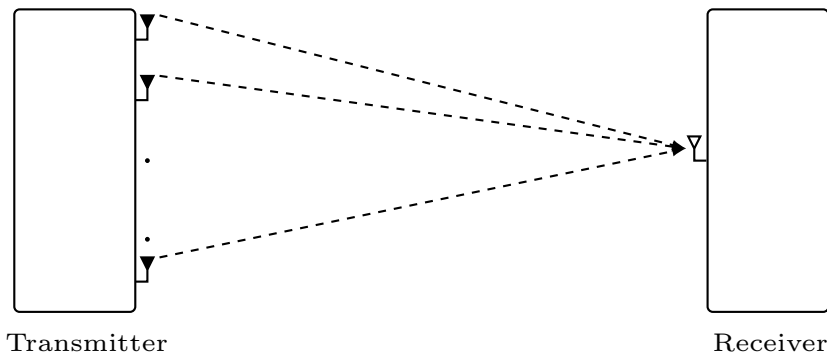


Figure 1.1. Illustration of the transmit diversity technique using multiple antennas at the transmitter.

STCs, which are used in MIMO systems achieve both, spatial and temporal diversity and do not require channel state information (CSI). The CSI can be obtained at the transmitter either by exploiting the channel reciprocity in the uplink channel in the time division duplex (TDD) systems or through a feedback channel using pilots in the downlink channel such that the receiver sends the channels estimation back to the transmitter in frequency division duplex (FDD) systems [TU07]. In both cases, an

overhead is associated with the acquisition of the CSI. Using STCs, multiple information signals are encoded over space and time and transmitted via multiple antennas during various time slots. Hence, reducing the effect of channel fading, minimizing the error rate and increasing the diversity without sacrificing the precious bandwidth resources. It is worth noting that STCs do not achieve the maximum rate obtained by the spatial multiplexing techniques.

In the following, several STCs are presented briefly. Furthermore, the performance gains and drawbacks are highlighted.

Orthogonal space-time block codes (OSTBCs) are a special kind of STCs, where each column of the code matrix is orthogonal to the other columns. The orthogonality of OSTBCs allows a simple symbol-by-symbol decoding at the receiver. A special simple case of OSTBCs was introduced by Alamouti [Ala98] for two transmit antennas. The Alamouti code provides full-diversity gain but no coding gain, where the coding gain is defined as the power gain of the coded system over an uncoded system for the same diversity gain and the same error probability. Furthermore, the diversity gain is a measure of the slope of the error probability plotted as a function of the signal-to-noise ratio (SNR) [VY03].

The orthogonality property of the Alamouti code has encouraged the researchers to explore OSTBCs for transmit systems with more than two antennas. OSTBCs were first introduced in [STC99b]. OSTBCs enjoy full-diversity and simple symbol-by-symbol decoding schemes. However, for MIMO systems with more than two transmit antennas, the full transmission rate of one symbol per time slot cannot be achieved using complex symbols in OSTBCs [STC99a].

Quasi orthogonal space-time block codes (QOSTBCs) were designed to achieve the full transmission rate by sacrificing the orthogonality of OSTBCs. Thus, the decoding complexity of QOSTBCs is higher compared with OSTBCs. Moreover, QOSTBCs have a partial diversity compared with OSTBCs [Jaf01]. A simple rotation technique as in [SP03, SX04] provides full-diversity QOSTBCs.

Space-time trellis codes (STTCs) were first proposed by the authors in [STC98] and are designed to combine error control, modulation and transmit and receive diversity. Thus, STTCs are capable of reducing the multi-path effect and delivering performance gains in terms of coding gain, diversity gain and spectral efficiency. Depending on the number of transmit and receive antennas, STTCs can be designed based on either the rank and determinant criteria or the trace criteria [VY03]. Applying the suitable design criteria for various modulation constellations and number of transmit antennas results

in optimum STTCs in terms of coding and diversity gains [VY03]. However, high decoding complexity and latency at the receiver are the main drawbacks of STTCs.

### 1.1.2 Transmit Beamforming

Transmit beamforming is a very powerful technique to send separate data streams using different antennas of a multi-antenna BS to a single user or multiple users simultaneously. MIMO processing and transmit beamforming has first made its way into standards in the 4G 3GPP standard LTE (Release 8) and WLAN 801.11n and 801.11ac protocols. Transmit beamforming can be used in different network scenarios [GSS<sup>+</sup>10].

- Single-group multicasting networks: The same data is sent to a single group of users simultaneously.
- Multi-group Multicasting networks: Different data is sent to a number of groups of users simultaneously. Each user in the same group receives the same information.
- Unicasting networks: Different data is sent to each user in the network at the same time.

Figure 1.2 illustrates the different transmit beamforming networks.

Transmit beamforming techniques are designed to steer the transmission of information in the direction of the network users. Thus, focusing the transmit power in the desired directions instead of broadcasting it isotropically as in traditional single antenna networks. On the other hand, transmit beamforming techniques minimize the interference at the non-intended directions. The knowledge of CSI for each user in the network is used in designing the beamformer at the BS, such that the signals add constructively at the desired directions and destructively at non-desired directions.

In practice, two widely popular approaches are employed to design the beamforming matrices at the BS. Both of the transmit beamforming designs consider the SINR at the receivers, which in turn directly affects the users' transmission rate and symbol error rate. In this sense, both designs use the SINR to measure the quality-of-service (QoS) of the system. The first approach is known as the QoS optimization problem and the later one max-min fair (MMF) beamforming design [SDL06, GSS<sup>+</sup>10]. The

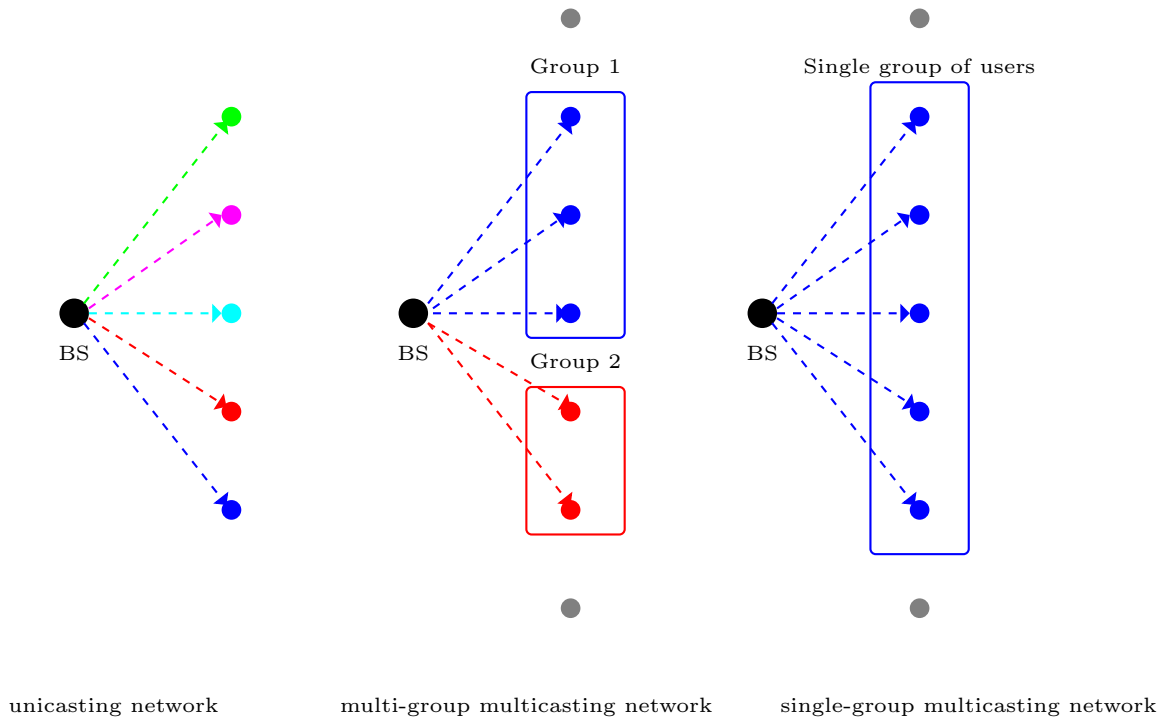


Figure 1.2. Illustration of transmit beamforming networks.

QoS optimization problem minimizes the transmit power while satisfying the SINR constraints at all the subscribed users, thus saving the power consumption at the serving BS, while assuring a desired performance for the network users. In the MMF design, the smallest SINR value among all subscribed users is maximized given the transmit power upper bound at the BS. Thus, the beamformers are designed fairly to improve the performance for the users with the worst SINR, assuming a given transmit power constraint at the BS.

In this dissertation, transmit beamforming techniques for single-group multicasting networks are studied.

### 1.1.3 Rank Reduction Techniques

Optimal solutions of the QoS and MMF problems are the best feasible solutions in terms of the design objective. However, both optimization problems are non-convex and non-deterministic polynomial-time hard (NP-hard) [GS05, TSS05, GSS<sup>+</sup>10, SDL06, LSTZ07], and there is non known algorithm capable of solving either one of them in polynomial time.

A powerful and well established technique known as semi-definite relaxation (SDR), has been suggested to relax the non-convex optimization problems of QoS and MMF, hence yielding convex problems that can be efficiently solved using, e.g., numerical gradient based methods or interior point solvers [SDL06]. However, due to the relaxation technique, the optimization solutions are only optimal, when their rank is equal to one. Otherwise, the obtained solutions are suboptimal. This approach is known as the rank one beamforming problem. Unfortunately, rank one optimal solutions are only obtained for networks with comparably low number of users [WMS13]. When the number of users increases, the rank of the beamforming solutions increases as well. Thus, the SDR technique's performance degrades dramatically for networks with large number of users.

A pioneer work was introduced by the authors in [HP10b], where a rank reduction algorithm was suggested to generate optimal beamformer when the rank of the optimization problem solutions is not larger than a predetermined upper bound. Moreover, in the same paper it was proven that the obtained upper bound scales with the number of network users.

The widely known randomization procedure can be employed to further reduce the rank of the beamforming solutions to one and generate feasible solutions. However, the obtained beamformers are generally suboptimal for networks with large number of users [LMS<sup>+</sup>10, KSL08a].

Rank two beamforming problem has been presented in [WLAP12, WMS13] to overcome the performance degradation of rank one beamforming problem. The Alamouti code was utilized to double the degrees of freedom, thus serving more users optimally compared with the rank one beamforming design. However, as the number of users grows further, the rank of the beamforming problem increases and the performance of the rank two beamforming design degrades consequently.

## 1.2 Contributions and Thesis Overview

In this dissertation, single group multicasting networks are considered, where streaming data services such as video or gaming applications are provided to the users based on their subscription. As mentioned in Section 1.1.2. In contrast to unicasting and multi-group multicasting networks, where each user or group of users, as appropriate, receives a different stream of data service from the BS, single group multicasting only allows for one group of users. In multicasting networks, the data is transmitted towards

the desired directions using optimization techniques. Yet, the problem is challenging for networks with relatively large number of users, because only a suboptimal feasible solution can be obtained with reasonable effort, which adversely affects the total system performance in terms of reliability and capacity. In rank one beamforming methods for multicasting networks, a single vector is utilized at the BS to beam the information in the direction of desired users, thus minimizing the interference at the other directions.

In this thesis, we consider beamformer designs based on either the QoS or the MMF problem. As mentioned earlier in 1.1.3, the solutions of both optimization methods are optimal if the rank of the obtained solutions equals to one. Higher rank ( $> 1$ ) solutions are more likely to arise as the number of users increases [HP10b], thus the obtained beamforming solutions are not optimal in terms of the design objectives.

In this dissertation, higher rank ( $> 1$ ) beamforming solutions are combined with a variety of space-time block codes (STBCs) with different characteristics with the objective of increasing the degrees of freedom and obtaining general rank beamforming solutions, meanwhile overcoming the issue that the rank two beamforming design is the only OSTBC, that enjoys full rate of one symbol per time slot. Moreover, the innovative STBCs based beamforming designs address the issues of the rank one and the rank two beamforming designs for single group multicasting networks, where STBCs are selected accordingly to obtain near optimal beamforming solutions and enhance the overall system performance in terms of reliability and capacity.

Furthermore, a new rank reduction technique is developed and employed to reduce the rank of the beamforming solution to the desired value.

Each of the following chapters is organized such that a brief introduction of the related works and the impact of the proposed approach is presented, the system model of the general rank optimization problem and the performance analysis are provided, the simulation results and comparisons to the other state-of-the-art designs are depicted, finally a summary of the proposed approach and its contributions is delivered.

**Chapter 2** introduces the state-of-the-art designs for beamforming techniques in single group multicasting networks. The rank one and the rank two beamforming designs for a single group of users are presented. Both QoS and MMF approaches are discussed in detail for both designs. Moreover, the powerful SDR technique is utilized, in which a variable transformation is introduced that lifts the variable space onto a larger dimensional space and in which the non-convex (rank one/ rank two) constraint in the optimization problem is relaxed. The resulting problem is solved optimally. Due to the relaxation technique, the solutions of the QoS and MMF problems enjoy an acceptable

performance for a group with a small number of users. However, the performance of the obtained solutions degrades severely when the number of users increases.

In **Chapter 3**, numerous technical contributions are established to overcome the drawbacks of the rank one and the rank two beamforming designs as presented in Chapter 2. Various general rank beamforming problems for single group multicasting networks, namely STTCs, OSTBCs, real-valued OSTBCs and STBCs based beamforming, are introduced to enhance the overall system performance for networks with a large number of users.

STTCs based general rank beamforming design is presented in Section 3.1. Increasing the number of users in the network results in increasing the rank of the beamforming solutions. STTCs are used to accompany the increasing rank and provide a flexible general rank design for the beamforming solutions. The maximum rank is determined by the choice of the STTC. STTCs are powerful codes, which provide error correcting capabilities, diversity and coding gain. Hence, STTCs outperform OSTBCs, where only diversity gain is delivered. However, STTCs are associated with increased decoding complexity compared to OSTBCs at the users side. The MMF problem is considered and the SDR technique is used to obtain the beamforming solutions. Moreover, the rank of the solutions is matched to the STTCs codes. As will be shown later, the simulation results demonstrate that the STTCs based beamforming approach significantly outperforms the state-of-the-art rank one and rank two beamforming designs.

General rank beamforming design using higher order ( $> 2$ ) OSTBCs is introduced in Section 3.2. The proposed approach is motivated to overcome the degraded performance of the Alamouti based beamforming design for the scenario of large number of users and the high decoding complexity of STTCs based beamforming approach at the user's side. Combining OSTBCs with beamforming yields a larger number of diverse beamformers that provide flexibility to serve users with diverse channels, thus providing larger degree of freedom and increasing the system reliability. However, higher order ( $> 2$ ) OSTBCs do not enjoy full transmission rate of one symbol per user and transmission time. In the proposed approach, the rate is compensated using either higher modulation schemes or channel codes with higher rates than the competing designs. A fair comparison with the other approaches is guaranteed by maintaining the same rate. The main drawback of this design is that the modulation or the channel code cannot be chosen independently of the utilized OSTBCs. Simulation results show that the proposed approach achieves significant reliability improvements compared with the state-of-the-art designs.

In Section 3.3, a general rank beamforming design using higher order ( $> 2$ ) real-valued



full rate OSTBCs is introduced. The proposed approach provides general beamforming solutions for networks with a large number of users, where the degrees of freedom required to design the beamforming vectors are not sufficient. The presented work uses the orthogonality of OSTBCs to provide symbol-by-symbol decoding, which can be used efficiently at each network user to retrieve the transmitted information with low complexity. The simulation results illustrate improved bit-error rate (BER) performance compared with the state-of-the-art rank one and rank two beamforming designs. It can be noted that the real-valued modulated OSTBCs reflect on the performance of this design, thus the other introduced designs provide better performance gains in terms of BER.

In STBCs based beamforming techniques in Section 3.6, the orthogonality of the OSTBCs based beamforming design is sacrificed and full rate STBCs are employed instead. The non-orthogonal STBCs increase the decoding complexity at the users' side compared with OSTBCs. An alternative and powerful design criterion is provided to minimize the worst user pairwise error probability (PEP) for a given transmit power budget. The non-convex problem is approximated using the first order Taylor approximation and an iterative algorithm is devised to yield the beamforming solutions. The performance of the proposed approach is evaluated using the QOSTBCs as example of the full rate STBCs. Simulation results depict that the proposed approach has a superior performance in terms of BER compared with the state-of-the-art rank one, rank two, real-valued OSTBC and OSTBC based beamforming designs.

This chapter is based on the following publications

- D. Taleb, S. Alabed, and M. Pesavento, "Optimal general-rank transmit beamforming technique for single-group multicasting service in modern wireless networks using STTC," **Best Paper Award** at the 9th International ITG Workshop on Smart Antennas. (WSA 2015), pp. 1–7, 3-5 Mar. 2015.
- D. Taleb, Y. Liu, and M. Pesavento, "Full-rate general rank beamforming in single-group multicasting networks using non-orthogonal STBC," 24th European Signal Processing Conference (EUSIPCO 2016), pp. 2365–2369, 29 Aug.-2 Sep. 2016.
- D. Schenck, D. Taleb, M. Pesavento, and A. Sezgin, "General rank beamforming using high order OSTBC for multicasting networks," 21th International ITG Workshop on Smart Antennas. (WSA 2017), pp. 175–181, 15-17 Mar. 2017.

- D. Taleb, and M. Pesavento, "General rank beamforming using full rate real-value OSTBC for multicasting networks," 24th International ITG Workshop on Smart Antennas (WSA 2020), 18.-20.02.2020

In **Chapter 4** a compelling optimization problem to reduce the rank of the beamforming solutions is presented. A smooth approximation of the rank function is employed. The non-convex surrogate function is linearized using the first order Taylor approximation. Two different algorithms are provided to reduce the rank iteratively. In the two scale algorithm, two loops are employed. The inner loop runs till the convergence criterion is met. In the outer loop, a regularization variable is smoothly decreased until the desired rank is reached. The exhaustive search of the two scale algorithm is accompanied with high computational complexity. A faster one scale algorithm is proposed to scale the regularization variable according to the eigenvalue of the beamforming solutions. A generalization to the general rank beamforming scenario of several state-of-the-art procedures, namely randomization, inner approximation, multiplicative update (MU), alternating direction method of multipliers (ADMM), successive linear approximation (SLA) and MU-SLA is provided. The simulation results demonstrate that the proposed rank reduction approach outperforms the competing approaches.

This chapter is based on the following publication

- D.Taleb, and M. Pesavento, "Rank regularized beamforming in single group multicasting networks," 11th IEEE Sensor Array and Multichannel Signal Processing Workshop (SAM 2020), 08.-11.06.2020

**Chapter 5** provides the final discussion and the conclusion of this work.

---

## Chapter 2

### State of the art

#### 2.1 Introduction

Single group multicasting beamforming has its own merit in applications, where multiple users receive the same information. Unlike unicasting and multigroup multicasting networks, where the interference at the unintended directions is minimized, the transmit power in single group multicasting networks is exploited to send only the intended information in the desired directions of users, as the interference is absent for this scenario. The BS in single group multicasting networks can even serve multiple users in the same group with slightly different information, where the uninteresting data can be discarded at the receivers' side. Moreover, the transmission power can be increased up to the maximum permitted limit to satisfy the QoS objectives at the users' side.

Multicasting services have been provided in the LTE network through enhanced multimedia broadcast multicast service [MSG13], where live television, video on demand, live coverage and firmware updates can be delivered to the intended users simultaneously. Several subscriber groups could operate on different frequencies, hence without interfering to each other by means of single group multicasting techniques instead of multigroup multicasting.

In this chapter, the state-of-the-art transmit beamforming techniques, namely rank one and rank two beamforming designs, are presented in Section 2.3 and 2.4 for a single group multicasting network scenario, where a multi-antenna BS transmits the same information to a group of users subscribed to a particular service. Beamforming techniques are devised to steer the transmitted information to the desired direction of the users such that there is no interference at the users' side. This is achieved by weighting the users' information by beamforming matrices [SDL06, BO99, BO01]. In the rank one beamforming design, the SDR technique is employed to obtain a single beamforming vector. However, the rank one beamforming problem for the single group multicasting networks is challenging, when the number of users grows due to the diversity of the communication channels. Thus, the rank two based beamforming using Alamouti code was introduced in [WMS13, LWTP15], where two beamforming vectors are utilized to double the degrees of freedom and serve more users optimally. Unfortunately, the performance of the rank two beamforming design degrades when

the number of users grows further. Thus, more general STCs are studied to provide a general rank beamforming design, which increases the degrees of freedom compared with the rank two beamforming design and provides optimal beamforming solution in terms of the design objectives as will be shown in Chapter 3. A detailed description of the STBCs, namely Alamouti, OSTBCs and STTCs, is provided in the following.

## 2.2 Space-time Block Codes

### 2.2.1 Alamouti Space-time Block Code

The Alamouti code is the simplest kind of OSTBCs, where two symbols are transmitted, e.g., from two antennas using two time slots. Thus, Alamouti code enjoys full rate code.

Assuming  $\mathbf{s} \triangleq [s_1 \ s_2]^T$  is the symbols vector, where  $s_1$  and  $s_2$  are quadrature phase shift keying (QPSK) modulated symbols, the transmission matrix is given by

$$\mathbf{S} \triangleq \begin{bmatrix} s_1 & s_2 \\ -s_2^* & s_1^* \end{bmatrix}. \quad (2.1)$$

The orthogonality of Alamouti code can be proven using

$$\mathbf{S}\mathbf{S}^H = \mathbf{S}^H\mathbf{S} = (|s_1|^2 + |s_2|^2) \mathbf{I}_2. \quad (2.2)$$

The orthogonality of  $\mathbf{S}$  in (2.2) simplifies the decoding procedure as will be shown through the rest of this section.

The channels are assumed to be quasi static block fading such that the channel coefficients of the  $j$ th user,  $\mathbf{h}_j$  remain constant over the transmission of one Alamouti block and the symbols are uncorrelated in each transmission matrix  $\mathbf{S}$ .

The signal  $\mathbf{y}_j$  received by the  $j$ th user during the transmission of two time slots is given by

$$\mathbf{y}_j = \mathbf{S}\mathbf{h}_j + \mathbf{n}_j, \quad (2.3)$$

where  $\mathbf{y}_j \triangleq [y_{j,1} \ y_{j,2}]^T$ ,  $\mathbf{h}_j \triangleq [h_{j,1} \ h_{j,2}]^T$  and  $\mathbf{n}_j \triangleq [n_{j,1} \ n_{j,2}]^T$  are the received signal, the  $j$ th user's channel and receiver noise with zero mean and  $\sigma_j^2$  variance, respectively, at the first and the second time slots.

Using the equivalent channel representation of Alamouti code [Ala98], equation (2.3) can be written as

$$\tilde{\mathbf{y}}_j = \tilde{\mathbf{H}}_j\mathbf{s} + \tilde{\mathbf{n}}_j, \quad (2.4)$$

where  $\tilde{\mathbf{y}} \triangleq [y_{j,1} \ y_{j,2}^*]^\text{T}$ ,  $\tilde{\mathbf{H}}_j \triangleq \begin{bmatrix} h_{j,1} & h_{j,2} \\ h_{j,2}^* & -h_{j,1}^* \end{bmatrix}$  and  $\tilde{\mathbf{n}}_j \triangleq [n_{j,1} \ n_{j,2}^*]^\text{T}$ .

Multiplying both sides of equation (2.4) by  $\tilde{\mathbf{H}}_j^\text{H}$  and dividing by  $\frac{1}{|h_{j,1}|^2 + |h_{j,2}|^2}$ , the received symbol at the  $j$ th user is given by

$$\begin{aligned} \hat{\mathbf{s}} &= \frac{1}{|h_{j,1}|^2 + |h_{j,2}|^2} \tilde{\mathbf{H}}_j^\text{H} \tilde{\mathbf{y}}_j \\ &= \mathbf{s} + \hat{\mathbf{n}}_j, \end{aligned} \quad (2.5)$$

where  $\hat{\mathbf{s}} \triangleq [\hat{s}_1 \ \hat{s}_2]^\text{T}$  and  $\hat{\mathbf{n}}_j \triangleq \frac{1}{|h_{j,1}|^2 + |h_{j,2}|^2} \begin{bmatrix} h_{j,1}^* n_{j,1} + h_{j,2} n_{j,2}^* \\ h_{j,2}^* n_{j,1} - h_{j,1} n_{j,2}^* \end{bmatrix}$ .

This simple symbol-by-symbol detection procedure allows the receiver to detect two symbols in two time slots.

### 2.2.2 Higher Order OSTBCs

The simplicity of the Alamouti code has motivated the design of higher order OSTBCs. However, the Alamouti code is the only known OSTBC that enjoys full transmission rate of one symbol per time slot for two transmit antennas. Consider a BS with  $N$  transmit antennas. A number of  $K$  symbols,  $s_1, s_2, \dots, s_K$  are transmitted during  $T$  time slots. Therefore the OSTBC code rate is  $L = \frac{K}{T}$ . The OSTBC transmission matrix  $\mathbf{S} \in \mathbb{C}^{T \times N}$  enjoys the orthogonality property such as

$$\mathbf{S}^\text{H} \mathbf{S} = (|s_1|^2 + |s_2|^2 + \dots + |s_K|^2) \mathbf{I}_N. \quad (2.6)$$

The signal  $\mathbf{y}_j$  received by the  $j$ th user during the transmission of  $T$  time slots is given by

$$\mathbf{y}_j = \mathbf{S} \mathbf{h}_j + \mathbf{n}_j, \quad (2.7)$$

where  $\mathbf{y}_j \triangleq [y_{j,1} \ y_{j,2} \ \dots \ y_{j,T}]^\text{T}$ ,  $\mathbf{h}_j \triangleq [h_{j,1} \ h_{j,2} \ \dots \ h_{j,T}]^\text{T}$  and  $\mathbf{n}_j \triangleq [n_{j,1} \ n_{j,2} \ \dots \ n_{j,T}]^\text{T}$  are the received signal, the  $j$ th user's quasi static block fading channel and receiver noise with zero mean and  $\sigma_j^2$  variance, respectively, during the transmission of  $T$  time slots.

The orthogonality property of (2.6) reduces the complexity of the decoding procedure such that the transmitted symbols can be decoded independently using the maximum likelihood (ML) scheme [Jaf05].

### Example

Consider the OSTBC matrix  $\mathbf{S} \in \mathbb{C}^{4 \times 4}$  with  $N = 4$  transmit antennas,  $T = 4$  time slots and  $K = 3$  QPSK modulated symbols given by  $s_1$ ,  $s_2$ , and  $s_3$ . Therefore, the OSTBC code rate is  $L = \frac{3}{4}$ . Assuming  $\mathbf{s} \triangleq [s_1 \ s_2 \ s_3]^T$ , the OSTBC transmission matrix is given by

$$\mathbf{S} = \begin{bmatrix} s_1 & s_2 & s_3 & 0 \\ -s_2^* & s_1^* & 0 & s_3 \\ s_3^* & 0 & -s_1^* & s_2 \\ 0 & s_3^* & -s_2^* & -s_1 \end{bmatrix}. \quad (2.8)$$

Using (2.6), it can be proven that the OSTBC code described in (2.8) is orthogonal and has a diversity gain of four, such that each of the three symbol is transmitted over all four independently fading channels.

## 2.2.3 Space-time Trellis Codes

In this section, STTCs will be introduced in detail. OSTBCs are very attractive due to their coding and decoding simplicity. However, they do not offer coding gain. On the other hand, STTCs offer coding gain by combining the error correction properties with the modulation scheme. Moreover, STTCs provide transmit and receive diversity.

### 2.2.3.1 STTCs Encoding

Consider a STTC encoder with  $N$  transmit antennas and a binary input stream given by  $[\mathbf{c}_1, \mathbf{c}_2, \dots, \mathbf{c}_t, \dots, \mathbf{c}_T]$ , where  $\mathbf{c}_t \triangleq [c_t^1, c_t^2, \dots, c_t^m]$  is a vector of  $m$  binary information bits at the  $t$ th time slot and  $T$  is the total number of time slots. The encoder maps the binary inputs  $\mathbf{c}_t$ , at time slot  $t$ , to modulation symbols  $\mathbf{s}(t)$ , at the output  $\mathbf{S} \in \mathbb{C}^{T \times N}$ , given by

$$\mathbf{S} \triangleq \begin{bmatrix} \mathbf{s}(1) \\ \vdots \\ \mathbf{s}(t) \\ \vdots \\ \mathbf{s}(T) \end{bmatrix}, \quad (2.9)$$

where  $\mathbf{s}(t) \triangleq [s_1(t), s_2(t), \dots, s_N(t)]$  and  $s_i(t)$  is the STTC signal at the  $i$ th transmit antenna and at the  $t$ th time slot.

The signal  $\mathbf{y}_j$  received by the  $j$ th user during the transmission of  $T$  time slots is given by

$$\mathbf{y}_j = \mathbf{S}\mathbf{h}_j + \mathbf{n}_j, \quad (2.10)$$

where  $\mathbf{y}_j \triangleq [y_{j,1} \ y_{j,2} \ \cdots \ y_{j,T}]^T$ ,  $\mathbf{h}_j \triangleq [h_{j,1} \ h_{j,2} \ \cdots \ h_{j,T}]^T$  and  $\mathbf{n}_j \triangleq [n_{j,1} \ n_{j,2} \ \cdots \ n_{j,T}]^T$  are the received signal, the  $j$ th user's quasi static block fading channel and receiver noise with zero mean and  $\sigma_j^2$  variance, respectively, during the transmission of  $T$  time slots.

Figure 2.1 illustrates the encoder of the STTCs. At each time slot  $t$ ,  $m$  binary bits are fed simultaneously into the encoder, where they are multiplied by the coefficients  $g_{n,i}^k$  of the generator matrices, where  $k = 1, \dots, m$ ,  $i = 1, \dots, N$ ,  $n = 0, \dots, v_k$  for a memory order  $v_k$  of the shift register  $D$  at the  $k$ th branch.

The output of the encoder is the summation of the values of all the shift registers using modulo  $\mathcal{M}$  arithmetics, where  $\mathcal{M} = 2^m$ , given by

$$s_i(t) = \sum_{n=0}^{v_k} \sum_{k=1}^m g_{n,i}^k c_{t-i}^k \bmod \mathcal{M}, \quad i = 1, \dots, N. \quad (2.11)$$

The encoding procedure is illustrated in the following example.

### Example

An encoder with  $N = 3$  transmit antennas as shown in Figure 2.2 is considered.

The total memory order is  $v = 2$ . Thus, the number of states produced by the bits in the shift registers is  $2^2 = 4$ . Assuming the QPSK modulation scheme, the generator matrices are given by [VY03]

$$\begin{aligned} \mathbf{G}^{(1)} &\triangleq \begin{bmatrix} 0 & 2 & 2 \\ 1 & 2 & 3 \end{bmatrix} \\ \mathbf{G}^{(2)} &\triangleq \begin{bmatrix} 2 & 3 & 3 \\ 2 & 0 & 2 \end{bmatrix}. \end{aligned} \quad (2.12)$$

The output of the STTC encoder at the  $t$ th time slot is given by

$$s_i(t) = \sum_{n=1}^2 \sum_{k=1}^2 g_{n,i}^k c_{t-i}^k \bmod \mathcal{M}, \quad i = 1, \dots, N, \quad (2.13)$$

where  $\mathcal{M} = 4$ .

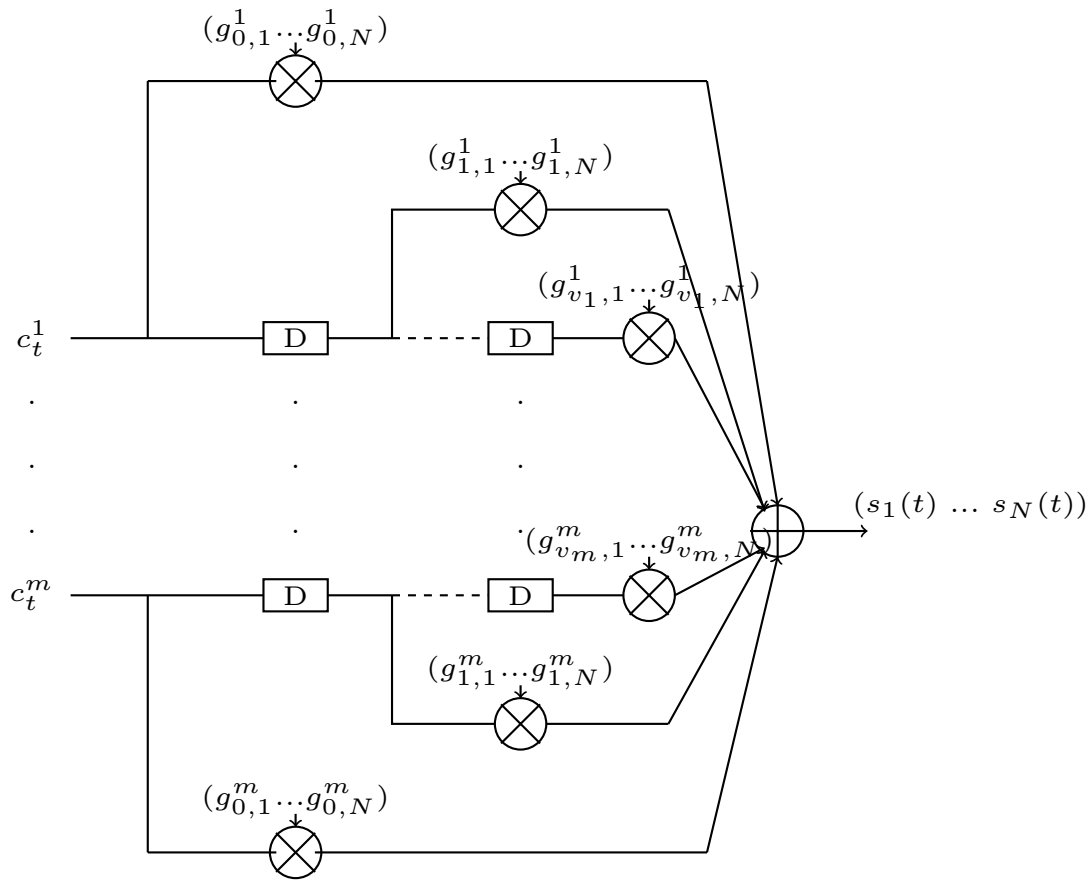


Figure 2.1. STTC encoder with  $m$  binary input bits and  $N$  transmit antennas.

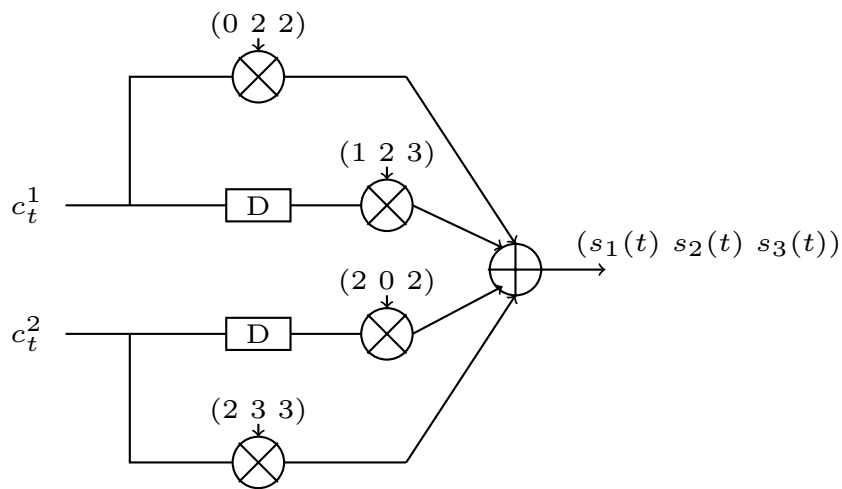


Figure 2.2. Example of a STTC encoder with 3 transmit antennas.



The trellis diagram of the corresponding encoder is shown in Figure 2.3, where the states are given by 00, 01, 10, 11 and the label  $\mathbf{c}_t/\mathbf{s}(t)$  at each branch indicates the input and the output of the encoder. For example, if the current state is 01 and the input of the encoder is 10 the output will be 220 and the next state will be 10. At the first time slot, the shift registers have the values of 0. Thus, the encoder starts with state 00. The last time slot of each frame must contain 00 at the encoder input. This assures a path that begins and ends with state 00 at the decoding side. Assuming, for example, a binary input  $\mathbf{c} = [00\ 10\ 10\ 11\ 00\ 00]$ , the corresponding STTC output  $\mathbf{S} \in \mathbb{C}^{T \times N}$  is given by

$$\mathbf{S} = \begin{bmatrix} 0 & 0 & 0 \\ 0 & 2 & 2 \\ 1 & 0 & 1 \\ 3 & 3 & 0 \\ 3 & 2 & 1 \\ 0 & 0 & 0 \end{bmatrix}. \quad (2.14)$$

Subsequently, the symbols 0, 1, 2, 3 in equation (2.14) are mapped to QPSK modulation symbols to produce

$$\frac{1}{\sqrt{2}} \begin{bmatrix} +1 + 1i & +1 + 1i & +1 + 1i \\ +1 + 1i & -1 - 1i & -1 - 1i \\ -1 + 1i & +1 + 1i & -1 + 1i \\ +1 - 1i & +1 - 1i & +1 + 1i \\ +1 - 1i & -1 - 1i & -1 + 1i \\ +1 + 1i & +1 + 1i & +1 + 1i \end{bmatrix}. \quad (2.15)$$

### 2.2.3.2 Decoding

The decoding procedure is performed at the user side using the established Viterbi algorithm, where the ML decoding scheme is employed and the path with the minimum path gain is chosen for the decoding [Jaf05, VY03]. Assuming perfect CSI available at the  $j$ th user, the branch metric for each received symbol  $y_j(t)$  at the  $t$ th time slot is calculated using the squared Euclidean distance between the actual received symbol and all possible constellation symbols, which is given by

$$\left| y_j(t) - \sum_{i=1}^N h_{j,i} s_i(t) \right|^2, \quad (2.16)$$

where  $h_{j,i}$  is the channel coefficient between the  $i$ th transmit antenna and the  $j$ th user and  $s_i(t)$  is the hypothesized transmitted symbol from the  $i$ th antenna.

The path metric is the summation of all branch metrics after receiving  $T = l + v$  symbols, where  $v = \sum_{k=1}^m v_k$  is the total memory order. The selected path is the path that starts and ends with state 00 and has the minimum squared Euclidean distance [Jaf05, VY03]. The ML decoder determines the symbols that form a valid path and solve the minimization problem denoted by

$$\min_{\mathbf{s}} \sum_{t=1}^{T+v} \left| y_j(t) - \sum_{i=1}^N h_{j,i} s_i(t) \right|^2. \quad (2.17)$$

The decoding complexity of the recent STTCs increases exponentially with the number of transmit antennas  $N$  at the BS, the trellis code rate  $r$  and the constellation order  $m$  and linearly with the trellis length  $T$ , hence the complexity order is given by  $O(TR2^{(rR+1)m})$  [KG10]. In spite of the high complexity of STTCs, multiple works have proposed its application for diverse scenarios and fields, for up to four transmit antennas, in which the complexity is kept upper-bounded. [SL01, GZCVCV10, ZBR-CVCV15, SS10]. Moreover, recent works have been published in which the decoding complexity of the Viterbi decoder has been addressed, by reducing the complexity of the branch metric calculation as in [KC08, NC00], or by using binary tree comparison [SCH10].

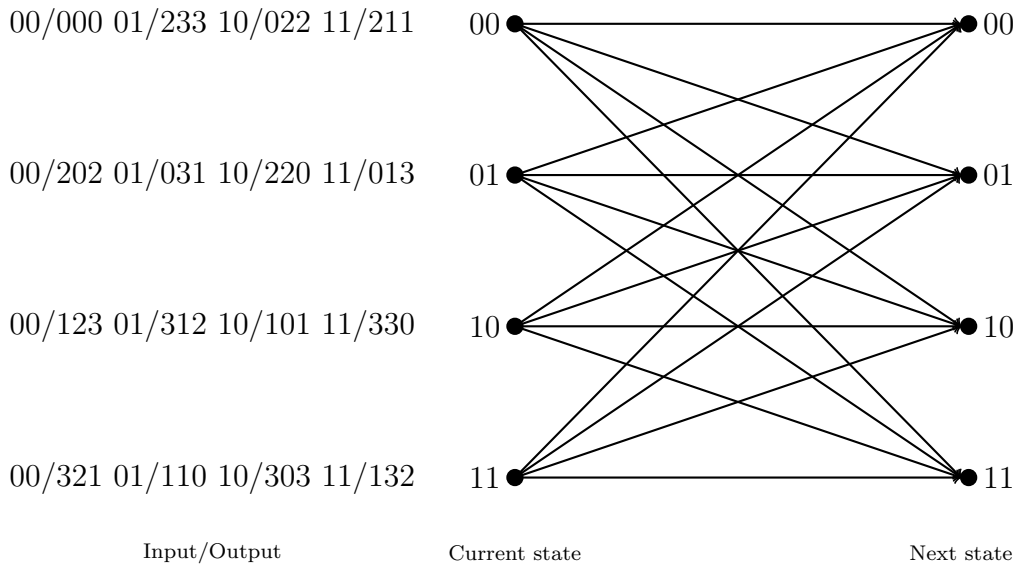


Figure 2.3. Trellis diagram for the encoder example.

## 2.3 Rank One Transmit Beamforming For Single Group Multicasting

In this section an overview of the rank one technique for single group multicasting networks is provided. Two widely known designs are devised to obtain the beamforming matrices at the BS. The first design is known as the QoS optimization problem and the later one is the MMF beamforming problem [SDL06, GSS<sup>+</sup>10].

### 2.3.1 System Model

The scenario of the single group wireless multicasting system is considered, where a BS equipped with  $N$  transmit antennas serves a group of  $M$  single antenna users. Both the BS and the users are assumed to have perfect CSI. In the rank one beamforming design, the information is steered towards the desired users' channel using a single beamforming vector. Denote  $s$  as the zero-mean unit power information symbol and  $\mathbf{w} \in \mathbb{C}^{N \times 1}$  as the beamforming vector. Figure 2.4 illustrates the system model.

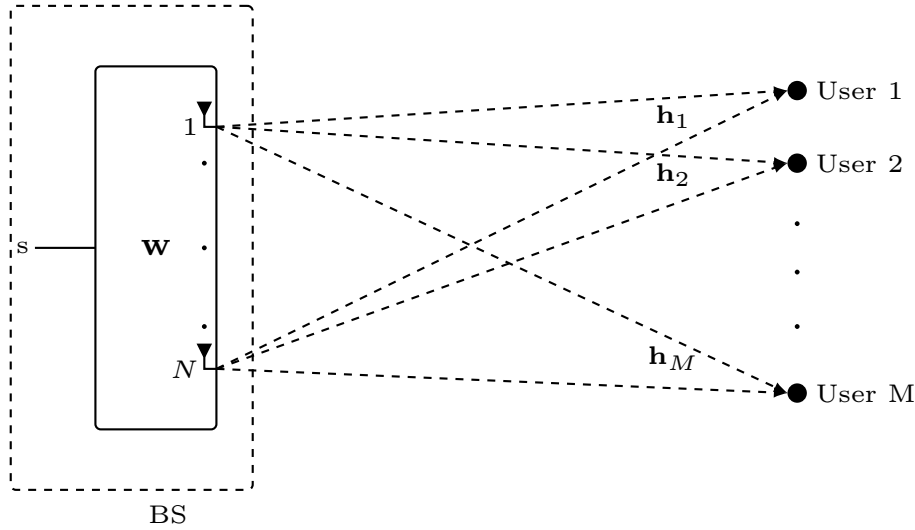


Figure 2.4. System model for rank one transmit beamforming.

The signal  $y_j$  received by the  $j$ th user is given by

$$y_j = s\mathbf{w}^H\mathbf{h}_j + n_j, \quad (2.18)$$

where  $\mathbf{h}_j \in \mathbb{C}^{N \times 1}$  is the  $j$ th user channel,  $n_j$  is the  $j$ th receiver additive white Gaussian noise with  $n_j \sim \mathcal{CN}(0, \sigma_j^2)$  and  $\sigma_j^2$  is the noise variance.

### 2.3.2 QoS Optimization Problem

In the conventional QoS optimization approach, the total transmit power  $P$  at the serving BS is minimized subject to SNR constraints at each subscribed user. This preserves the transmit power at the BS and assures a minimum QoS at the subscribed users. The transmit power at the BS is given by

$$\begin{aligned}
 P &\triangleq \mathbb{E}_s \left[ \|s \mathbf{w}^H\|_F^2 \right] \\
 &= \mathbb{E}_s \left[ \text{tr} \left( (s \mathbf{w}^H) (s \mathbf{w}^H)^H \right) \right] \\
 &= \text{tr} \left( \mathbb{E}_s \left[ \mathbf{w} s s^* \mathbf{w}^H \right] \right) \\
 &= \text{tr} \left( \mathbf{w} \mathbf{w}^H \right),
 \end{aligned} \tag{2.19}$$

where the trace rotation property is applied and  $\mathbb{E} [|s|^2] = 1$ .

Note that the trace rotation property is given by  $\text{tr}(\mathbf{A}\mathbf{B}) = \text{tr}(\mathbf{B}\mathbf{A})$  if the products  $\mathbf{A}\mathbf{B} \neq \mathbf{0}$  and  $\mathbf{B}\mathbf{A} \neq \mathbf{0}$ , and  $\|\cdot\|_F$  is the Frobenius norm.

The SNR constraint at the  $j$ th user is given by

$$\begin{aligned}
 \text{SNR}_j &\triangleq \mathbb{E}_s \left[ \frac{\|s \mathbf{w}^H \mathbf{h}_j\|_F^2}{|n_j|^2} \right] \\
 &= \frac{\mathbb{E}_s \left[ \text{tr} \left( (s \mathbf{w}^H \mathbf{h}_j) ((s \mathbf{w}^H \mathbf{h}_j)^H) \right) \right]}{\sigma_j^2} \\
 &= \frac{\text{tr} \left( \mathbb{E}_s \left[ \mathbf{w} s s^* \mathbf{w}^H \mathbf{h}_j \mathbf{h}_j^H \right] \right)}{\sigma_j^2} \\
 &= \frac{\text{tr} \left( \mathbf{w} \mathbf{w}^H \mathbf{h}_j \mathbf{h}_j^H \right)}{\sigma_j^2},
 \end{aligned} \tag{2.20}$$

where the information symbols  $s$  and the noise  $n_j$  at user  $j$  are considered statistically independent.

Assuming that  $\mathbf{H}_j \triangleq \mathbf{h}_j \mathbf{h}_j^H$  and  $\gamma_j$  is the SNR threshold at the  $j$ th user, the QoS optimization problem can be formulated as

$$\begin{aligned}
 \min_{\mathbf{w}} \quad & \text{tr} \left( \mathbf{w} \mathbf{w}^H \right) \\
 \text{s.t.} \quad & \frac{\text{tr} \left( \mathbf{w} \mathbf{w}^H \mathbf{H}_j \right)}{\sigma_j^2} \geq \gamma_j, \quad j = 1, \dots, M.
 \end{aligned} \tag{2.21}$$

The QoS problem is NP-hard in general [GS05, TSS05, GSS<sup>+</sup>10, SDL06, LSTZ07]. In order to solve the given optimization problem, SDR technique was introduced

in [SDL06]. The SDR technique is capable of relaxing non-convex quadratically constrained quadratic problems into convex semi-definite problems. Therefore, the SDR technique can be employed to obtain a suboptimal solution. Define

$$\mathbf{X} \triangleq \mathbf{w}\mathbf{w}^H \Leftrightarrow \mathbf{X} \succeq \mathbf{0} \text{ and } \text{rank}(\mathbf{X}) = 1, \quad (2.22)$$

where a matrix  $\mathbf{A} \in \mathbb{C}^{n \times n}$  is positive semi-definite,  $\mathbf{A} \succeq \mathbf{0}$ , when  $\mathbf{x}^H \mathbf{A} \mathbf{x} \geq 0$  for all  $\mathbf{x} \in \mathbb{C}^n$ . The symbol  $P \Leftrightarrow Q$  in (2.22) expresses equivalence, such that  $P$  implies  $Q$  and the other way around.

Using (2.22), the optimization problem of (2.21) can be written as

$$\min_{\mathbf{X}} \text{tr}(\mathbf{X}) \quad (2.23a)$$

$$\text{s.t.} \quad \frac{\text{tr}(\mathbf{X}\mathbf{H}_j)}{\sigma_j^2} \geq \gamma_j, \quad j = 1, \dots, M, \quad (2.23b)$$

$$\mathbf{X} \succeq \mathbf{0}, \quad (2.23c)$$

$$\text{rank}(\mathbf{X}) = 1. \quad (2.23d)$$

It can be noticed that constraint (2.23b) is affine, (2.23c) is positive semi-definite, but the rank constraint in (2.23d) is non-convex. Thus, the problem of (2.23) is non-convex. However, a convex version is obtained using the SDR technique to drop the non-convex constraint of (2.23d). Consequently, the relaxed problem is given by

$$\min_{\mathbf{X}} \text{tr}(\mathbf{X}) \quad (2.24a)$$

$$\text{s.t.} \quad \frac{\text{tr}(\mathbf{X}\mathbf{H}_j)}{\sigma_j^2} \geq \gamma_j, \quad j = 1, \dots, M, \quad (2.24b)$$

$$\mathbf{X} \succeq \mathbf{0}. \quad (2.24c)$$

### 2.3.3 MMF Optimization Problem

The conventional MMF optimization problem tries to improve the total system performance by maximizing the worst user SNR value given a predetermined transmit power constraint at the BS. Thus improving the whole system performance as specified by the minimum user SNR given a power budget at the system operator. This problem can be formulated as

$$\max_{\mathbf{w}} \min_{j=1, \dots, M} \text{SNR}_j \quad (2.25a)$$

$$\text{s.t.} \quad P \leq P_{\max}, \quad (2.25b)$$

where  $P_{\max}$  is the maximum transmit power at the BS. Making use of the expression derived for the transmit power (2.19) and the user SNR (2.20), the problem of (2.25) can be written as

$$\max_{\mathbf{w}} \min_{j=1, \dots, M} \frac{\text{tr}(\mathbf{w}\mathbf{w}^H \mathbf{H}_j)}{\sigma_j^2} \quad (2.26a)$$

$$\text{s.t.} \quad \text{tr}(\mathbf{w}\mathbf{w}^H) \leq P_{\max}. \quad (2.26b)$$

The optimization problem of (2.26) is NP-hard, thus the SDR technique is employed to obtain an approximate solution. Using the equivalence of (2.22), the optimization problem of (2.26) can be expressed as

$$\max_{\mathbf{X}} \min_{j=1, \dots, M} \frac{\text{tr}(\mathbf{X}\mathbf{H}_j)}{\sigma_j^2} \quad (2.27a)$$

$$\text{s.t.} \quad \text{tr}(\mathbf{X}) \leq P_{\max}, \quad (2.27b)$$

$$\mathbf{X} \succeq \mathbf{0}, \quad (2.27c)$$

$$\text{rank}(\mathbf{X}) = 1. \quad (2.27d)$$

The problem of (2.27) is non-convex. However, it can be solved using the SDR relaxation by dropping the rank constraint in (2.27d). The relaxed problem is given by

$$\max_{\mathbf{X}} \min_{j=1, \dots, M} \frac{\text{tr}(\mathbf{X}\mathbf{H}_j)}{\sigma_j^2} \quad (2.28a)$$

$$\text{s.t.} \quad \text{tr}(\mathbf{X}) \leq P_{\max}, \quad (2.28b)$$

$$\mathbf{X} \succeq \mathbf{0}.$$

The solutions of QoS and MMF problems are equivalent to each other except for a scaling factor [SDL06, GSS<sup>+</sup>10].

The rank of the optimal beamforming solutions obtained using (2.24) and (2.28) is upper bounded by a threshold given by the square root of the number of network users  $M$  [HP10b, HP10a]. On the other hand, the solutions of the optimization problems (2.24) and (2.28) are optimal, when they enjoy a rank equal to one. Unfortunately, when the number of users surpasses  $M = 2$ , the solutions produced by the SDR technique are of rank larger than one, thus they are not optimal [WMS13]. Furthermore, the SDR performance degrades severely for networks with larger number of users.

Many algorithms have addressed the performance degradation of the SDR technique and proposed enhancements, see, e.g., [WM11, AGS10, Loz07, LMS<sup>+</sup>10].

In order to decrease the rank of the solutions to one, rank reduction algorithm [HP10b, HP10a, Pat98] and randomization technique should be devised [LMS<sup>+</sup>10, KSL08a]. Multiple beamforming vectors are generated randomly and scaled to satisfy the problem constraints. The best vector in terms of the problem objective is chosen. The randomization procedure produces feasible beamforming solutions. However, they are generally suboptimal.

Transmit beamforming is combined with space-time coding in plenty of designs to improve the performance degradation of the SDR technique, see for example [JSB02, ZG02, ZG03, LJ05]. A linear-transformation-based beamforming technique is proposed in [JSB02], where the side information of the channel estimates is employed in a convex optimization problem to design the linear beamformer required to transmit the OSTBC matrix. Quasi-orthogonal space-time beamforming is employed rather than OSTBC in [LJ05]. However, the system design is similar to [JSB02]. Based on the mean value of the channel feedback, two dimensional beamformers are designed in [ZG02]. Combining the beamformer with Alamouti [Ala98], has an impact on improving the system performance. A similar design to [ZG02] is suggested in [ZG03], using the second order channel statistics. All the above-mentioned designs [JSB02, ZG02, ZG03, LJ05] consider a simple scenario of a single-user in a MIMO network.

The non-convex term in the QoS problem is approximated using Taylor expansion to obtain a linear optimization problem in [THJ14]. Using the multiplicative update (MU) algorithm to initialize the design of [THJ14], leads to further performance enhancement in [GS15].

In [HS16] the non-convex quadratically constrained quadratic problem is partitioned into multiple sub-optimization problems with a single SNR constraint. Thus, reducing the overall computational complexity in comparison to [GS15].

The performance of all the aforementioned designs degrades as the number of users in the system increases. This is due to the degrees of freedom, which are insufficient to meet the system requirements with large number of users.

## 2.4 Rank Two Transmit Beamforming Technique

The rank two transmit beamforming design was introduced in [WMS13, WSM12, WLAP12] to enhance the performance and the suboptimality of the rank one beamforming approach in the case that a higher rank SDR solution is obtained. Two beamforming vectors can be utilized simultaneously to transmit the Alamouti code in (2.1)

during the transmission time of two symbols. The usage of two beamforming vectors rather than only one as in rank one beamforming approach enhances the system performance. Moreover, the degrees of freedom in the beamformer design are doubled. Thus, slightly more users can be served optimally when the rank of the beamforming matrix does not exceed two.

The QoS problem of rank two transmit beamforming is solved employing the SDR technique. The obtained relaxed optimization problem is identical to rank one optimization problem. The orthogonality of the Alamouti code (see also (2.2)) allows a very simple symbol-by-symbol detection at the end user. Moreover, Alamouti is a full rate code, which maintains the same data rate as in the conventional rank one beamforming approach [Jaf05]. However, when the number of users is larger than eight, the approximate solutions of the SDR technique exhibit a rank larger than two, thus they are not optimal [WMS13]. The Alamouti based transmit beamforming design is illus-

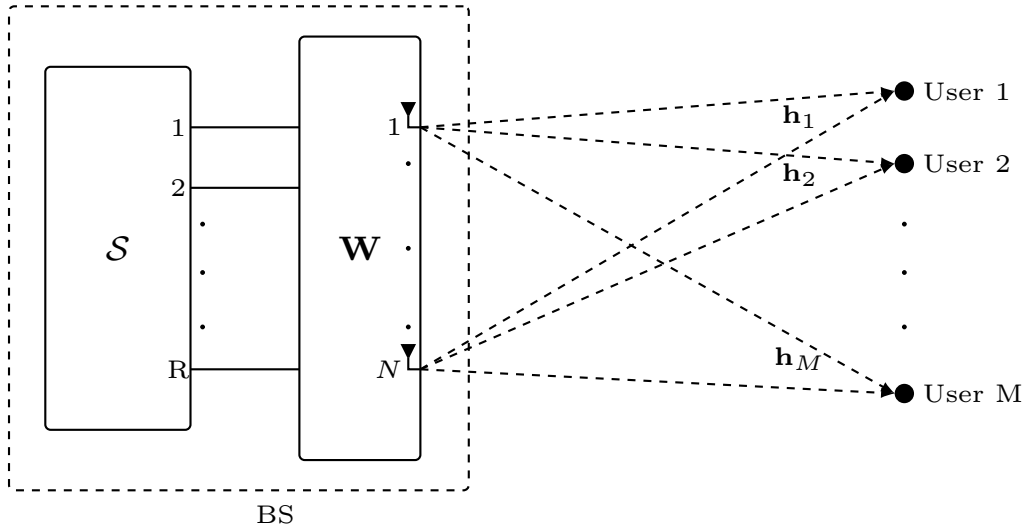


Figure 2.5. System model.

trated in Figure 2.5, where  $R$  is the number of parallel spatial streams corresponding to an individual beamformer used to transmit the encoding matrix  $\mathbf{S}$  in (2.1). For rank two based transmit beamforming,  $R = 2$ , thus two symbols  $s_1$  and  $s_2$  are transmitted during two time slots.

Assume that  $\mathbf{W} \triangleq [\mathbf{w}_1 \ \mathbf{w}_2]$  is the  $N \times 2$  transmit beamforming matrix and the channels are quasi static block fading as in Section 2.2.1.

The signal  $\mathbf{y}_j$  received by the  $j$ th user during the transmission of two time slots is given by

$$\mathbf{y}_j = \mathbf{S}\mathbf{W}^H\mathbf{h}_j + \mathbf{n}_j. \quad (2.29)$$



Assume  $\tilde{\mathbf{h}}_j \triangleq \mathbf{W}^H \mathbf{h}_j = [\mathbf{w}_1^H \mathbf{h}_j \ \mathbf{w}_2^H \mathbf{h}_j]^T$  is the virtual channel of the  $j$ th user,

$$\mathbf{y}_j = \mathbf{S} \tilde{\mathbf{h}}_j + \mathbf{n}_j. \quad (2.30)$$

From the system model in (2.30), it can be concluded that the transmit beamforming system has two virtual antennas. The virtual channels are illustrated in Figure 2.6. Similar steps can be followed as in Section 2.2.1 for the decoding of the symbol vectors

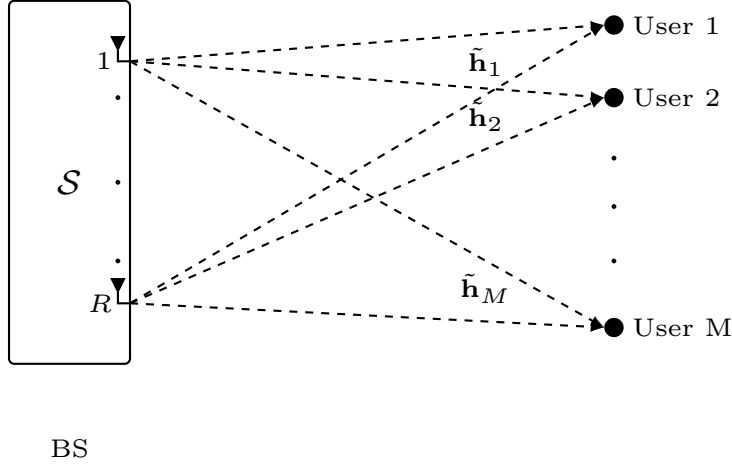


Figure 2.6. System illustration using the virtual channels.

at the users.

### 2.4.1 Optimization Problem

Similar to the rank one design, the total transmit power  $P$  at the serving BS is minimized subject to SNR constraints at each user in the multicasting network.

The transmit power at each time slot at the serving station is given by

$$\begin{aligned} P &\triangleq \mathbb{E}_{s_1, s_2} [\|\mathbf{S}\mathbf{W}^H\|_F^2] \\ &= \mathbb{E}_{s_1, s_2} \left[ \text{tr} \left( (\mathbf{S}\mathbf{W}^H) (\mathbf{S}\mathbf{W}^H)^H \right) \right] \\ &= \text{tr} \left( \mathbb{E}_{s_1, s_2} [\mathbf{W}\mathbf{S}\mathbf{S}^H\mathbf{W}^H] \right) \\ &= \eta \text{tr} (\mathbf{W}\mathbf{W}^H), \end{aligned} \quad (2.31)$$

where the orthogonality property of (2.2) is used and  $\eta$  is a scaling factor such that  $\eta = \mathbb{E}_{s_1, s_2} [|s_1|^2 + |s_2|^2]$ .

Similarly, the SNR constraint at the  $j$ th user is given by

$$\begin{aligned}
\text{SNR}_j &\triangleq \mathbb{E}_{s_1, s_2} \left[ \frac{\| \mathbf{S} \mathbf{W}^H \mathbf{h}_j \|^2_F}{\| \mathbf{n}_j \|^2_F} \right] & (2.32) \\
&= \frac{\mathbb{E}_{s_1, s_2} \left[ \text{tr} \left( (\mathbf{S} \mathbf{W}^H \mathbf{h}_j) (\mathbf{S} \mathbf{W}^H \mathbf{h}_j)^H \right) \right]}{\sigma_j^2} \\
&= \frac{\text{tr} \left( \mathbb{E}_{s_1, s_2} [\mathbf{W} \mathbf{S}^H \mathbf{S} \mathbf{W}^H \mathbf{h}_j \mathbf{h}_j^H] \right)}{\sigma_j^2} \\
&= \eta \frac{\text{tr} (\mathbf{W} \mathbf{W}^H \mathbf{h}_j \mathbf{h}_j^H)}{\sigma_j^2} = \gamma_j,
\end{aligned}$$

where the information matrix  $\mathbf{S}$  and the noise vector  $\mathbf{n}_j$  at user  $j$  are statistically independent.

The QoS optimization problem can be formulated as

$$\min_{\mathbf{w}} \text{tr} (\mathbf{W} \mathbf{W}^H) \quad (2.33a)$$

$$\text{s.t.} \quad \frac{\text{tr} (\mathbf{W} \mathbf{W}^H \mathbf{H}_j)}{\sigma_j^2} \geq \gamma_j, \quad j = 1, \dots, M. \quad (2.33b)$$

The problem of (2.33) is NP-hard. However, the SDR approximation can be employed to obtain a suboptimal solution.

Define

$$\mathbf{X} \triangleq \mathbf{W} \mathbf{W}^H. \quad (2.34)$$

Using the definition of (2.34), assume that

$$\mathbf{X} \Leftrightarrow \mathbf{X} \succeq \mathbf{0} \text{ and } \text{rank}(\mathbf{X}) = 2, \quad (2.35)$$

the optimization problem of (2.33) can be reformulated as

$$\min_{\mathbf{X}} \text{tr} (\mathbf{X}) \quad (2.36a)$$

$$\text{s.t.} \quad \frac{\text{tr} (\mathbf{X} \mathbf{H}_j)}{\sigma_j^2} \geq \gamma_j, \quad j = 1, \dots, M, \quad (2.36b)$$

$$\mathbf{X} \succeq \mathbf{0}, \quad (2.36c)$$

$$\text{rank}(\mathbf{X}) = 2. \quad (2.36d)$$

The problem of (2.36) is non-convex due to the rank constraint of (2.36d). However, a convex problem approximation can be obtained using the SDR technique to drop the non-convex constraint.

The relaxed problem is given by

$$\min_{\mathbf{X}} \quad \text{tr}(\mathbf{X}) \quad (2.37a)$$

$$\text{s.t.} \quad \frac{\text{tr}(\mathbf{X}\mathbf{H}_j)}{\sigma_j^2} \geq \gamma_j, \quad j = 1, \dots, M, \quad (2.37b)$$

$$\mathbf{X} \succeq \mathbf{0}. \quad (2.37c)$$

It can be seen that the problem of (2.37) is identical to the relaxed conventional problem (2.24). However, due to rank two relaxation, the solution is optimal only if it enjoys a rank less or equals to two. If the rank of beamforming solution equals to one, a single beamforming vector  $\mathbf{w}_1$  is employed and  $\mathbf{w}_2$  is assumed to be a vector full of zeros.

Higher rank solutions are obtained for networks with large number of users. It has been proven that rank two beamforming is optimal for a network with maximum eight users [HP10b,HP10a]. Thus, the randomization procedure should be devised [LMS<sup>+</sup>10, KSL08a], which is highly suboptimal.

In the next chapter, various higher rank beamforming designs will be introduced, which mark the main contribution of this thesis. The presented approaches provide general beamforming solutions for single group multicasting networks with relatively large number of users. Each beamforming design has its own merit and contributes to enhance the performance gains in terms of reliability and capacity based on different design aspects, and outperforms the state-of-the-art rank one and rank two techniques in the case of a large number of users in the system.



## Chapter 3

# General Rank Transmit Beamforming

In this chapter, the general rank transmit beamforming designs are introduced, where various STBC codes, namely STTC, OSTBC, real-valued OSTBC and QOSTBC, are combined with beamforming for the scenario of multicasting networks. All the presented approaches are motivated by the degraded performance of rank one and Alamouti based transmit beamforming designs for networks with a large number of users, due to the insufficient degrees of freedom in the beamforming designs.

As mentioned in Chapter 2, the rank of the beamforming solutions is generally larger than two for networks with more than eight users [WMS13]. The concept of rank two transmit beamforming [WMS13, WSM12, WLAP12] is extended using STBC codes. The provided designs increase the degrees of freedom, such that more beamformers can be steered towards the desired users' channels without degrading the system performance. The increased degrees of freedom result in an optimal beamforming design and improved reliability for scenarios with larger number of users.

Moreover, considerable performance gains in terms of BER and achievable data rate are obtained compared with the best known techniques, namely rank one [SDL06] and rank two based beamforming [WMS13].

Through this chapter, CSI of all users is assumed to be available at the serving station and each user has the CSI of its own channel and the beamformer vectors. Moreover, the channels are assumed to be quasi static block fading, i.e., the channels remain constant during the transmission of one block. These assumptions are common and the same as in [WLAP12, WMS13, WSM12].

### 3.1 STTCs Based Transmit Beamforming

A general rank single-group multicast beamforming approach using STTCs is presented in this section, where a BS transmits common information to a group of single-antenna receivers subscribed to the same service. Combining beamforming with STTCs increases the degrees of freedom, which allows serving more users optimally compared with the state-of-the-art rank one and rank two transmit beamforming. STTCs enjoys higher diversity and coding gain. This is due to the redundancy introduced in the channel code and the error correcting properties of STTCs

[Jaf05, VY03, LV06, YLV05, CY05]. Thus, STTCs outperform OSTBCs which only provide diversity gain [ATP98, STC98]. However, STTCs are associated with a significant increase in the decoding complexity.

In the proposed design, STTC is applied to obtain the  $T \times R$  encoding matrix  $\mathbf{S}$ , as illustrated in Figure 2.5. The trellis encoder has been discussed in details in Section 2.2.3.1. The encoded matrix  $\mathbf{S}$  is transmitted over  $T$  time slots. For more details about the encoding and the decoding procedures for STTCs please refer to Section 2.2.3.

Assume that  $\mathbf{W} \triangleq [\mathbf{w}_1, \dots, \mathbf{w}_R]$  is the  $N \times R$  beamforming matrix, hence the  $l$ th column of the code matrix is weighted with beamforming vector  $\mathbf{w}_l$ , which can also be considered as a virtual MIMO antenna from which the STTC code matrix  $\mathbf{S}$  is transmitted to a group of single-antenna users.

The received signal at the  $j$ th user is given by

$$y_j(t) = \sum_{i=1}^R s_i(t) \mathbf{w}_i^H \mathbf{h}_j + n_j(t) \quad t = 1, \dots, T, \quad (3.1)$$

$$j = 1, \dots, M.$$

Using the matrix notation, equation (3.1) can be expressed as

$$\begin{bmatrix} y_j(1) \\ \vdots \\ y_j(T) \end{bmatrix} = \begin{bmatrix} s_1(1) & \cdots & s_R(1) \\ \vdots & \ddots & \vdots \\ s_1(T) & \cdots & s_R(T) \end{bmatrix} \begin{bmatrix} \mathbf{w}_1^H \mathbf{h}_j \\ \vdots \\ \mathbf{w}_R^H \mathbf{h}_j \end{bmatrix} + \begin{bmatrix} n_j(1) \\ \vdots \\ n_j(T) \end{bmatrix}. \quad (3.2)$$

The virtual channel vector corresponding to the  $j$ th user can be defined as

$$\tilde{\mathbf{h}}_j \triangleq \mathbf{W}^H \mathbf{h}_j = [\mathbf{w}_1^H \mathbf{h}_j, \dots, \mathbf{w}_R^H \mathbf{h}_j]^T. \quad (3.3)$$

Assume  $\mathbf{n}_j \triangleq [n_j(1), \dots, n_j(T)]^T$  is additive white Gaussian receiver noise with  $\mathbf{n}_j \sim \mathcal{CN}(\mathbf{0}, \sigma_j^2 \mathbf{I}_T)$  and  $\mathbf{y}_j \triangleq [y_j(1), \dots, y_j(T)]^T$  is the received signal vector at the  $j$ th user, equation (3.2) can be compactly written as

$$\mathbf{y}_j = \mathbf{S} \tilde{\mathbf{h}}_j + \mathbf{n}_j. \quad (3.4)$$

Notice that equation (3.4) is similar to equation (2.30) for the received signal of rank two based beamforming design. However, the dimension of the vectors and matrices is no longer restricted to two and the code matrix  $\mathbf{S}$  is of non-square dimension  $T \times R$ . Moreover, for  $R = 1$ , the system model of the proposed design in equation (3.2) is identical to the conventional system model in (2.18).

### 3.1.1 Optimization Problem

In this section, the optimization problem of the proposed approach is discussed. The MMF design for the general rank transmit beamforming approach is adopted.

The SNR of the received signal of equation (3.4) at the  $j$ th user is denoted by

$$\begin{aligned} \text{SNR}_j &\triangleq \mathbb{E} \left[ \frac{|\mathbf{S}\mathbf{W}^H\mathbf{h}_j|^2}{|\mathbf{n}_j|^2} \right] \\ &= \frac{\text{tr} \left( \mathbb{E} \left[ (\mathbf{S}\mathbf{W}^H\mathbf{h}_j)^H (\mathbf{S}\mathbf{W}^H\mathbf{h}_j) \right] \right)}{\sigma_j^2} \\ &= \frac{\text{tr} \left( \mathbb{E} \left[ \mathbf{h}_j^H \mathbf{W} \mathbf{S}^H \mathbf{S} \mathbf{W}^H \mathbf{h}_j \right] \right)}{\sigma_j^2}, \end{aligned} \quad (3.5)$$

where the information symbols  $s$  and the noise  $n_j$  at user  $j$  are statistically independent.

The symbols generated in each time slot are assumed uncorrelated. Thus, using  $\mathbb{E} [\mathbf{S}^H \mathbf{S}] = \mu \mathbf{I}_R$ , where  $\mu$  is a scaling factor, equation (3.5) can be written similar to equation (2.31).

Similarly, the transmit power at the  $j$ th user is given by equation (2.32)

The general rank MMF optimization problem is expressed by

$$\max_{\mathbf{W}} \min_{j=1, \dots, M} \frac{\text{tr} (\mathbf{W}\mathbf{W}^H \mathbf{H}_j)}{\sigma_j^2} \quad (3.6a)$$

$$\text{s.t.} \quad \text{tr} (\mathbf{W}\mathbf{W}^H) \leq P_{\max}. \quad (3.6b)$$

Using the definition

$$\mathbf{X} \triangleq \mathbf{W}\mathbf{W}^H \quad \Leftrightarrow \quad \mathbf{X} \succeq \mathbf{0} \text{ and } \text{rank} (\mathbf{X}) \leq R, \quad (3.7)$$

where  $R$  is the number of the STTC outputs and the number of virtual antennas as introduced in Section 2.4.

Problem (3.6) can be equivalently written as

$$\max_{\mathbf{X}} \min_{j=1, \dots, M} \frac{\text{tr} (\mathbf{X}\mathbf{H}_j)}{\sigma_j^2} \quad (3.8a)$$

$$\text{s.t.} \quad \text{tr} (\mathbf{W}) \leq P_{\max}, \quad (3.8b)$$

$$\mathbf{W} \succeq \mathbf{0}, \quad (3.8c)$$

$$\text{rank} (\mathbf{W}) \leq R. \quad (3.8d)$$

We observe that (2.27) is a special case of the problem (3.8) when the number of virtual antennas  $R = 1$ .

Similar to Section 2.3, the SDR technique is employed to drop the non-convex rank constraint of (3.8d) and obtain the relaxed convex problem given by

$$\max_{\mathbf{X}} \min_{j=1, \dots, M} \frac{\text{tr}(\mathbf{X}\mathbf{H}_j)}{\sigma_j^2} \quad (3.9a)$$

$$\text{s.t.} \quad \text{tr}(\mathbf{W}) \leq P_{\max}, \quad (3.9b)$$

$$\mathbf{W} \succeq 0. \quad (3.9c)$$

The rank of  $\mathbf{X}$  generally exceeds two for groups with more than 8 users. This leads to the conclusion that the designed approach has a better performance compared with both the rank one [SDL06] and the rank two based beamforming approaches [WMS13].

### 3.1.2 Simulation Results

In the simulation results, a Rayleigh fading channel with independent identical distributed circularly symmetric unit-variance channel coefficients is considered. The BS is assumed to have  $N = 4$  or  $N = 3$  transmit antennas and a maximum transmit power  $P_{\max} = 1$ .

The simulation results are performed for a frame length of  $T = 120$  and number of  $10^4$  Monte-Carlo runs using the QPSK constellations. The proposed approach is compared with the rank two and rank one beamforming designs. Moreover, STTCs based rank two beamforming is considered using the system model in (2.29), where the maximum number of spatial stream equals two. The generator matrices given by

$$\begin{aligned} \mathbf{G}^{(1)} &= \begin{bmatrix} 0 & 2 \\ 2 & 0 \end{bmatrix}, \\ \mathbf{G}^{(2)} &= \begin{bmatrix} 0 & 1 \\ 1 & 0 \end{bmatrix}, \end{aligned} \quad (3.10)$$

are used to obtain the STTC encoder output  $\mathbf{S}$  of the STTC based rank two beamforming approach using the equations (2.9) and (2.11).

The rank one beamforming design is combined with the convolutional code, with a constraint length of 7 and code generator polynomials 171 and 131 in octal, and a code rate of 1/2, which is equal to the code rate of the employed STTC.



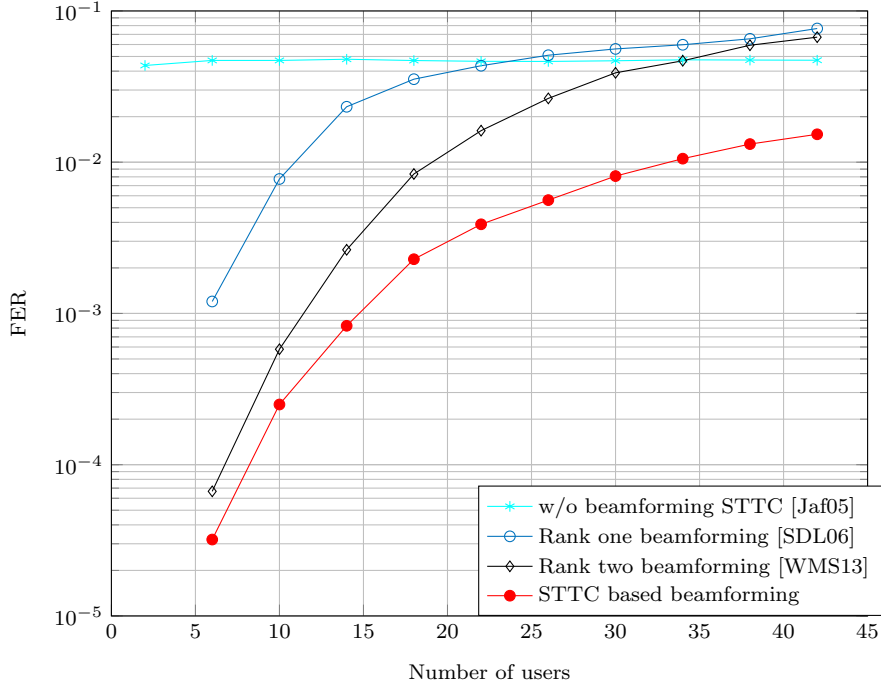


Figure 3.1. System performance of FER with varying number of users for  $N = 3$  transmit antennas and  $\text{SNR} = 20$  dB

A fair comparison to the other existing designs is guaranteed using the frame-error rate (FER) as a performance metric. The FER is defined as the average rate a transmitted code matrix frame  $\mathcal{S}$  is wrongly detected at the receiver side to the total number of frames sent. Figure 3.1 depicts the FER versus the number of users for BS with  $N = 3$  transmit elements and SNR equals to 20 dB. The proposed approach is compared to the performance of STTC described by the generator matrices of (2.12), rank one beamforming combined with convolutional coding, and rank two beamforming combined with STTC with the generator matrices of (3.10). The generator matrices of (2.12) are used for the proposed approach. The chosen STTC code is based on the trace criteria [LV06] to provide the optimal code, which provides coding gain advantage.

As seen from Figure 3.1 the proposed approach has the best performance compared with the state-of-the-art approaches. The performance gains can be explained by the increased degrees of freedom using more spatial streams and the error correction properties of STTCs. Moreover, the performance of rank one and rank two beamforming degrades as the number of users increases.

In Figure 3.2, the spectral efficiency versus the number of users is shown for a BS with  $N = 4$  transmit antennas and a group of  $M = 32$  users. The spectral efficiency equation

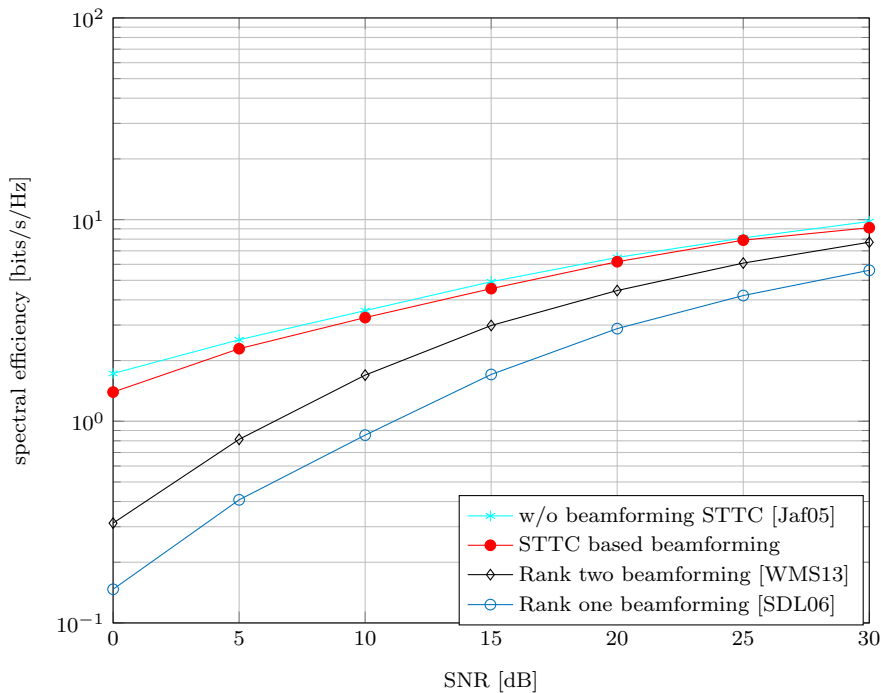


Figure 3.2. System performance of capacity plotted against SNR in dB for  $N = 4$  transmit antennas and  $M = 32$  users

is given by [Jaf05]

$$C = \mathbb{E}_{\mathbf{H}_j} \left[ \log_2 \left( 1 + \frac{1}{N\sigma_j^2} \text{tr}(\mathbf{H}_j) \right) \right]. \quad (3.11)$$

The spectral efficiency of the STTC based beamforming design can be expressed as

$$C = \mathbb{E}_{\mathbf{H}_j} \left[ \log_2 \left( 1 + \frac{1}{N} \text{SNR}_j \right) \right], \quad (3.12)$$

where  $\text{SNR}_j$  is given by equation (3.5). For a fair comparison between all approaches, the spectral efficiency is considered only for the correctly detected frames. It can be observed from Figure 3.2 that the STTC has the best spectral efficiency and outperforms the STTC based beamforming design slightly. Moreover, higher spectral efficiency of the STTC based beamforming design can be achieved compared with rank one and rank two beamforming methods.

In Figure 3.3, the rank of the beamforming solutions versus the number of users is displayed for  $N = 3$  and  $\text{SNR} = 20$  dB. The number of higher rank solutions increases with the number of users, i.e. for a group of  $M = 18$  users approximately 76% of the number of the solutions are either rank one or two and 24% of the solutions are rank three and when  $M = 42$  the rank of the beamforming matrices increases such that 98.5% of the solutions are either of rank two or three, and more than 50% of

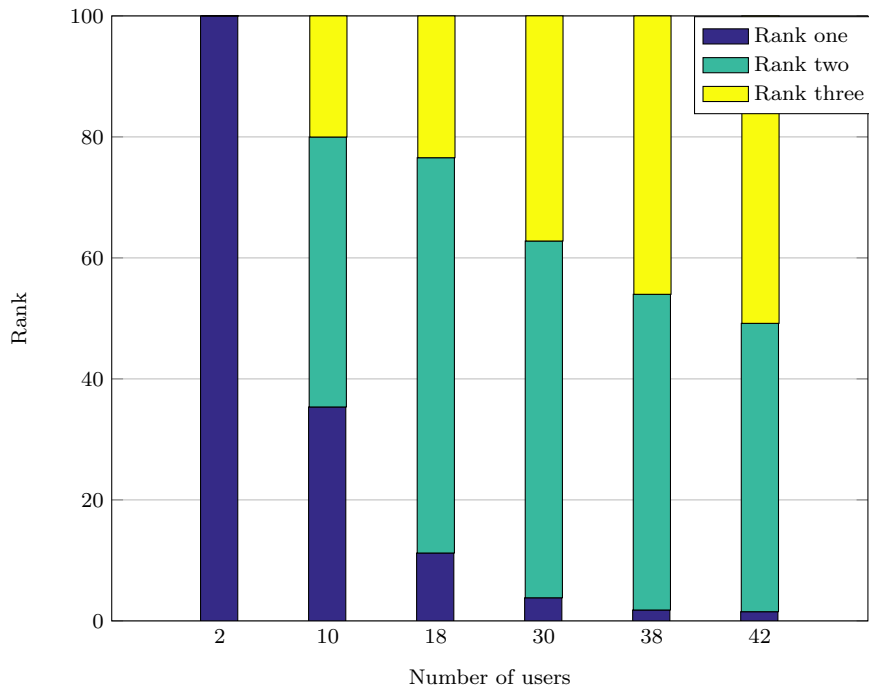


Figure 3.3. Rank percentage of the matrix  $\mathbf{X}$  with varying number of users

the matrices have a rank of three. This implies that the general rank STTCs based beamforming approach provides optimal solutions for networks with large number of users. On the contrary, the performance of the state-of-the-art designs degrades, due to the insufficient degrees of freedom required for the design of the beamforming solutions.

## 3.2 High Order OSTBCs Based Beamforming

In this section, the higher order OSTBCs based beamforming approach is presented. Although the STTCs based beamforming design provides general rank beamforming solutions with higher performance gains for networks of large number of users, such design has high decoding complexity on the users' side. OSTBC codes enjoy a simple one-by-one symbol decoding method. Unfortunately, higher order OSTBCs do not enjoy the full transmission rate property of one symbol per channel use as shown in Section 2.2.2. Assume  $R$  is the rank of the optimal beamforming problem. Let  $R_0$  be an integer given by  $R_0 = \frac{R}{2}$  or  $R_0 = \frac{R+1}{2}$ , then the maximum achievable rate for OSTBC is given by  $L_{\text{OSTBC}} = \frac{R_0+1}{2R_0}$ . For  $R = 4$ , the maximum achievable rate equals  $L_{\text{OSTBC}} = \frac{3}{4}$ . However, the increased number of virtual antennas in the beamforming

design results in better system performance in terms of transmit power or average minimum user SNR. Therefore, rate loss associated with the non-full rate OSTBC based beamforming approach may be compensated by the performance gains in the beamforming design.

The same transmission rate for each approach can be imposed to provide a fair comparison. This can be achieved either by applying in the higher order OSTBC case a channel code with higher rate, or using a larger modulation scheme. A channel code with higher rate is applied to the higher rank beamforming design and lower rate channel code is applied to the compared state-of-the-art approaches.

Assuming  $L_c$  is the rate of the employed channel code and  $b$  is the number of bits per symbol, then the bit rate is given by

$$L = L_{\text{OSTBC}}L_cb. \quad (3.13)$$

When  $L_c = 1$ , i.e., no channel code is employed, a higher modulation scheme is applied to the proposed approach than in the competing designs. Hence, rate penalties can be balanced.

For simplicity of presentation and without loss of generality, we use the code given in Section 2.2.2 for the proposed OSTBC based transmit beamforming approach, where a number of  $K = 3$  symbols  $s_1$ ,  $s_2$ , and  $s_3$  are transmitted during  $T = 4$  time slots. However, other OSTBCs with larger  $K$  and  $T$  can be utilized.

Assume that  $\mathbf{W} \triangleq [\mathbf{w}_1 \ \mathbf{w}_2 \ \mathbf{w}_3 \ \mathbf{w}_4]$  is the  $N \times 4$  transmit beamforming matrix, the channels coefficients are quasi static block fading as in Section 2.2.1, and the symbols are independent in each transmission matrix.

The transmitted signal at the serving BS,  $\mathbf{X}_W$  is given by  $\mathbf{X}_W \triangleq \mathbf{S}\mathbf{W}^H = [\mathbf{x}_1 \ \mathbf{x}_2 \ \mathbf{x}_3 \ \mathbf{x}_4]^T$ , where  $\mathbf{S}$  is given in Section 2.2.2 and

$$\mathbf{x}_1^T \triangleq s_1\mathbf{w}_1^H + s_2\mathbf{w}_2^H + s_3\mathbf{w}_3^H + 0\mathbf{w}_4^H, \quad (3.14)$$

$$\mathbf{x}_2^T \triangleq -s_2^*\mathbf{w}_1^H + s_1^*\mathbf{w}_2^H + 0\mathbf{w}_3^H + s_3\mathbf{w}_4^H, \quad (3.15)$$

$$\mathbf{x}_3^T \triangleq s_3^*\mathbf{w}_1^H + 0\mathbf{w}_2^H - s_1^*\mathbf{w}_3^H + s_2\mathbf{w}_4^H, \quad (3.16)$$

$$\mathbf{x}_4^T \triangleq 0\mathbf{w}_1^H + s_3^*\mathbf{w}_2^H - s_2^*\mathbf{w}_3^H - s_1\mathbf{w}_4^H. \quad (3.17)$$

The signal  $\mathbf{y}_j$  received at the  $j$ th user during four time slots can be written as

$$\begin{bmatrix} y_{j,1} \\ y_{j,2} \\ y_{j,3} \\ y_{j,4} \end{bmatrix} = \begin{bmatrix} s_1 & s_2 & s_3 & 0 \\ -s_2^* & s_1^* & 0 & s_3 \\ s_3^* & 0 & -s_1^* & s_2 \\ 0 & s_3^* & -s_2^* & -s_1 \end{bmatrix} \begin{bmatrix} \mathbf{w}_1^H \mathbf{h}_j \\ \mathbf{w}_2^H \mathbf{h}_j \\ \mathbf{w}_3^H \mathbf{h}_j \\ \mathbf{w}_4^H \mathbf{h}_j \end{bmatrix} + \begin{bmatrix} n_{j,1} \\ n_{j,2} \\ n_{j,3} \\ n_{j,4} \end{bmatrix}. \quad (3.18)$$

The system model of (3.18) can be expressed compactly as in (2.29).

The virtual user channel of the  $j$ th user is given by  $\tilde{\mathbf{h}}_j \triangleq \mathbf{W}^H \mathbf{h}_j = [\mathbf{w}_1^H \mathbf{h}_j \ \mathbf{w}_2^H \mathbf{h}_j \ \mathbf{w}_3^H \mathbf{h}_j \ \mathbf{w}_4^H \mathbf{h}_j]^T = [\tilde{h}_{j,1} \ \tilde{h}_{j,2} \ \tilde{h}_{j,3} \ \tilde{h}_{j,4}]^T$ .

Figure 2.5 illustrates the system model.

Equation (3.18) can also be expressed using the equivalent channel model

$$\tilde{\mathbf{y}}_j = \tilde{\mathbf{H}}_j \tilde{\mathbf{s}} + \tilde{\mathbf{n}}_j, \quad (3.19)$$

where

$$\tilde{\mathbf{y}}_j \triangleq \begin{bmatrix} \text{Re}(y_{j,1}) \\ \text{Im}(y_{j,1}) \\ \text{Re}(y_{j,2}) \\ \text{Im}(y_{j,2}) \\ \text{Re}(y_{j,3}) \\ \text{Im}(y_{j,3}) \\ \text{Re}(y_{j,4}) \\ \text{Im}(y_{j,4}) \end{bmatrix}, \quad \tilde{\mathbf{s}}_j \triangleq \begin{bmatrix} \text{Re}(s_1) \\ \text{Im}(s_1) \\ \text{Re}(s_2) \\ \text{Im}(s_2) \\ \text{Re}(s_3) \\ \text{Im}(s_3) \end{bmatrix}, \quad \tilde{\mathbf{n}}_j \triangleq \begin{bmatrix} \text{Re}(n_{j,1}) \\ \text{Im}(n_{j,1}) \\ \text{Re}(n_{j,2}) \\ \text{Im}(n_{j,2}) \\ \text{Re}(n_{j,3}) \\ \text{Im}(n_{j,3}) \\ \text{Re}(n_{j,4}) \\ \text{Im}(n_{j,4}) \end{bmatrix}, \quad (3.20)$$

and

$$\tilde{\mathbf{H}}_j \triangleq \begin{bmatrix} \text{Re}(\tilde{h}_{j,1}) & -\text{Im}(\tilde{h}_{j,1}) & \text{Re}(\tilde{h}_{j,2}) & -\text{Im}(\tilde{h}_{j,2}) & \text{Re}(\tilde{h}_{j,3}) & -\text{Im}(\tilde{h}_{j,3}) \\ \text{Im}(\tilde{h}_{j,1}) & \text{Re}(\tilde{h}_{j,1}) & \text{Im}(\tilde{h}_{j,2}) & \text{Re}(\tilde{h}_{j,2}) & \text{Im}(\tilde{h}_{j,3}) & \text{Re}(\tilde{h}_{j,3}) \\ \text{Re}(\tilde{h}_{j,2}) & \text{Im}(\tilde{h}_{j,2}) & -\text{Re}(\tilde{h}_{j,1}) & -\text{Im}(\tilde{h}_{j,1}) & \text{Re}(\tilde{h}_{j,4}) & -\text{Im}(\tilde{h}_{j,4}) \\ \text{Im}(\tilde{h}_{j,2}) & -\text{Re}(\tilde{h}_{j,2}) & -\text{Im}(\tilde{h}_{j,1}) & \text{Re}(\tilde{h}_{j,1}) & \text{Im}(\tilde{h}_{j,4}) & \text{Re}(\tilde{h}_{j,4}) \\ -\text{Re}(\tilde{h}_{j,3}) & -\text{Im}(\tilde{h}_{j,3}) & \text{Re}(\tilde{h}_{j,4}) & -\text{Im}(\tilde{h}_{j,4}) & \text{Re}(\tilde{h}_{j,1}) & \text{Im}(\tilde{h}_{j,1}) \\ -\text{Im}(\tilde{h}_{j,3}) & \text{Re}(\tilde{h}_{j,3}) & \text{Im}(\tilde{h}_{j,4}) & \text{Re}(\tilde{h}_{j,4}) & \text{Im}(\tilde{h}_{j,1}) & -\text{Re}(\tilde{h}_{j,1}) \\ -\text{Re}(\tilde{h}_{j,4}) & \text{Im}(\tilde{h}_{j,4}) & -\text{Re}(\tilde{h}_{j,3}) & -\text{Im}(\tilde{h}_{j,3}) & \text{Re}(\tilde{h}_{j,2}) & \text{Im}(\tilde{h}_{j,2}) \\ -\text{Im}(\tilde{h}_{j,4}) & -\text{Re}(\tilde{h}_{j,4}) & -\text{Im}(\tilde{h}_{j,3}) & \text{Re}(\tilde{h}_{j,3}) & \text{Im}(\tilde{h}_{j,2}) & -\text{Re}(\tilde{h}_{j,2}) \end{bmatrix}. \quad (3.21)$$

It can be proven that  $\tilde{\mathbf{H}}_j$  is semi-orthogonal, where  $\tilde{\mathbf{H}}_j^T \tilde{\mathbf{H}}_j = \|\tilde{\mathbf{h}}_j\|_F^2 \mathbf{I}_6$ .

Multiplying both side of equation (3.19) by  $\tilde{\mathbf{H}}_j^T$ , dividing by  $\|\tilde{\mathbf{h}}_j\|_F^2$ , and using the semi-orthogonality property of equivalent channel, the received symbol vector at the  $j$ th user is given by

$$\begin{aligned}\hat{\mathbf{s}} &= \frac{1}{\|\tilde{\mathbf{h}}_j\|_F^2} \tilde{\mathbf{H}}_j^T \tilde{\mathbf{y}}_j \\ &= \mathbf{s} + \hat{\mathbf{n}}_j,\end{aligned}\quad (3.22)$$

where  $\hat{\mathbf{n}}_j \triangleq \frac{1}{\|\tilde{\mathbf{h}}_j\|_F^2} \tilde{\mathbf{H}}_j^T \tilde{\mathbf{n}}_j$ , and

$$\hat{s}_1 \triangleq \frac{\tilde{h}_{j,1}^* y_{j,1} + \tilde{h}_{j,2} y_{j,2}^* - \tilde{h}_{j,3} y_{j,3}^* - \tilde{h}_{j,4}^* y_{j,4}}{|\tilde{h}_{j,1}|^2 + |\tilde{h}_{j,2}|^2 + |\tilde{h}_{j,3}|^2 + |\tilde{h}_{j,4}|^2}, \quad (3.23)$$

$$\hat{s}_2 \triangleq \frac{\tilde{h}_{j,2}^* y_{j,1} - \tilde{h}_{j,1} y_{j,2}^* + \tilde{h}_{j,4}^* y_{j,3} - \tilde{h}_{j,2} y_{j,4}^*}{|\tilde{h}_{j,1}|^2 + |\tilde{h}_{j,2}|^2 + |\tilde{h}_{j,3}|^2 + |\tilde{h}_{j,4}|^2}, \quad (3.24)$$

$$\hat{s}_3 \triangleq \frac{\tilde{h}_{j,3}^* y_{j,1} + \tilde{h}_{j,4}^* y_{j,2} + \tilde{h}_{j,1} y_{j,3}^* + \tilde{h}_{j,2} y_{j,4}^*}{|\tilde{h}_{j,1}|^2 + |\tilde{h}_{j,2}|^2 + |\tilde{h}_{j,3}|^2 + |\tilde{h}_{j,4}|^2}, \quad (3.25)$$

Thus, three symbols can be detected in four time slots at the receiver.

The average transmit power for the OSTBC based transmit beamforming is given by

$$\begin{aligned}P_t &\triangleq \frac{1}{T} \sum_{t=1}^4 \mathbb{E} [\|\mathbf{x}_t\|_F^2] \\ &= \frac{1}{4} \mathbb{E} \left[ \text{tr} \left( (\mathbf{S}\mathbf{W}) (\mathbf{S}\mathbf{W})^H \right) \right] \\ &= \frac{1}{4} \text{tr} \left( \mathbb{E} [\mathbf{W}^H \mathbf{S} \mathbf{S}^H \mathbf{W}] \right) \\ &= \frac{3}{4} \|\mathbf{W}\|_F^2,\end{aligned}\quad (3.26)$$

where the orthogonality property in (2.6) is used such that  $\mathbf{S}\mathbf{S}^H = \mathbb{E} [|s_1|^2 + |s_2|^2 + |s_3|^2] \mathbf{I}_4$ . Equation (3.26) means that the transmit power per time slot is  $\frac{3}{4}$  of the maximum allowed transmit power.

### 3.2.1 Optimization Problem

In this section, the general rank transmit beamforming approach is discussed, where the MMF approach is employed. Hence, the minimum user SNR is maximized subject to the transmit power constraint. The expression for the average transmit power at the

BS is given by equation (2.31), where the properties of trace rotation and orthogonality of the OSTBCs are used. Using the same properties, the SNR constraint at the  $j$ th user is expressed by equation (2.32). The MMF optimization problem is identical to the problem of (3.6).

The same approach is followed to relax the NP-hard problem using the same SDR approximation in (3.7), where  $R = 4$  for this scenario. The same steps are applied here as in (3.8) to drop the non-convex rank constraint and get an approximation problem as given in (3.9).

The problem of (3.9) is identical to the relaxed conventional MMF problem (2.28). However, the problem of (3.9) enjoy optimal solutions for all the beamforming matrices with rank less or equal to four. The beamforming vectors are the principle components of the beamforming solution matrices.

The number of linearly independent principle components of the beamforming solution matrix  $\mathbf{X}$  defines its rank. However, if the rank is smaller than four, then the beamforming matrix  $\mathbf{W}$  is formulated using the obtained principle vectors and the remaining beamforming vectors are set to zero. For example, if the rank of  $\mathbf{X}$  equals two then the matrix  $\mathbf{W}$  has the principle components of  $\mathbf{X}$  in the first two columns, while the second two columns of  $\mathbf{W}$  are set to be zero.

As seen previously, the transmit power is  $P_t = \frac{3}{4}P$ . However, the average available transmit power per block is  $P$ . Thus, the OSTBC matrix  $\mathbf{S}$  is scaled such that  $P_t = \alpha P$ , where  $\alpha = \frac{4}{3}$ .

### 3.2.2 Randomization Procedure

In this section, an extended version of the randomization procedure proposed in [WMS13] for rank one transmit beamforming is presented. When the rank of the beamforming matrix  $\mathbf{X}$  is larger than four, the randomization algorithm is applied to obtain feasible but suboptimal rank four solutions in general.

The randomization Algorithm 1 is run over  $\kappa$  different iterations. For each iteration  $k$ , four beamforming candidates vectors  $\mathbf{w}_1^{(k)}$ ,  $\mathbf{w}_2^{(k)}$ ,  $\mathbf{w}_3^{(k)}$ ,  $\mathbf{w}_4^{(k)}$  are generated using the singular value decomposition of the beamforming solution  $\mathbf{X} = \mathbf{U}\mathbf{S}\mathbf{U}^H$  such that

$$\mathbf{W}^{(k)} \triangleq \mathbf{U}\mathbf{S}^{1/2}\mathbf{E}^{(k)}, \quad (3.27)$$

where the  $N \times 1$  vectors  $\mathbf{E}^{(k)} \triangleq [\mathbf{e}_1^{(k)}, \dots, \mathbf{e}_4^{(k)}]$  are randomly generated with independent circularly white Gaussian distribution. The beamforming candidate matrix  $\mathbf{W}^{(k)} \triangleq [\mathbf{w}_1^{(k)} \ \mathbf{w}_2^{(k)} \ \mathbf{w}_3^{(k)} \ \mathbf{w}_4^{(k)}]$  is normalized such that  $\|\mathbf{W}^{(k)}\|_F = \sqrt{P}$ . The candidate beamforming matrix, which yields the largest minimum user SNR over  $\kappa$  cycles is selected.

**Algorithm 1:** The randomization technique

<p><b>Input:</b> <math>U, \kappa, M, \sigma_j, \mathbf{H}_j, j = 1, \dots, M</math></p> <p><b>begin</b></p> <p>1    <b>for</b> <math>k \in \{1, \dots, \kappa\}</math> <b>do</b></p> <p>2        Generate <math>\mathbf{e}_1^{(k)}, \dots, \mathbf{e}_4^{(k)}</math> with independent circularly white Gaussian distribution.</p> <p>3        Generate <math>\mathbf{w}_1^{(k)}, \mathbf{w}_2^{(k)}, \mathbf{w}_3^{(k)}</math>, and <math>\mathbf{w}_4^{(k)}</math> using equation (3.27).</p> <p>4        Set <math>\mathbf{W}^{(k)} \triangleq [\mathbf{w}_1^{(k)} \ \mathbf{w}_2^{(k)} \ \mathbf{w}_3^{(k)} \ \mathbf{w}_4^{(k)}]</math> and scale <math>\ \mathbf{W}^{(k)}\ _F</math> to <math>\sqrt{P}</math>.</p> <p>      <b>end</b></p> <p>5        <math>k^* = \arg \max_{k=1, \dots, \kappa} \min_{j=1, \dots, M} \left\{ \frac{\text{tr}(\mathbf{W}^{(k)} \mathbf{W}^{(k)H} \mathbf{H}_j)}{\sigma_j^2} \right\}</math>.</p> <p>6        Set <math>\mathbf{W} \triangleq [\mathbf{w}_1^{(k^*)} \ \mathbf{w}_2^{(k^*)} \ \mathbf{w}_3^{(k^*)} \ \mathbf{w}_4^{(k^*)}]</math>.</p> <p>      <b>end</b></p> <p>      <b>return</b> <math>\mathbf{W}</math>.</p>
--

### 3.2.3 Simulation Results

In this subsection, the same assumptions regarding the network channels are made as in Section 3.1.2. The BS is equipped with  $N = 6$  transmit elements, and a maximum transmit power  $P_{\max} = 1$ . A fair comparison between the proposed design and the state-of-the-art designs is guaranteed using the same transmit power and the same rate for each approach. The randomization procedure of Algorithm 1 is carried out for  $\kappa = 1000$  cycles.

The BER is used as the performance metric. In the simulation results, "Method [SDL06]" refers to the rank one transmit beamforming, using the randomization procedure in [SDL06] for three candidate vectors in each iteration. "Method [WMS13]" refers to Alamouti based transmit beamforming using the randomization procedure in as specified in [WMS13].

In Figure 3.4, the same bit rate of  $L = 3$  bpcu is provided for each approach assuming no channel codes  $L_c = 1$ , using phase shift keying (PSK) 8-PSK modulation for Method



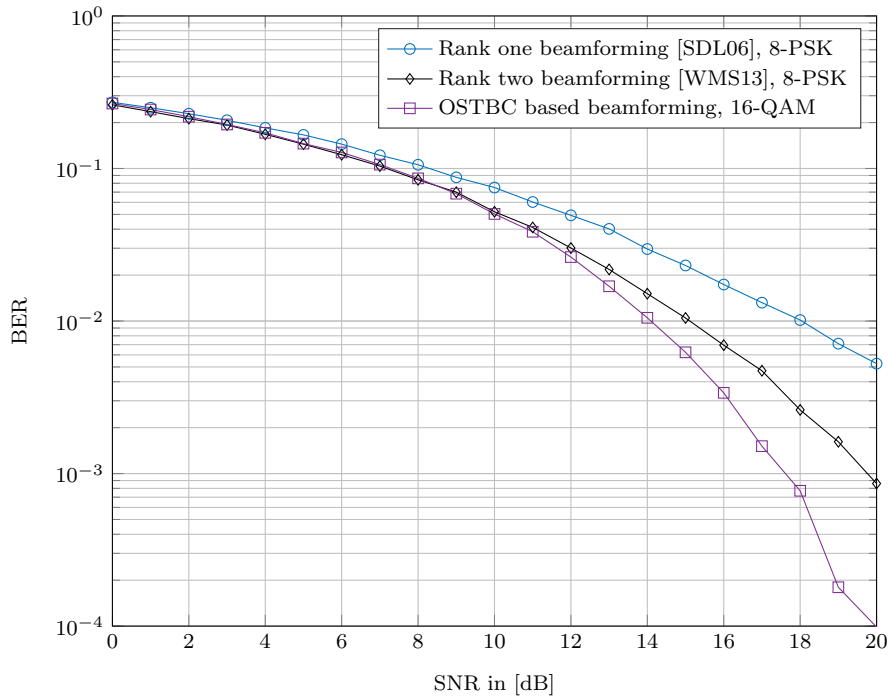


Figure 3.4. System performance of BER plotted against SNR in dB for bit rate of  $L = 3$  bpcu,  $N = 6$  transmit antennas and  $M = 64$  users

[SDL06] and Method [WMS13] and quadrature amplitude modulation (QAM) 16-QAM for the proposed approach. Furthermore, a system with a single group of  $M = 64$  users is assumed.

The rank one beamforming approach performs significantly worse than the other approaches. Although Method [WMS13] and the proposed approach use different modulation schemes, they perform equally well up to an SNR of 10 dB. For SNR values exceeding 10 dB, the proposed approach performs gradually better compared with the state-of-the-art approaches.

In Figure 3.5, different modulation schemes are employed to provide the same transmission rate of  $L = 3$  bpcu for all approaches. The SNR is assumed to be equal to 13 dB. Figure 3.5 depicts the average BER versus the number of users. For groups with small number of users, Method [WMS13] 8-PSK performs best. However, the proposed 16-QAM approach has larger rank, thus shows better results for scenarios with more than 12 users, where the degrees of freedom in the beamforming design are insufficient to serve the users using only two beamformers as in Method [WMS13]. The rank one approach [SDL06] shows the worst performance compared to the other approaches.

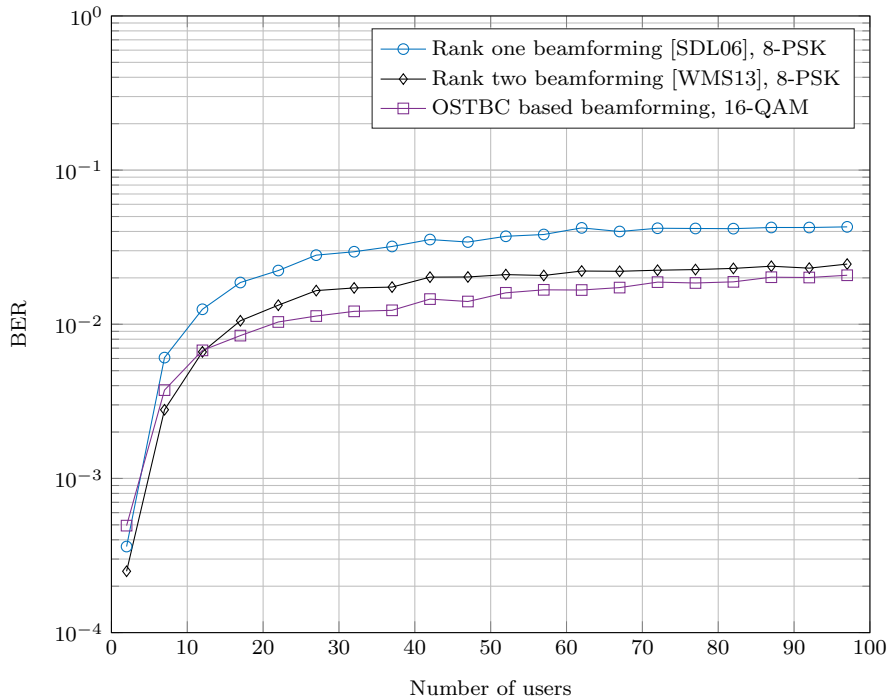


Figure 3.5. System performance of BER with varying number of Users for  $N = 6$  transmit antennas and  $\text{SNR} = 13$  dB

We observe that the OSTBCs based beamforming approach has much better over-all performance in terms of BER compared to the state-of-the-art approaches especially for higher SNRs.

The histogram in Figure 3.6 displays the rank of the beamforming solution  $\mathbf{X}$  versus the number of users. The simulation has been performed over 300 different Monte-Carlo runs for a fixed SNR of 10 dB. The simulation results show that the probability to obtain solutions  $\mathbf{X}$  of rank one or rank two is very high for scenarios with smaller numbers of users. However, the probability to obtain higher rank solutions drastically increases with increasing the numbers of users, while the probability for smaller rank solution decreases. As previously mentioned, the proposed approach provides optimal solutions up to rank four. Higher order OSTBCs with larger  $K$  and  $T$  can be utilized to obtain  $K$  spatial streams. Meanwhile, the drop of the code rate can be compensated using channel code or higher constellation scheme. However, it is only possible to obtain optimal beamforming matrices up to a rank two using the method of [WMS13]. Therefore, the proposed OSTBCs based beamforming approach performs better than the state-of-the-art beamforming designs in wireless networks with larger number of users as the beamforming solutions are more likely to exhibit higher rank.

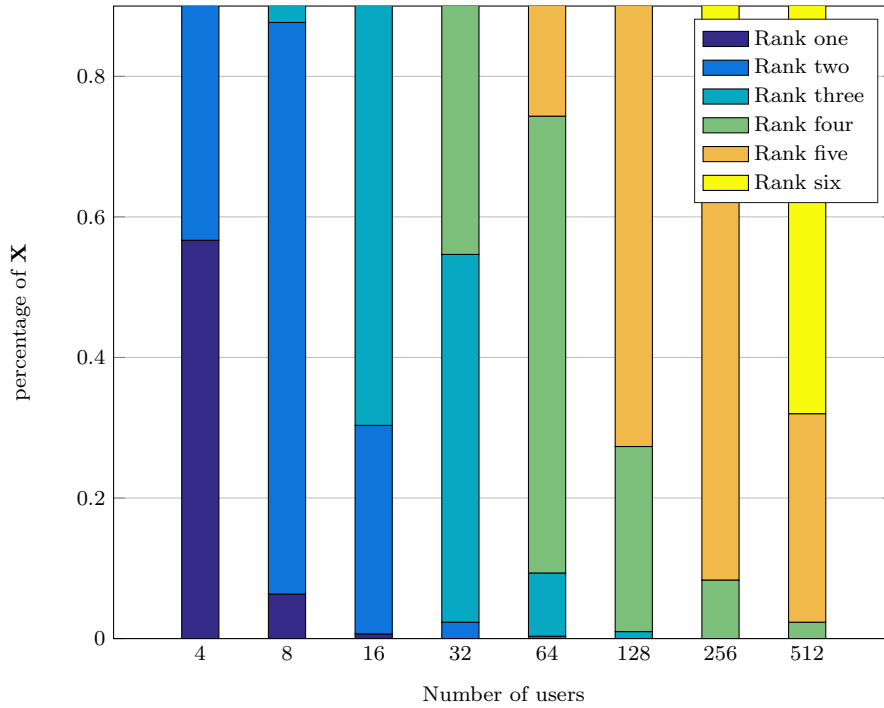


Figure 3.6. Rank percentage of the matrix  $\mathbf{X}$  with varying number of users and  $N = 6$  transmit antennas

### 3.3 Real-valued OSTBCs Based Beamforming

In this Section, the problem of insufficient degrees of freedom in single group multicasting networks is addressed and general rank beamforming solutions are provided. It has been shown in Section 3.2 that OSTBCs based beamforming provides higher rank beamforming solutions, however the design does not enjoy full code rate. The proposed approach in this section provides full rate code using the real-valued OSTBCs. The quality of service optimization problem is solved and the beamforming solutions are combined with the proposed OSTBC. Similar to OSTBCs, real-valued OSTBCs provides simple symbol-by-symbol decoding to efficiently retrieve the transmitted information at each network user.

The simple decoding scheme at the receivers, is combined with an increased BER performance compared with the state-of-the-art designs as will be illustrated in the simulation results shown in Section 3.5.

Denote  $\mathbf{s}$  as the  $R \times 1$  real-valued transmit symbol vector. For simplicity of presentation, but without loss of generality, the OSTBC with order equals to 4 will be considered, such that  $R = 4$  and  $\mathbf{s} = [s_1 \ s_2 \ s_3 \ s_4]^T$ .

The OSTBC matrix is given by

$$\mathbf{S} \triangleq \begin{bmatrix} s_1 & s_2 & s_3 & s_4 \\ -s_2 & s_1 & -s_4 & s_3 \\ -s_3 & s_4 & s_1 & -s_2 \\ -s_4 & -s_3 & s_2 & s_1 \end{bmatrix}. \quad (3.28)$$

Note that the transmitted matrix is orthogonal, hence  $\mathbf{S}^T \mathbf{S} = (|s_1|^2 + |s_2|^2 + |s_3|^2 + |s_4|^2) \mathbf{I}_4$ .

As illustrated in Figure 2.5, the OSTBC matrix  $\mathbf{S}$  is transmitted to the users using  $N \times R$  beamforming matrix  $\mathbf{W}$ . The received signal at the  $j$ th user is given by (2.30).

### 3.3.1 Optimization Problem

A similar approach is followed here as in Section 3.2 to design the beamforming vectors, which will act as virtual antennas from which the real-valued OSTBC is transmitted. The QoS beamforming problem is considered. The beamformers are optimized such that the transmit power  $P$  is minimized given the SNR constraints for each user [SDL06].

The average transmit power is given by equation (2.31), where the orthogonality property of OSTBC  $\mathbf{S}^T \mathbf{S} = \mu \mathbf{I}_4$  is employed, where  $\mu = (|s_1|^2 + |s_2|^2 + |s_3|^2 + |s_4|^2)$ .

The SNR at each user  $j$  is computed according to equation (2.32).

Hence, the OSTBCs based beamforming optimization problem can be formulated similar to the rank two beamforming problem of (2.33).

The problem of (2.33) is NP-hard. Therefore, the semi-definite relaxation technique is employed to obtain a generally suboptimal solution [SDL06, WMS13, WSM12, WLAP12, LWTP15, WXH<sup>+</sup>17, TAP15, TLP16, STPS17].

The same equivalence of (3.7) is used for  $R = 4$  and substituted in (2.33) to obtain a problem as formulated in

$$\min_{\mathbf{X}} \quad \text{tr}(\mathbf{X}) \quad (3.29a)$$

$$\text{s.t.} \quad \text{tr}(\mathbf{X} \mathbf{H}_j) \geq \gamma_j \sigma_j^2, \quad j = 1, \dots, M,$$

$$\mathbf{X} \succeq \mathbf{0},$$

$$\text{rank}(\mathbf{X}) = R. \quad (3.29b)$$

In problem (3.29) the rank constraint is non-convex, thus a relaxed version of the optimization problem is obtained by neglecting the constraint. The resulted problem is identical to rank two problem of (2.37).

An optimal solution  $\mathbf{X}$  of problem (3.29) has a rank equal to  $R$ . However, if the rank is larger than  $R$ , the rank reduction technique [HP10b, HP10a] and the randomization technique [SDL06] are devised to yield beamforming solutions with the desired rank.

The randomization procedure followed for this approach is similar to the one applied in Section 3.2.2.

### 3.4 Detection Method

Using Equation (3.3), the equivalent channel  $\tilde{\mathbf{h}}_j$  for  $R = 4$  of the  $j$ th user is given by

$$\tilde{\mathbf{h}}_j = [\tilde{h}_{j,1} \ \tilde{h}_{j,2} \ \tilde{h}_{j,3} \ \tilde{h}_{j,4}]^T, \quad (3.30)$$

where  $\tilde{\mathbf{h}}_j \triangleq \mathbf{W}^H \mathbf{h}_j = [\mathbf{w}_1^H \mathbf{h}_j \ \mathbf{w}_2^H \mathbf{h}_j \ \mathbf{w}_3^H \mathbf{h}_j \ \mathbf{w}_4^H \mathbf{h}_j]^T = [\tilde{h}_{j,1} \ \tilde{h}_{j,2} \ \tilde{h}_{j,3} \ \tilde{h}_{j,4}]^T$ .

Equation (3.4) represents the received signal at the  $j$ th user, thus can be expressed in matrix using (3.30) and (3.28) by

$$\begin{bmatrix} y_{j,1} \\ y_{j,2} \\ y_{j,3} \\ y_{j,4} \end{bmatrix} = \begin{bmatrix} s_1 & s_2 & s_3 & s_4 \\ -s_2 & s_1 & -s_4 & s_3 \\ s_3 & s_4 & s_1 & -s_2 \\ -s_4 & -s_3 & s_2 & s_1 \end{bmatrix} \begin{bmatrix} \tilde{h}_{j,1} \\ \tilde{h}_{j,2} \\ \tilde{h}_{j,3} \\ \tilde{h}_{j,4} \end{bmatrix} + \begin{bmatrix} n_{j,1} \\ n_{j,2} \\ n_{j,3} \\ n_{j,4} \end{bmatrix}. \quad (3.31)$$

The equivalent received signal model is written as

$$\begin{bmatrix} y_{j,1} \\ y_{j,2} \\ y_{j,3} \\ y_{j,4} \end{bmatrix} = \begin{bmatrix} \tilde{h}_{j,1} & \tilde{h}_{j,2} & \tilde{h}_{j,3} & \tilde{h}_{j,4} \\ \tilde{h}_{j,2} & -\tilde{h}_{j,1} & \tilde{h}_{j,4} & -\tilde{h}_{j,3} \\ \tilde{h}_{j,3} & -\tilde{h}_{j,4} & -\tilde{h}_{j,1} & \tilde{h}_{j,2} \\ \tilde{h}_{j,4} & \tilde{h}_{j,3} & -\tilde{h}_{j,2} & -\tilde{h}_{j,1} \end{bmatrix} \begin{bmatrix} s_1 \\ s_2 \\ s_3 \\ s_4 \end{bmatrix} + \begin{bmatrix} n_{j,1} \\ n_{j,2} \\ n_{j,3} \\ n_{j,4} \end{bmatrix}. \quad (3.32)$$

Assume

$$\tilde{\mathbf{H}}_j = \begin{bmatrix} \tilde{h}_{j,1} & \tilde{h}_{j,2} & \tilde{h}_{j,3} & \tilde{h}_{j,4} \\ \tilde{h}_{j,2} & -\tilde{h}_{j,1} & \tilde{h}_{j,4} & -\tilde{h}_{j,3} \\ \tilde{h}_{j,3} & -\tilde{h}_{j,4} & -\tilde{h}_{j,1} & \tilde{h}_{j,2} \\ \tilde{h}_{j,4} & \tilde{h}_{j,3} & -\tilde{h}_{j,2} & -\tilde{h}_{j,1} \end{bmatrix}. \quad (3.33)$$

Using (3.33), equation (3.32) can be written as in (2.30).

For the simplicity of presentation, assume that  $a = \tilde{h}_{j,1}$ ,  $b = \tilde{h}_{j,2}$ ,  $c = \tilde{h}_{j,3}$  and  $d = \tilde{h}_{j,4}$ . Notice that  $\tilde{\mathbf{H}}^H \tilde{\mathbf{H}}_j$  is written as

$$\tilde{\mathbf{H}}^H \tilde{\mathbf{H}}_j = \begin{bmatrix} a^* & b^* & c^* & d^* \\ b^* & -a^* & -d^* & c^* \\ c^* & d^* & -a^* & -b^* \\ d^* & -c^* & b^* & -a^* \end{bmatrix} \begin{bmatrix} a & b & c & d \\ b & -a & d & -c \\ c & -d & -a & b \\ d & c & -b & -a \end{bmatrix}, \quad (3.34)$$

which is equal to

$$\begin{bmatrix} |a|^2+|b|^2+|c|^2+|d|^2 & a^*b-b^*a-c^*d+d^*c & a^*c+b^*d-ac^*-bd^* & a^*d-b^*c+bc^*-ad^* \\ ab^*-a^*b-cd^*+c^*d & |a|^2+|b|^2+|c|^2+|d|^2 & b^*c-a^*d+ad^*-bc^* & b^*d+a^*c-bd^*-ac^* \\ ac^*+bd^*-a^*c-b^*d & bc^*-ad^*+a^*d-b^*c & |a|^2+|b|^2+|c|^2+|d|^2 & c^*d-cd^*-a^*b+ab^* \\ ad^*-bc^*+b^*c-a^*d & bd^*+ac^*-b^*d-a^*c & cd^*-c^*d-ab^*+a^*b & |a|^2+|b|^2+|c|^2+|d|^2 \end{bmatrix}. \quad (3.35)$$

Using the property of  $x - x^* = 2\text{Im}(x)$ , (3.35) can be simplified to

$$\begin{bmatrix} |a|^2+|b|^2+|c|^2+|d|^2 & 2\text{Im}(a^*b)+2\text{Im}(d^*c) & 2\text{Im}(a^*c)+2\text{Im}(b^*d) & 2\text{Im}(a^*d)+2\text{Im}(b^*c) \\ 2\text{Im}(ab^*)+2\text{Im}(c^*d) & |a|^2+|b|^2+|c|^2+|d|^2 & 2\text{Im}(b^*c)+2\text{Im}(ad^*) & 2\text{Im}(b^*d)+2\text{Im}(a^*c) \\ 2\text{Im}(ac^*)+2\text{Im}(bd^*) & 2\text{Im}(bc^*)+2\text{Im}(a^*d) & |a|^2+|b|^2+|c|^2+|d|^2 & 2\text{Im}(c^*d)+2\text{Im}(ab^*) \\ 2\text{Im}(ad^*)+2\text{Im}(b^*c) & 2\text{Im}(bd^*)+2\text{Im}(ac^*) & 2\text{Im}(cd^*)+2\text{Im}(a^*b) & |a|^2+|b|^2+|c|^2+|d|^2 \end{bmatrix}. \quad (3.36)$$

From (3.36), the virtual channel matrix given in (3.33) satisfies

$$\text{Re} \left( \tilde{\mathbf{H}}^H \tilde{\mathbf{H}} \right) = \alpha \mathbf{I}_4, \quad (3.37)$$

where  $\alpha$  is a scalar variable.

Multiplying both sides of the equivalence channel model as in equation (2.30) by  $\tilde{\mathbf{H}}^H$  and using the property of (3.37), the received symbols can be decoded under the observation that  $\mathbf{s}$  is real-valued using

$$\hat{\mathbf{s}} = \text{Re} \left( \tilde{\mathbf{H}}^H \mathbf{y}_j / \alpha \right). \quad (3.38)$$

It can be observed from equation (3.38) that the detection at the user side is done in symbol-by-symbol manner. Hence, the detection complexity is equivalent to the conventional OSTBC schemes.

### 3.5 Simulation results

A BS with  $N = 6$  and a single group multicasting network with  $M = 64$  users is considered. The real-valued symbols used for OSTBC code at the transmitter side are given by  $\mathbf{s} = \sqrt{\frac{1}{5}}[-3 \quad -1 \quad 1 \quad 3]^T$ , where the averaged symbol energy equals to one.

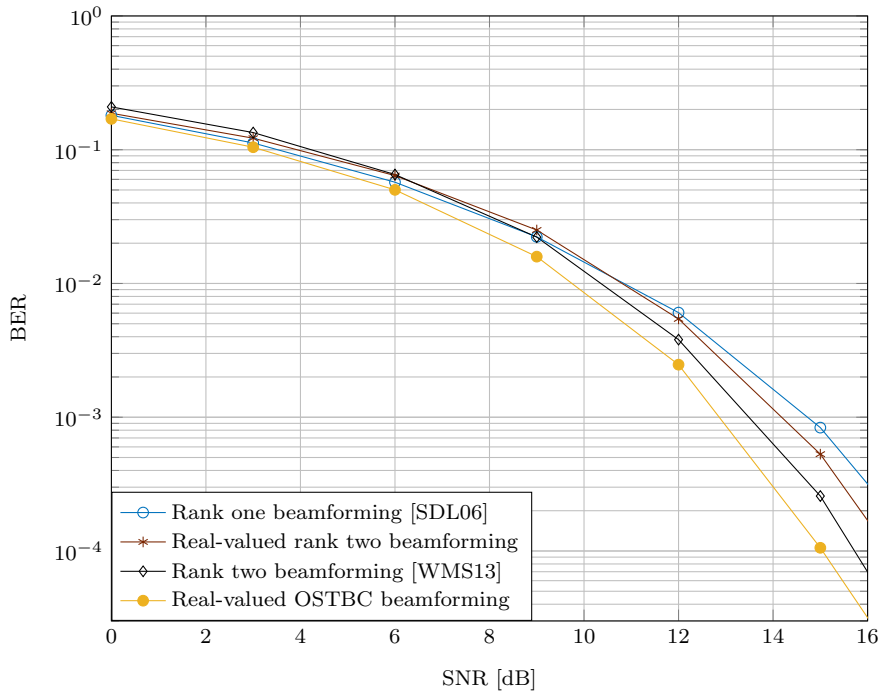


Figure 3.7. System performance of BER plotted against SNR in dB for  $N = 6$  transmit antennas and  $M = 64$  users

The transmit power for each approach is scaled to be one to guarantee a fair comparison between them all. The simulation results are averaged over  $10^6$  Monte-Carlo runs.

In Figure 3.7, the performance of the real-valued OSTBC based beamforming approach in terms of the BER versus the SNR is compared with the performance of Alamouti based rank two beamforming [WMS13, WSM12, WLAP12], rank one beamforming design [SDL06] and Alamouti based rank two beamforming using real-valued symbols. For rank one and rank two beamforming the transmitted symbols are QPSK modulated.

It can be observed that rank one beamforming has comparatively the worst performance for a large number of network users. It can be also seen that the proposed approach outperforms rank one and rank two beamforming designs, e.g., for  $\text{BER} = 10^{-3}$  the proposed approach performs approximately 1 dB better than the rank two based design of [WMS13]. Moreover, rank two beamforming approach using real-valued symbols has a performance, which is worse than rank two beamforming using complex constellations symbols.

Table 3.1 displays the percentage rank of  $\mathbf{X}$  using a number of Monte-Carlo runs equals to 100,  $N = 6$  and  $\gamma_j = \text{SNR}_j$  at each user.

Rank \ SNR[dB]	0	3	6	9	12	15	18	21
1	0	0	0	0	0	0	0	0
2	0	0	0	0	0	0	0	0
3	43	44	45	47	44	45	45	46
4	56	55	54	52	55	54	55	53
5	1	1	1	1	1	1	0	1

Table 3.1. The rank percentage obtained from QoS problem for  $N = 6$  transmit antennas and  $M = 64$  users

It can be noticed that most of the solutions are either of rank equals to 3 or rank equals to 4 for different SNR values. Moreover, the rank of the solutions is distributed approximately uniformly over all SNR values. This can be explained by the fixed number of users  $M = 64$  for this simulation, which keeps the number of degrees of freedom unchanged for different values of SNR.

In the next set of simulations, the number of users is changed considering the  $\text{SNR}_j = 12$  dB at each user. Figure 3.8 demonstrates the BER versus the number of users for the proposed approach, real-valued rank two beamforming, rank two beamforming design [WMS13, WSM12, WLAP12] and rank one beamforming design [SDL06]. It can be observed that rank one and rank two beamforming approaches have the best performance in terms of BER for a number of users equals to two. As the number of users increases to 8, the performance of rank one beamforming decreases, because the rank of beamforming solutions increases as can be observed from Table 3.2. Both rank one and rank two beamforming designs perform better than the proposed approach and real-valued rank two beamforming for relatively small number of users because of the complex modulated constellations employed in rank one and rank two designs. However, as the number of users increases, the proposed approach starts to deliver better results than the state-of-the-art designs. It can be observed that for the number of users exceeding approximately 40, the number of degrees of freedom is not sufficient for the rank two beamforming design, thus the proposed approach performs better. The real-valued rank two beamforming approach performs worse than the rank two beamforming approach for each simulation scenario. The performance loss can be easily explained by the real-valued constellations. For a number of users exceeding approximately 50, real-valued rank two beamforming performs better than rank one beamforming design.

Table 3.2 displays the rank of the beamforming solutions of problem (3.29) for different numbers of users using a number of Monte-Carlo runs equals to 100 and  $\gamma_j = 12$  dB



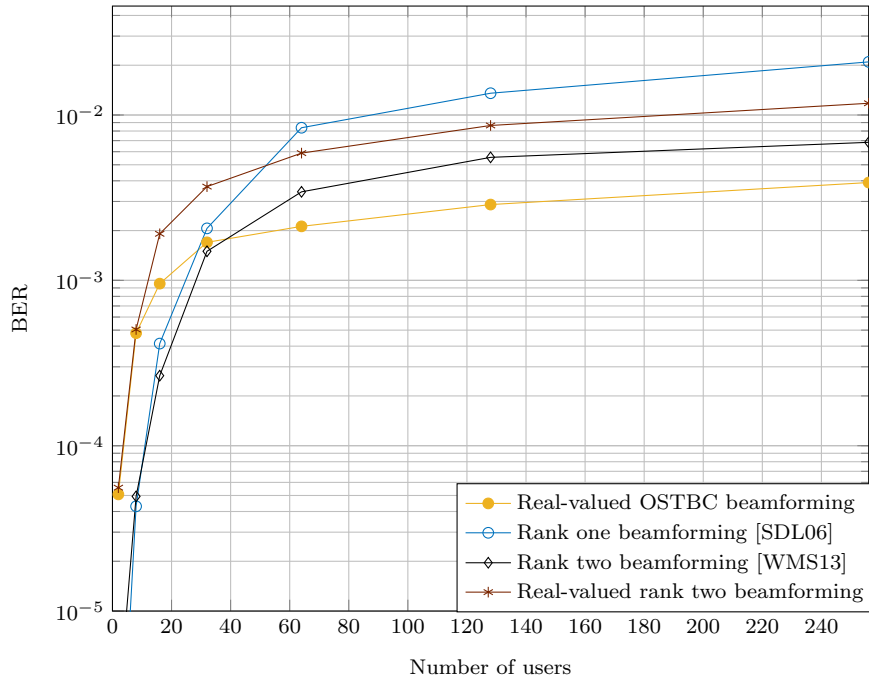


Figure 3.8. System performance of BER with varying number of users for  $N = 6$  transmit antennas and  $\text{SNR} = 12$  dB

at each user. It can be observed that the rank increases by increasing the number of users. For  $M = 2$  all beamforming solutions have a rank of one. As the number of users increases to 8 the rank of the most of the beamforming solutions is increased to 2. For  $M = 64$  most of the beamforming solutions are of rank equals to 3 or 4, which explains the improved performance of our approach as compared to the state-of-the-art designs.

## 3.6 STBCs Based Beamforming

In this section, the general rank beamforming problem for single group multicasting networks is introduced from a new perspective. The optimization problem is designed based on a different criterion compared with the conventional optimization problems. In order to further increase the degrees of freedom and enjoy a full rate code, STBC is employed, which is non-orthogonal in general. The simple decoding property of symbol-wise detection of the OSTBCs is sacrificed in the designed approach. The symbol-wise post detection SNR, which is devised to assess the users' QoS in the rank one and rank two beamforming is no longer meaningful. Thus, an alternative design criterion to measure the performance of a beamforming matrix is employed. In the STBC based

M \ Rank	Rank					
	1	2	3	4	5	6
2	100	0	0	0	0	0
8	32	68	0	0	0	0
16	3	82	15	0	0	0
32	0	11	83	6	0	0
64	0	1	49	50	0	0
128	0	0	1	79	19	1
256	0	0	0	24	70	6

Table 3.2. The rank percentage obtained from QoS problem for  $N = 6$  transmit antennas and SNR= 12 dB

beamforming design, the worst user's Euclidean distance of the decision region is maximized instead of maximizing the worst user's SNR. Thus, the worst user's PEP is minimized for a given transmit power constraint at the serving BS. Therefore, a modified max-min fair (MMMF) optimization problem is formulated. However, the resulting problem is non-convex and NP-hard. An iterative inner approximation algorithm is employed to solve the problem. At each iteration, a first-order Taylor approximation is devised to linearize the non-convex quadratically constrained quadratic program. The approximate problem is convex and can be solved efficiently. The proposed design can be applied to any STBC non-orthogonal code. The simulation results depict better performance than the state-of-the-art methods in terms of the FER, especially for systems with a large number of users.

Consider a wireless single group multicasting network, where a BS applies STBC to obtain the  $T \times R$  code matrix  $\mathbf{S} \in \mathcal{K}_{\mathcal{P}}$ , where  $\mathcal{K}_{\mathcal{P}}$  is the set of STBC matrices of cardinality  $\mathcal{P}$ . The STBC matrix  $\mathbf{S}$  is multicasted to all the users in a specific service area using the  $N \times R$  beamforming matrix  $\mathbf{W} \triangleq [\mathbf{w}_1, \dots, \mathbf{w}_R]$ .  $R$  beamformers are considered assuming  $R > 2$ . Therefore, the degrees of freedom in the beamforming design is increased, which allows to accommodate a large number of constraints in the proposed beamforming design, thus a large number of users in the network system.

The corresponding system model is shown in Figure 2.5, which is the same as all the proposed general rank beamforming designs.

The  $T \times 1$  received signal  $\mathbf{y}_j$  at the  $j$ th user is given by (2.30). The beamforming matrix  $\mathbf{W}$  at the serving BS is designed to minimize the pairwise error probability of the worst user given a total transmit power constraint, as discussed in the next section.

### 3.6.1 Optimization Problem

A general STBC is employed in the proposed general rank beamforming design, which is generally non-orthogonal but enjoys full rate. The use of a non-orthogonal STBC yields more decoding complexity at the receiver compared with the Alamouti based beamforming design, where the orthogonality enables the receivers to apply a simple symbol-by-symbol detector. Thus, a vector-wise detector is devised at the receivers. Moreover, the symbol-wise post-detection SNR expressions used in the state-of-the-art designs to validate the QoS requirements at the receiver are no longer meaningful in the non-orthogonal STBC based beamforming. Alternatively, the proposed approach is designed based on the PEP expression, which is a valid metric for any STBC to evaluate the vector-wise decoding performance.

First the PEP expression is given at a specific user, then the worst user's PEP is employed as the objective of the beamforming optimization problem.

Assuming a known CSI at the  $j$ th user, the conditional PEP using maximum-likelihood decoding is given by [Jaf05]

$$\begin{aligned} \text{PEP} &= \Pr(\mathcal{S}^m \rightarrow \mathcal{S}^n | \mathbf{h}_j) \\ &= Q\left(\sqrt{\frac{1}{2\sigma_j^2} \text{tr}(\mathbf{h}_j^H \mathbf{W} (\mathcal{S}^m - \mathcal{S}^n)^H (\mathcal{S}^m - \mathcal{S}^n) \mathbf{W}^H \mathbf{h}_j)}\right), \end{aligned} \quad (3.39)$$

where  $\mathcal{S}^m \in \mathcal{K}_{\mathcal{P}}$  denotes the  $m$ th STBC matrix correctly transmitted by the serving BS and  $\mathcal{S}^n \in \mathcal{K}_{\mathcal{P}}$  ( $n \neq m$ ) denotes the wrongly decoded STBC matrix at the  $j$ th user.

The beamforming matrix  $\mathbf{W}$  is designed such that the worst user's PEP is minimized assuming a total transmit power budget at the BS for single-group multicasting networks using STBCs.

The proposed beamforming design is independent of the actual transmitted symbol and the same beamforming matrix can be used for multiple symbols in the coherence time. This approach is different from the recent methods that use symbol level precoding or constructive interference as in [LLLS21, ASK<sup>+</sup>17].

With the monotonically decreasing property of the Q-function, the optimization problem of (3.39) can be formulated as

$$\gamma_{\text{BF-STBC}} \triangleq \max_{\mathbf{W}} \min_{j=1, \dots, M} \min_{\substack{\mathcal{S}^m, \mathcal{S}^n \in \mathcal{K}_{\mathcal{P}}; \\ n \neq m}} \text{tr} \left( \frac{\mathbf{W} (\mathcal{S}^m - \mathcal{S}^n)^H (\mathcal{S}^m - \mathcal{S}^n) \mathbf{W}^H \mathbf{H}_j}{\sigma_j^2} \right) \quad (3.40a)$$

$$\text{s.t.} \quad \text{tr}(\mathbf{W} \mathbf{W}^H) \leq P_{\max}. \quad (3.40b)$$

Assuming that  $\mathbf{D}_{mn} \triangleq \mathbf{S}^m - \mathbf{S}^n$  is the code difference matrix and  $\tilde{\mathbf{D}}_{mn} \triangleq \mathbf{D}_{mn}^H \mathbf{D}_{mn}$  is the distance matrix [Jaf05], the MMMF problem of (3.40) can be written as

$$\gamma_{\text{BF-STBC}} \triangleq \max_{\mathbf{W}} \min_{j=1, \dots, M} \min_{\mathbf{S}^m, \mathbf{S}^n \in \mathcal{K}_{\mathcal{P}}; n \neq m} \text{tr} \left( \frac{\mathbf{W} \tilde{\mathbf{D}}_{mn} \mathbf{W}^H \mathbf{H}_j}{\sigma_j^2} \right) \quad (3.41a)$$

$$\text{s.t.} \quad \text{tr}(\mathbf{W} \mathbf{W}^H) \leq P_{\max}, \quad (3.41b)$$

Define  $\tilde{\mathcal{D}} \triangleq \left\{ \tilde{\mathbf{D}}_{mn} \right\}_{\substack{m, n=1 \\ m \neq n}}^{\mathcal{P}}$  as the set of matrices which contains all the distance matrices  $\tilde{\mathbf{D}}_{mn}$  created by distinct codewords.

Solving the optimization problem of (3.41) over all distance matrices  $\tilde{\mathbf{D}}_{mn} \in \tilde{\mathcal{D}}$  is computationally very complex due to the cardinality of  $\tilde{\mathcal{D}}$ , given by  $\mathcal{P}^2 - 1$ , which increases dramatically by increasing the rank of the STBC.

The computational complexity is reduced, using a smaller subset  $\tilde{\mathcal{D}}_{\text{sub}}$  of  $\tilde{\mathcal{D}}$ , where  $\tilde{\mathcal{D}}_{\text{sub}} \triangleq \left\{ \tilde{\mathbf{D}}_1, \dots, \tilde{\mathbf{D}}_{\mathcal{L}} \right\}$ . A matrix  $\tilde{\mathbf{D}}_{mn}$  is not contained in  $\tilde{\mathcal{D}}_{\text{sub}}$  if there exists another matrix  $\tilde{\mathbf{D}}_l \in \tilde{\mathcal{D}}_{\text{sub}}$  ( $l = 1, \dots, \mathcal{L}$ ), which satisfies  $\tilde{\mathbf{D}}_{mn} \succ \tilde{\mathbf{D}}_l$ .

**Lemma 1.** *Given three positive definite Hermitian matrices  $\Sigma$ ,  $\Delta_1$  and  $\Delta_2$ . If  $\Delta_1 \succ \Delta_2$ , then  $\text{tr}(\Sigma \Delta_1) > \text{tr}(\Sigma \Delta_2)$ .*

*Proof.* Rewrite  $\Sigma \triangleq \Lambda^H \Lambda$ . Given  $\Delta_1 \succeq \Delta_2$ , thus  $\text{tr}(\Sigma \Delta_1) - \text{tr}(\Sigma \Delta_2) = \text{tr}(\Lambda^H \Lambda (\Delta_1 - \Delta_2)) = \text{tr}(\Lambda (\Delta_1 - \Delta_2) \Lambda^H) > 0$ , which follows from the definition of positive definite matrices.  $\square$

Following **Lemma 1**, along with the definition of  $\tilde{\mathcal{D}}_{\text{sub}}$ , gives  $\text{tr} \left( \frac{\mathbf{W} \tilde{\mathbf{D}}_{mn} \mathbf{W}^H \mathbf{H}_j}{\sigma_j^2} \right) > \text{tr} \left( \frac{\mathbf{W} \tilde{\mathbf{D}}_l \mathbf{W}^H \mathbf{H}_j}{\sigma_j^2} \right)$ . Therefore, both minimization  $\min_{\mathbf{S}^m, \mathbf{S}^n \in \mathcal{K}_{\mathcal{P}}; n \neq m} \text{tr} \left( \frac{\mathbf{W} \tilde{\mathbf{D}}_{mn} \mathbf{W}^H \mathbf{H}_j}{\sigma_j^2} \right)$  in (3.41) and  $\min_{l=1, \dots, \mathcal{L}} \text{tr} \left( \frac{\mathbf{W} \tilde{\mathbf{D}}_l \mathbf{W}^H \mathbf{H}_j}{\sigma_j^2} \right)$  are equivalent and the problem (3.41) is can be written as

$$\gamma_{\text{BF-STBC}} \triangleq \max_{\mathbf{W}} \min_{j=1, \dots, M} \min_{l=1, \dots, \mathcal{L}} \text{tr} \left( \frac{\mathbf{W} \tilde{\mathbf{D}}_l \mathbf{W}^H \mathbf{H}_j}{\sigma_j^2} \right) \quad (3.42a)$$

$$\text{s.t.} \quad \text{tr}(\mathbf{W} \mathbf{W}^H) \leq P_{\max}. \quad (3.42b)$$

In general,  $\mathcal{L}$  is much smaller than  $\mathcal{P}^2 - 1$  for practical STBCs. Therefore, the computational complexity of the problem (3.42) is significantly lower compared with the complexity of the problem (3.41).

The optimization problem (3.42) belongs to the class of non-convex quadratically constrained quadratic programs, thus it is difficult to solve and NP-hard in general [BV04]. A theoretical optimal solution can be obtained by employing the vectorization properties and using the SDR technique. An iterative algorithm is employed, where the optimization problem of (3.42) is solved using a sequence of inner approximation problems. The solutions of the approximated problems are always feasible for the original problem (3.42), assuming a feasible initialization point.

### 3.6.2 Theoretically Upper Bound

In this section, the vectorization technique is employed to reformulate the objective function (3.42a) and obtain a convex problem, which can be relaxed using the SDR technique.

Using the vectorization properties [PP12] given by

$$\text{tr}(\mathbf{A}^T \mathbf{B}) = \text{vec}(\mathbf{A})^T \text{vec}(\mathbf{B}), \quad (3.43)$$

$$\text{vec}(\mathbf{A} \mathbf{G} \mathbf{B}) = (\mathbf{B}^T \otimes \mathbf{A}) \text{vec}(\mathbf{G}), \quad (3.44)$$

and denoting  $\mathbf{w}_c \triangleq \text{vec}(\mathbf{W}^T)$ , problem (3.42) can be written as

$$\max_{\mathbf{w}_c \in \mathbb{C}^{N^2 \times 1}} \min_{\substack{j=1, \dots, M; \\ l=1, \dots, \mathcal{L}}} \text{tr} \left( \frac{\mathbf{w}_c \mathbf{w}_c^H (\tilde{\mathbf{D}}_l \otimes \mathbf{H}_j)}{\sigma_j^2} \right) \quad (3.45a)$$

$$\text{s.t.} \quad \text{tr}(\mathbf{w}_c \mathbf{w}_c^H) \leq P_{\max}, \quad (3.45b)$$

where the equality  $\text{tr}(\mathbf{W} \mathbf{W}^H) = \text{tr}(\mathbf{w}_c \mathbf{w}_c^H)$  is used.

The objective function (3.45a) is also non-convex and is NP-hard in general. In order to solve this problem, the SDR technique can be applied to relax the non-convex term and obtain a suboptimal solution.

Using the equivalence (2.22), the problem of (3.45) can be formulated as

$$\max_{\mathbf{X}} \min_{\substack{j=1, \dots, M; \\ l=1, \dots, \mathcal{L}}} \text{tr} \left( \frac{\mathbf{X} (\tilde{\mathbf{D}}_l \otimes \mathbf{H}_j)}{\sigma_j^2} \right) \quad (3.46a)$$

$$\text{s.t.} \quad \text{tr}(\mathbf{X}) \leq P_{\max}, \quad (3.46b)$$

$$\mathbf{X} \succeq 0, \quad (3.46c)$$

$$\text{rank}(\mathbf{X}) \leq 1, \quad (3.46d)$$

which is non-convex due to the rank constraint. Using SDR and dropping the rank yields a relaxed convex problem, given by

$$\max_{\mathbf{X}} \min_{\substack{j=1,\dots,M; \\ l=1,\dots,\mathcal{L}}} \operatorname{tr} \left( \frac{\mathbf{X} (\tilde{\mathbf{D}}_l \otimes \mathbf{H}_j)}{\sigma_j^2} \right) \quad (3.47a)$$

$$\text{s.t. } \operatorname{tr}(\mathbf{X}) \leq P_{\max}, \quad (3.47b)$$

$$\mathbf{X} \succeq 0, \quad (3.47c)$$

In general, the beamforming solutions obtained by solving the problem of (3.47) have a rank greater than one, which is due to the employed rank one relaxation. Moreover, the dimensions of the matrix  $\mathbf{X}$  is  $NR \times NR$ , due to the used vectorization operator. Thus, beamforming solutions with high rank are obtained with high probability. Moreover, The worst case computational complexity problem of (3.47) is  $O(\sqrt{NR}((NR)^3 + \mathcal{L}M(NR)^2)\log(1/\xi))$ , where  $\xi$  represents the solutions precision achieved at the interior iterative method [KSL08b, WSC<sup>+</sup>14]. Compared with the computational complexity of the rank one problem as in [KSL08b] given by  $O(\sqrt{N}(N^3 + MN^2)\log(1/\xi))$ , it can be seen that problem (3.47) has higher complexity, which further increases with  $\mathcal{L}$  and  $R$ .

### 3.6.3 Convex Approximation Technique

Another approach to solve the non-convex problem of (3.42) is presented in this section. An iterative algorithm is employed and first order Taylor expansion is used to linearize the problem of (3.42) and transform it to a convex one.

The optimization problem in (3.42) can be equivalently written as

$$\min_{\mathbf{W}, t} t \quad (3.48a)$$

$$\text{s.t. } t > 0, \quad (3.48b)$$

$$\operatorname{tr} \left( \frac{\mathbf{W} \tilde{\mathbf{D}}_l \mathbf{W}^H \mathbf{H}_j}{\sigma_j^2} \right) \geq \frac{1}{t}, \quad j = 1, \dots, M, \quad l = 1, \dots, \mathcal{L}, \quad (3.48c)$$

$$\operatorname{tr}(\mathbf{W} \mathbf{W}^H) \leq P_{\max}, \quad (3.48d)$$

where  $t$  is an auxiliary optimization variable.

The value of  $1/t$  in problem (3.48) represents a lower bound of  $\gamma_{\text{BF-STBC}}$  in (3.42).

The SNR threshold constraint (3.48c) can be rewritten as

$$\lambda_{j,l}(\mathbf{W}, t) \triangleq \frac{\sigma_j^2}{t} - \text{tr} \left( \mathbf{W} \tilde{\mathbf{D}}_l \mathbf{W}^H \mathbf{H}_j \right) \leq 0. \quad (3.49)$$

Note that the functions  $\sigma_j^2/t$  and  $\text{tr} \left( \mathbf{W} \tilde{\mathbf{D}}_l \mathbf{W}^H \mathbf{H}_j \right)$  in (3.49) are convex. This follows from the definition of  $\tilde{\mathbf{D}}_l$  and  $\mathbf{H}_j$ . Thus,  $\lambda_{j,l}(\mathbf{W}, t)$  given in (3.49) represents a difference of convex (DC) functions. Therefore, the optimization problem of (3.48) belongs to the class of DC programs [HT99, AT05, CP12, LTPD03, BV98]. Based on this observation, a procedure similar to the one proposed in [SLP15] is followed to approximate and solve the problem (3.48) iteratively.

Assume  $\mathbf{W}^{(k)}$  as the beamforming matrix generated at the  $k$ th iteration, the beamforming matrix at the  $(k+1)$ th iteration can be written as

$$\mathbf{W}^{(k+1)} \triangleq \mathbf{W}^{(k)} + \Delta \mathbf{W}^{(k)}, \quad (3.50)$$

where  $\Delta \mathbf{W}^{(k)}$  is the update solution at iteration  $k$ .

At each iteration step  $k$ , the first order Taylor expansion of the  $\lambda_{j,l}(\mathbf{W}, t)$  about the current solution  $\mathbf{W}^{(k)}$  is used to compute the update  $\Delta \mathbf{W}^{(k)}$ . The concave term  $\text{tr} \left( \mathbf{W} \tilde{\mathbf{D}}_l \mathbf{W}^H \mathbf{H}_j \right)$  is replaced in the constraint of (3.49) by its first order Taylor approximation, meanwhile keeping the convex term unchanged. Thus, the inequality of (3.49) can be approximated by

$$\bar{\lambda}_{j,l}^{(k)}(\Delta \mathbf{W}^{(k)}) \triangleq \frac{\sigma_j^2}{t} - \text{tr} \left( \mathbf{W}^{(k)} \tilde{\mathbf{D}}_l \mathbf{W}^{(k)H} \mathbf{H}_j \right) - 2 \text{tr} \left( \text{Re} \left( \mathbf{W}^{(k)} \tilde{\mathbf{D}}_l \Delta \mathbf{W}^{(k)H} \mathbf{H}_j \right) \right) \leq 0. \quad (3.51)$$

The inequalities (3.49) and (3.51) give

$$\lambda_{j,l}^{(k)}(\mathbf{W}^{(k)} + \Delta \mathbf{W}^{(k)}) \leq \bar{\lambda}_{j,l}^{(k)}(\Delta \mathbf{W}^{(k)}). \quad (3.52)$$

The right hand side term of inequality (3.52) represents a linearization of the non-convex part of (3.49).

Consider the sequential update of the beamforming matrix in (3.50). Assume  $\Delta \mathbf{W}^{(k)}$  is the new optimization variable, the optimization problem of (3.48) can be expressed as

$$\min_{\Delta \mathbf{W}^{(k)}, t^{(k)}} t^{(k)} \quad (3.53a)$$

$$\text{s.t. } t^{(k)} > 0, \quad (3.53b)$$

$$\bar{\lambda}_{j,l}^{(k)}(\Delta \mathbf{W}^{(k)}) \leq 0, \quad j = 1, \dots, M, \quad l = 1, \dots, \mathcal{L}, \quad (3.53c)$$

$$\text{tr} \left( (\mathbf{W}^{(k)} + \Delta \mathbf{W}^{(k)}) (\mathbf{W}^{(k)} + \Delta \mathbf{W}^{(k)})^H \right) \leq P_{\max}. \quad (3.53d)$$

Observing the inequality (3.52), it can be concluded that the problem (3.53) represents an inner approximation of the optimization problem (3.48). Hence, can be solved using any standard cvx solver eliminating the need for any further relaxation. Algorithm 2 summarizes the sequential approach to yield the beamforming solutions and solve the optimization problem of (3.53). A feasible initialization point is generated randomly, then the algorithm iterates until the convergence criteria is met, i.e., the relative difference in the objective function between two iterations  $\rho$  falls below a threshold value  $\epsilon$  determined previously.

**Algorithm 2:** Inner Approximation algorithm

**Input:**  $\tilde{\mathbf{D}}_l, \epsilon, P_{\max}, \sigma_j, \mathbf{H}_j, j = 1, \dots, M, l = 1, \dots, \mathcal{L}$

- 1 Set  $k = 0$ , choose  $\mathbf{W}^{(0)}$  randomly.  
Set  $t^{(0)} \triangleq 1/(\min_{j,l}(\mathbf{W}\tilde{\mathbf{D}}_l\mathbf{W}^H\mathbf{H}_j))$ .  
Set  $\rho > \epsilon$ .
- 2 **begin**
- 3     **while**  $\rho > \epsilon$  **do**
- 4          $k = k + 1$ .
- 5         Compute  $(\Delta\mathbf{W}^*, t^{(k)*})$  by solving (3.53).  
Update  $\mathbf{W}^{(k+1)} \triangleq \mathbf{W}^{(k)} + \Delta\mathbf{W}^*$  by using  $\mathbf{W}^{(k)}$ .
- 6         Calculate  $\rho \triangleq |t^{(k)} - t^{(k+1)}|/t^{(k)}$ .
- 7     **end**
- 8 **end**
- 9 **return**  $\mathbf{W}^{(k+1)}, t^{(k+1)}$ .

The iterative Algorithm 2 is globally convergent if the variables belong to a compact and closed set [SL09]. These conditions are satisfied in the proposed design, due to the power constraint of (3.53d) which sets an upper bound on the feasible solutions set and the auxiliary optimization variable  $t$  which is positive and minimized to a lower value.

The worst case computational complexity problem of (3.53) for a single iteration is  $O(\sqrt{N}(N^3 + \mathcal{L}MN^2)\log(1/\xi))$ . Thus, assuming that Algorithm 2 converges in  $K$  iterations, the overall complexity is given by  $O(\sqrt{N}K(N^3 + \mathcal{L}MN^2)\log(1/\xi))$ . It can be noted that the computational complexity of problem (3.53) is comparatively smaller than the complexity of problem (3.47).



### 3.6.4 QOSTBC Encoding and Decoding

In this section, a brief overview about QOSTBC is provided. QOSTBC will be used later in Section 3.6.5 to evaluate the performance of the proposed design.

Full rate OSTBC codes with complex elements are impossible for more than two spatial streams. QOSTBC provides full rate codes. However, the simple symbol-by-symbol property is sacrificed and pairwise decoding is performed.

Consider a QOSTBC encoder with  $R = 4$  spatial output streams and  $T = 4$  time slots and assume that the channel coefficients are quasi-static over one frame duration and may change arbitrarily from one frame to another. The  $T \times K$  encoded matrix  $\mathbf{S}$  is given by [Jaf05]

$$\mathbf{S} \triangleq \begin{bmatrix} s_1 & s_2 & s_3 & s_4 \\ -s_2^* & s_1^* & -s_4^* & s_3^* \\ -s_3^* & -s_4^* & s_1^* & s_2^* \\ s_4 & -s_3 & -s_2 & s_1 \end{bmatrix}, \quad (3.54)$$

with  $s_1, s_2, s_3$  and  $s_4$  being the QPSK modulated input symbols. Notice that four symbols are multicasted using four different time slots. Thus, the code rate equals to one. However, the minimum rank of the difference matrix  $\mathbf{D}_{mn}$  could be two. Hence, the diversity of the code is equal to two.

Assume  $\psi_i$  is the  $i$ th column of encoded matrix  $\mathbf{S}$ , then

$$\langle \psi_1, \psi_2 \rangle = \langle \psi_1, \psi_3 \rangle = \langle \psi_2, \psi_4 \rangle = \langle \psi_3, \psi_4 \rangle = 0, \quad (3.55)$$

where  $\langle \psi_i, \psi_j \rangle$  is the inner product of  $\psi_i$  and  $\psi_j$ . The subspace generated by  $\psi_1, \psi_4$  is orthogonal to the subspace generated by  $\psi_2, \psi_3$ . The orthogonality of both subspaces enables pairwise detection at the receiver's side as will be explained in the following.

Assume that  $\tilde{\mathbf{h}}_j \triangleq \mathbf{W}^H \mathbf{h}_j = [\tilde{h}_{j,1} \ \tilde{h}_{j,2} \ \tilde{h}_{j,3} \ \tilde{h}_{j,4}]^T$ , the ML decoding of the QOSTBC at the user  $j$  is given by [Jaf05]

$$\min_{s_1, s_2, s_3, s_4} \tilde{\mathbf{h}}_j^H \mathbf{S}^H \mathbf{S} \tilde{\mathbf{h}}_j - \tilde{\mathbf{h}}_j^H \mathbf{S}^H \mathbf{y}_j - \mathbf{y}_j^H \mathbf{S} \tilde{\mathbf{h}}_j, \quad (3.56)$$

which can be simplified to

$$\min_{s_1, s_2, s_3, s_4} f_{14}(s_1, s_4) + f_{23}(s_2, s_3), \quad (3.57)$$

where

$$\begin{aligned}
f_{14}(s_1, s_4) \triangleq & (|s_1|^2 + |s_4|^2) \sum_{n=1}^4 |\tilde{h}_{j,n}|^2 + 2\text{Re} \left( \left( -\tilde{h}_{j,1}y_{j,1}^* - \tilde{h}_{j,2}^*y_{j,2} - \tilde{h}_{j,3}^*y_{j,3} - \tilde{h}_{j,4}y_{j,4}^* \right) s_1 \right. \\
& \left. + \left( -\tilde{h}_{j,4}y_{j,1}^* + \tilde{h}_{j,3}^*y_{j,2} + \tilde{h}_{j,2}^*y_{j,3} - \tilde{h}_{j,1}y_{j,4}^* \right) s_4 \right) + 4\text{Re} \left( \tilde{h}_{j,1}\tilde{h}_{j,4}^* - \tilde{h}_{j,2}^*\tilde{h}_{j,3} \right) \text{Re}(s_1s_4^*),
\end{aligned} \tag{3.58}$$

$$\begin{aligned}
f_{23}(s_2, s_3) \triangleq & (|s_2|^2 + |s_3|^2) \sum_{n=1}^4 |\tilde{h}_{j,n}|^2 + 2\text{Re} \left( \left( -\tilde{h}_{j,2}y_{j,1}^* + \tilde{h}_{j,1}^*y_{j,2} - \tilde{h}_{j,4}^*y_{j,3} + \tilde{h}_{j,3}y_{j,4}^* \right) s_2 \right. \\
& \left. + \left( -\tilde{h}_{j,3}y_{j,1}^* - \tilde{h}_{j,4}^*y_{j,2} + \tilde{h}_{j,1}^*y_{j,3} + \tilde{h}_{j,2}y_{j,4}^* \right) s_3 \right) + 4\text{Re} \left( \tilde{h}_{j,2}\tilde{h}_{j,3}^* - \tilde{h}_{j,1}^*\tilde{h}_{j,4} \right) \text{Re}(s_2s_3^*),
\end{aligned} \tag{3.59}$$

and  $\mathbf{y}_j = [y_{j,1} \ y_{j,2} \ y_{j,3} \ y_{j,4}]^T$ . Notice that  $f_{14}$  is independent of  $s_2$  and  $s_3$  and  $f_{23}$  is independent of  $s_1$  and  $s_4$ . Hence,  $s_1, s_4$  can be decoded separately from  $s_2, s_3$  and detection is performed pairwise at the receiver' side.

The set  $\mathcal{K}_{\mathcal{P}}$  for the aforementioned QOSTBC code has a cardinality  $\mathcal{P} = 256$ . However, numerical results show that a much smaller subset of  $\mathcal{L} = 3$  in (3.42) can be obtained using **Lemma 1** in Section 3.6.1. Thus, the computational complexity of performing the minimization problem of (3.41) is significantly reduced. The  $\mathcal{L}$  corresponding matrices with the minimum distance are given by

$$\mathbf{D}_1 \triangleq \frac{1}{2} \sum_{i=1}^T |s_i|^2 \mathbf{I}_4, \tag{3.60a}$$

$$\mathbf{D}_2 \triangleq \sum_{i=1}^T |s_i|^2 (\mathbf{I}_4 + \overline{\text{diag}}(1, -1, -1, 1)), \tag{3.60b}$$

$$\mathbf{D}_3 \triangleq \sum_{i=1}^T |s_i|^2 (\mathbf{I}_4 + \overline{\text{diag}}(-1, 1, 1, -1)), \tag{3.60c}$$

where the transmit power of each symbol is normalized to one, i.e.,  $|s_i|^2 = 1, (i = 1, 2, 3, 4)$  and  $\overline{\text{diag}}(1, -1, -1, 1)$  is given by

$$\overline{\text{diag}}(1, -1, -1, 1) = \begin{bmatrix} 0 & 0 & 0 & 1 \\ 0 & 0 & -1 & 0 \\ 0 & -1 & 0 & 0 \\ 1 & 0 & 0 & 0 \end{bmatrix}. \tag{3.61}$$

### 3.6.5 Simulation Results

In the simulation results, a serving BS with  $N = 4$  antennas is assumed to apply transmit beamforming to multicast QOSTBC encoded matrix  $\mathbf{S}$  as in (3.54) during  $T = 4$  time slots,  $R = 4$  spatial streams. Thus,  $\mathcal{L} = 3$  and the minimum distance matrices are given by (3.60). A maximum transmit power of  $P_{\max} = 1$  is assumed.

The simulations are performed for  $10^4$  Monte-Carlo runs and 100 independent channel realizations.

In Algorithm 2, a precision threshold value  $\epsilon = 10^{-3}$  is assumed.

Figure 3.9 illustrates the obtained lower and upper bounds on  $\gamma_{\text{BF-STBC}}$  as defined in (3.42a) versus the number of users for different approaches. In this figure, the upper bound is obtained by solving the optimization problem of (3.47), thus obtaining the optimal theoretical value. The curve with the label ‘‘QOSTBC beamforming’’ represents the value of  $1/t^{(k+1)}$  in (3.48a) obtained using Algorithm 2 and the ‘‘First iteration’’ curve represents  $1/t^{(1)}$  obtained by running Algorithm 2 for a single iteration. Hence, producing the lower bound. The convergence of Algorithm 2 can be recognized by observing Figure 3.9. It can be noticed that the value of  $\gamma_{\text{BF-STBC}}$  obtained by Algorithm 2 converges to the theoretical upper bound, which indicates that the proposed approach produces near optimal solutions of problem (3.48). It can also be observed that the value of  $\gamma_{\text{BF-STBC}}$  for all the curves decreases by increasing the number of users.

Figure 3.10 depicts a histogram of the number of iterations required to achieve the convergence for a precision threshold of  $\epsilon = 10^{-3}$  in Algorithm 2. We consider a group of 64 users and SNR = 10 dB. It can be observed that the proposed algorithm converges after approximately 8 – 10 iterations. The convergence of Algorithm 2 is remarkably dependent on the initialization point. A proper initial value of leads to a faster convergence. However, the initialization point is chosen randomly in Algorithm 2.

Figure 3.11 displays the worst user’s FER performance of the beamforming design using Algorithm 2, compared with the best state-of-the-art beamforming techniques for this problem, i.e., rank one [SDL06] and rank two transmit beamforming designs [WMS13, WSM12]. In Figure 3.11, the FER of the conventional QOSTBC assuming no beamforming [Jaf05] is also plotted. A system with a group of 64 users is assumed. The worst user’s FER of the rank two beamforming design is calculated for

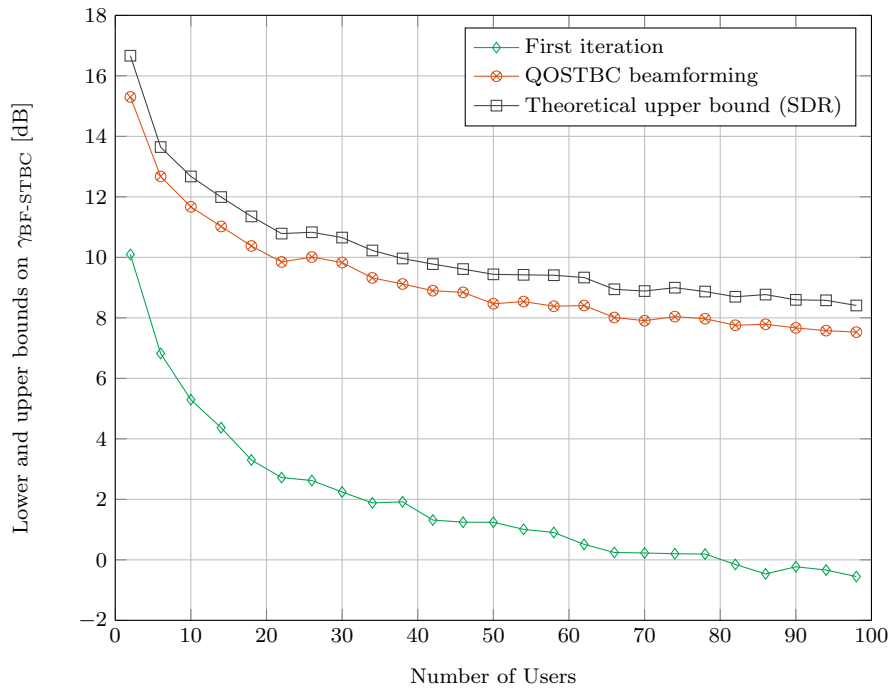


Figure 3.9. Lower and upper bounds on  $\gamma_{BF-STBC}$  at the worst user plotted against SNR in dB for  $N = 4$  transmit antenna

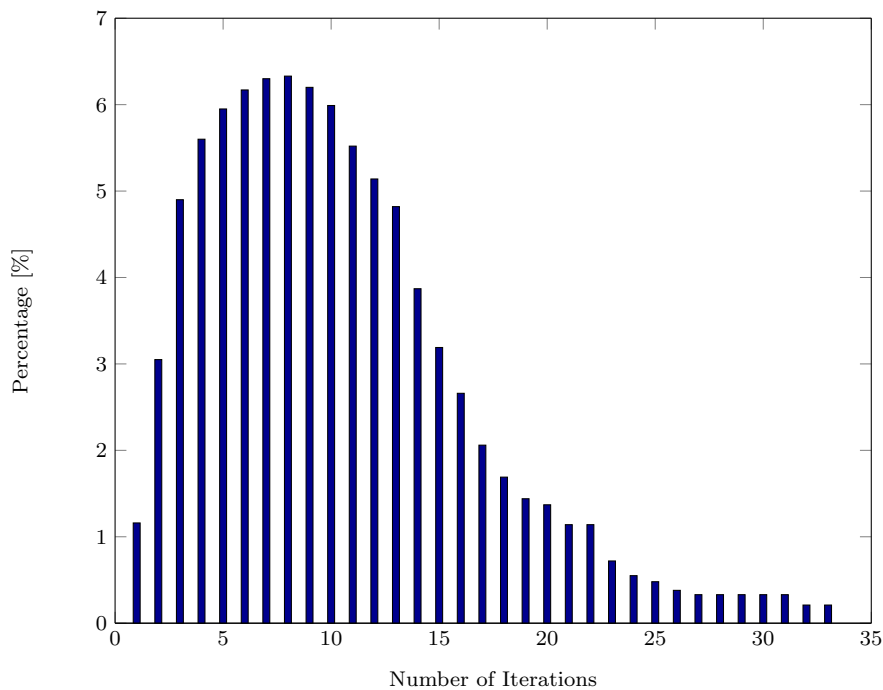


Figure 3.10. A histogram of the number of iterations for a system of 64 users and  $N = 4$  transmit antennas

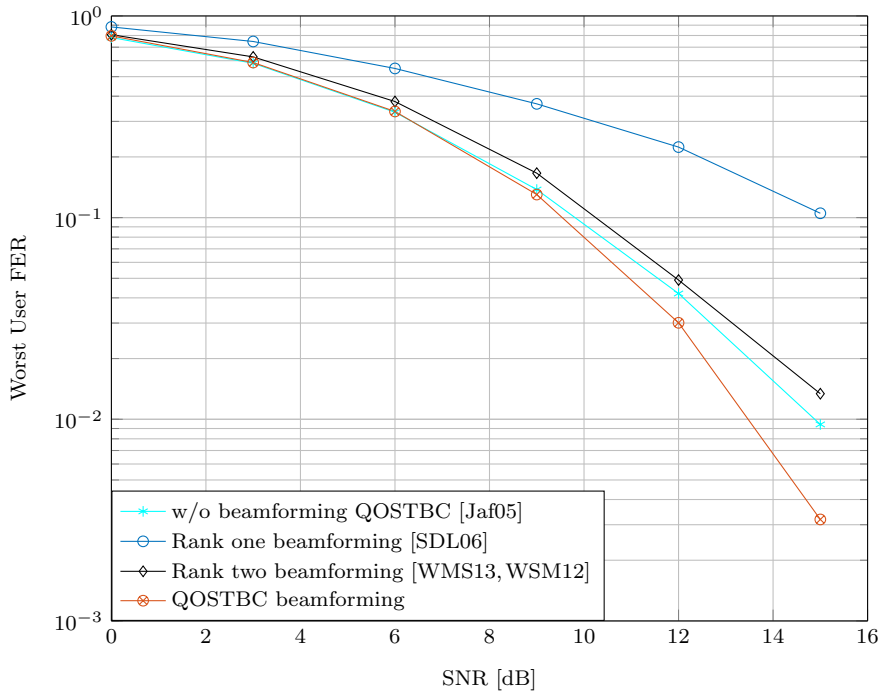


Figure 3.11. System performance of the worst user FER plotted against SNR in dB for a system of 64 users and  $N = 4$  transmit antennas

a frame composed of four symbols, each two symbols represent one Alamouti based beamforming matrix as in [WMS13, WSM12]. For the rank one beamforming design, the worst user's FER is calculated using a frame of four symbols. Each symbol is obtained from solving the rank one approach as in [SDL06]. A fair comparison is guaranteed assuming the same transmit power for all designs at each time slot  $P_{\max} = 1$ . From Figure 3.11, it can be seen that the performance of the proposed QOSTBC based beamforming approach significantly outperforms the state-of-the-art approaches and a gain of approximately 1 – 2 dB can be observed. Furthermore, the proposed approach yields a significantly higher diversity gain (defined as the slope of the FER curve in the high SNR region) than the conventional scheme without beamforming.

Figure 3.12 depicts a similar comparison as in Figure 3.11 for different numbers of users, assuming the SNR is 10 dB. It can be observed that rank one beamforming design exhibits the best performance for a small group consisted of 2 users. However, the performance of rank one beamforming design degrades severely as the number of users increases further. The rank two beamforming approach outperforms all compared approaches for a group of users of size 3 to 30. However, as the number of users further increases, the proposed approach starts to deliver the best performance compared with both of the rank one and rank two beamforming designs. The performance of the

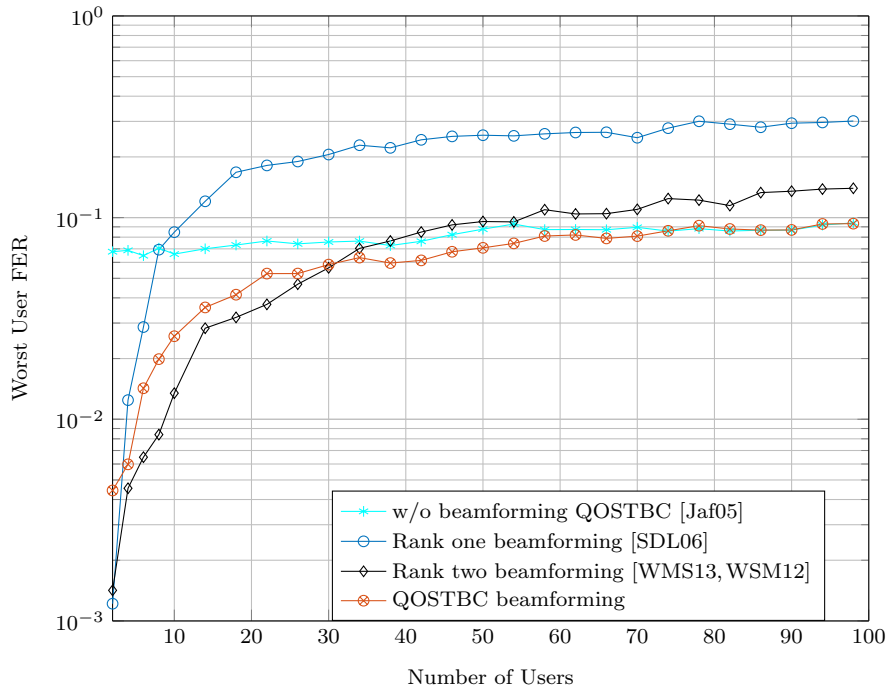


Figure 3.12. System performance of the worst user FER with varying number of users for SNR= 10 dB and  $N = 4$  transmit antennas

proposed approach converges to that of the conventional scheme without beamforming for a group with more than 74 users at SNR= 10 dB. Moreover, the performance of the proposed QOSTBC based beamforming approach does not degrade severely by increasing the number of users.

The increased degrees of freedom allows including more constraints in the optimization problem (3.42), i.e., additional shaping constraints [LWTP15, HP10b]. This is extremely practical in many applications, e.g., in the cognitive radio context. However, adding constraints is not possible in the conventional STBCs broadcasting schemes that do not use beamforming. This marks an important advantage of the proposed approach over the existing conventional STBCs broadcasting techniques.

In Figure 3.13 the performance measures in terms of BER for the general rank beamforming approaches compared with the state-of-the-art transmit beamforming designs and QOSTBC with 4 transmit antennas without beamforming. The same modulation scheme QPSK is used for QOSTBC, rank one, rank two, OSTBC, and QOSTBC based beamforming approaches. Moreover, real-valued symbols as in Section 3.5 are used for the real-valued OSTBC based beamforming method. However, the same rate is guaranteed using and different channel codes with different rates. All approaches enjoy the

same transmission rate of  $L = 1$  bpcu and a single-group of  $M = 64$  users is served. A convolutional code with rate  $1/2$  is combined with rank one Method [SDL06], rank two method [WMS13] beamforming, real-valued OSTBC and QOSTBC based beamforming. Moreover, a convolutional code of rate  $2/3$  is combined with OSTBC based beamforming approach. Convolutional encoders are used with the same memory length and almost identical channel coding gain for all approaches [Ode79, Vit71] to guarantee a fair comparison. The simulation results show that for SNRs smaller than 3 dB, all the methods perform almost the same, except the real-valued OSTBC based beamforming approach, where the real-valued modulated symbols have smaller Euclidean distance, thus higher BER values. All the proposed general rank beamforming methods perform better than the state-of-the-art designs. It can be observed that complex-valued OSTBC based beamforming performs better than the real-valued based one till SNR equals to 10 dB. For SNR larger than 10 dB the slope of the BER curve of the real-valued OSTBC based beamforming becomes steeper and it outperforms the complex-valued OSTBC based beamforming approach. It is possible to explain this by the difference in error correction capabilities between the employed convolutional codes of rates  $1/2$  and  $3/4$ . Moreover, QOSTBC based beamforming design outperforms all the other approaches due to the design of the optimization problem, which minimizes the worst user's PEP given the transmit power constraints. For  $\text{BER}=10^{-4}$  QOSTBC based beamforming approach has 2 dB performance gain compared with real-valued OSTBC based beamforming design.

### 3.7 Summary

In this chapter, novel approaches are presented to enhance the performance degradation of the rank one and the rank two based beamforming designs for multicasting networks of a single group of users. The increase of degrees of freedom enables the BS to simultaneously serve more users compared with the state-of-the-art approaches. STTCs based beamforming design is very promising as it provides substantially better performance compared with the state-of-the-art approaches. The simulation results depict high diversity and coding gain resulting from using STTC scheme. However, STTCs have a high decoding complexity at the subscribed user compared with the simple symbol-by-symbol detection of OSTBCs. A simpler approach is proposed using a high order ( $> 2$ ) OSTBC based beamforming design. Higher order OSTBCs enjoy a simple decoding at the subscribed user, but sacrifice the full code rate. The use of higher order OSTBC increases the degrees of freedom and allows serving more users at multicasting networks. Although full rate OSTBCs are impossible for higher order

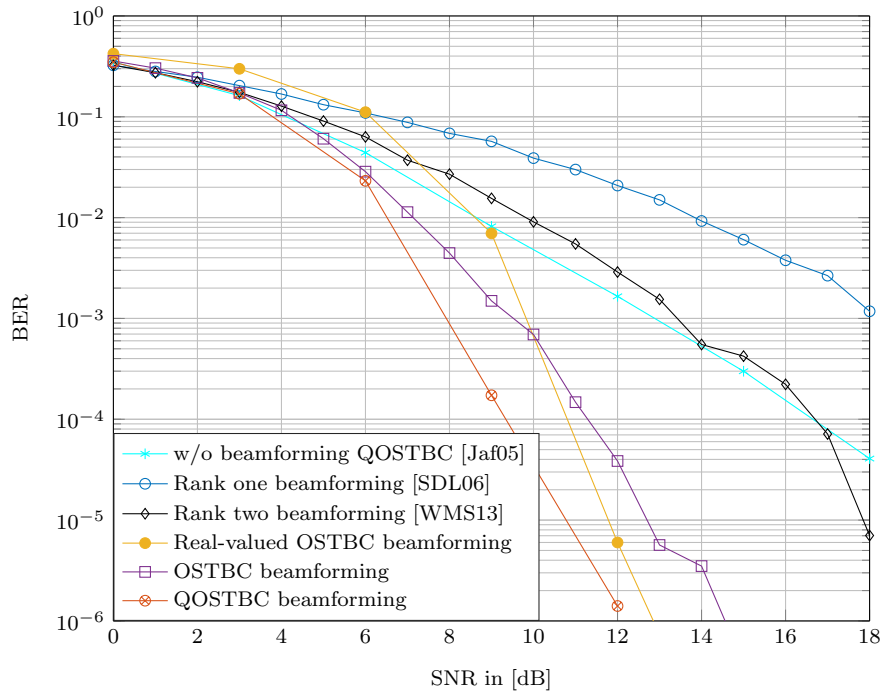


Figure 3.13. System performance of BER plotted against SNR in dB for transmission rate  $L = 1$  bpcu and  $M = 64$  users

(> 2) OSTBC matrices, the rate can be compensated using high modulation schemes. Furthermore, channel codes are practically used in wireless communication standards, thus the rate can be compensated also using channel codes with higher rate compared with the other designs. Simulation results depict that the proposed approach provides significant reliability improvements in communication scenarios even with large numbers of users compared to the state-of-the-art approaches.

The problem of insufficient degrees of freedom in the state-of-the-art beamforming designs (see Section 2.3.3 and 2.4.1) is addressed using real-valued OSTBCs for single group transmit beamforming networks. The proposed real-valued OSTBC codes enjoy full transmission rate and simple symbol-to-symbol decoding capability, thus the decoding complexity is not increased compared with the conventional OSTBCs design. It has been shown that the proposed approach delivers the best performance results in terms of BER compared to the rank one and rank two beamforming designs for scenarios of relatively large number of network users, where the rank of the beamforming is generally larger than one. One example has been provided for real-valued OSTBC with order equals to four. However, a generalization to higher orders real-valued OSTBC can be easily obtained such that networks with larger number of users can be served with no performance loss.



Full rate OSTBC using complex modulation symbols is impossible for higher order ( $> 2$ ) OSTBC matrices. However, the proposed QOSTBC based beamforming design enjoys full rate at the cost of increased decoding complexity at the subscribed user. Due to the non-orthogonal STBC based beamforming, post detection SNR based optimization design is no longer meaningful and new PEP design is applied to generate the beamforming matrices and improve the overall system performance.

A comparison between the state-of-the-art designs, complex-valued OSTBCs, real-valued OSTBCs and the QOSTBC based beamforming approaches is presented in the simulation results. The same transmission rate is guaranteed using channel codes to provide a fair comparison between all the transmit beamforming designs. The simulation results depict that QOSTBC based beamforming approach outperform all the other beamforming designs, however, at the cost of increased decoding complexity. real-valued OSTBCs based beamforming approach outperforms complex-valued OSTBCs based beamforming design for higher values of SNR ( $> 10$  dB). All the proposed beamforming approaches outperform the state-of-the-art rank one and rank two beamforming designs.



## Chapter 4

# Rank Regularized Beamforming

As seen in the previous chapters, the beamforming solutions enjoy a rank  $R$ , which increases with the number of network users  $M$  [WMS13]. Rank reduction solutions are devised, when  $R$  is larger than the number of columns in the STBC matrix. The early approach to solve the optimization problems using SDR technique was introduced in [SDL06]. The SDR optimization design yields suboptimal solutions, when the rank of the beamforming matrix is larger than one. For a larger number of users, it is generally observed that the rank of the optimization matrices  $\mathbf{X}$  in e.g. (3.29) is larger than one. Hence, the SDR performance degrades dramatically.

Many algorithms were proposed, see, e.g., [WM11, AGS10, Loz07, LMS<sup>+</sup>10] to improve the performance of solutions obtained with the SDR technique.

The authors of [HP10b] suggested a rank reduction algorithm to generate an optimal beamforming solution when its rank is larger than the square-root of the number of users, hence  $R > \sqrt{M}$ .

Randomization technique can be employed to further decrease the rank of the beamforming solutions, whenever the rank reduction technique cannot be applied [LMS<sup>+</sup>10, KSL08a]. The beamforming solutions produced by the randomization procedure are feasible but generally suboptimal for the original problem.

Improving the performance of the rank one beamforming design for the single group multicasting networks has been discussed in many works, see, e.g., [WMS13, WSM12, WLAP12, LWTP15, WXH<sup>+</sup>17, TAP15, TLP16, STPS17]. For all the general beamforming designs, the beamforming solutions are optimal if the rank of the solution matrix is less or equal to the number of columns in the STBC matrix. Otherwise the rank reduction procedure [HP10b, HP10a, Pat98] or the suboptimal randomization technique [LMS<sup>+</sup>10, KSL08a] can be devised to obtain the beamforming vectors. In single group multicasting networks the SDR beamforming solutions generally exhibit a high rank such that the optimal rank reduction procedure [HP10b] is not applicable since  $\sqrt{M} > R$ . To avoid the difficulties with the SDR solutions, an inner convex approximation algorithm was applied in Section 3.6 to provide general rank beamforming solutions using an iterative algorithm. However, the proposed procedure is associated with high computational complexity.

A similar idea based on the Taylor expansion to linearize the non-convex term of the optimization problem was proposed in [THJ14] and later improved by combining it with the multiplicative update (MU) algorithm, where the beamforming vector was updated iteratively using the inverse of the scaled SNR gradient vectors of all users in [GS15]. Rank one beamforming vectors were generated using the aforementioned procedures.

In [HS16], the non-convex quadratically constrained quadratic problem was solved using multiple sub-optimization problems, each satisfying a single SNR constraint at the time. The authors of [HS16] proof that the computational complexity is reduced in comparison with [GS15].

A rank regularization design using the logdet function as an approximation for the rank function was introduced in [Faz02]. The majorization-minimization procedure was employed to linearize the concave log function using Taylor expansion.

In this chapter, a rank regularization algorithm based on a modified version of the QoS design is introduced, where an approximation of the rank function is minimized given the users SNR targets. The idea of general rank beamforming is considered to reduce the rank of the beamforming solutions to the desired predetermined rank  $R$ . The logdet smooth surrogate of the rank function is employed to reduce the rank of the beamforming solutions in an approach similar to [Faz02]. A linearization of the non-convex function is obtained using the Taylor approximation. The problem is first solved by employing a two scale algorithm, where an iterative optimization scheme with two nested loops based on the majorization-minimization procedure and adaptive reweighting of the regularization term is used. Later on, a computationally simpler single scale algorithm is developed to reduce the computational complexity of the two scale algorithm. The regularization parameter is updated (during each iteration) to control the rank of the obtained beamforming solutions.

The general rank beamforming approach using OSTBCs is considered. The beamforming problem is non-convex and generally NP-hard. The semidefinite relaxation technique as presented in Section 3.2 is employed to solve the problem. Simulation results demonstrate that the proposed algorithms outperform the state-of-the-arts procedures in terms of the transmit power, average minimum SNR and SER. For a proper setting of the regularization variable, the one scale algorithm outperforms the best compared methods in terms of computational complexity.

$M$	$R_{\text{QoS}}$	$\lfloor \sqrt{M} \rfloor$
80	6	8
120	6	10
160	7	12
200	7	14
240	8	15
280	9	16
320	9	17
360	9	18
400	9	20

Table 4.1. Rank upper bound comparison between theoretical values and QoS problem

## 4.1 Motivation and Background

In this chapter, we follow the same assumptions as in Section 3.2. Similarly, perfect CSI both at the BS and users is assumed. The system model is given in (2.5). The OSTBC matrix  $\mathbf{S}$  is transmitted to the users using the  $N \times R$  beamforming matrix  $\mathbf{W}$ . This work suggests an optimization approach to design the beamformer matrix  $\mathbf{W}$ , which enjoys the required rank  $R$ .

Compared with the QoS approach, low rank solutions are provided. Two iterative algorithms are devised. Both satisfy the same constraints of the conventional QoS problem.

In order to investigate the rank of the solutions using the QoS optimization problem in (2.37), the rank of  $\mathbf{X}$  for different numbers of users is observed.

The rank obtained in Tables 3.2 and 3.1 shows that the rank of the solutions increases with the number of users  $M$ , thus the number of constraints.

Let us assume  $R_{\text{QoS}}$  is the maximum rank value of the solutions of the QoS problem, which are obtained from the simulations using 100 Monte-Carlo runs and compare  $R_{\text{QoS}}$  to the  $\lfloor \sqrt{M} \rfloor$  upper bound.

Table 4.1 shows that the rank obtained from the QoS optimization problem of (2.37) is always equal or smaller to the  $\lfloor \sqrt{M} \rfloor$  threshold. It can also be noticed that the gap expands as the number of users increases. Thus  $\lfloor \sqrt{M} \rfloor$  imposes a loose upper bound, especially for scenarios with a large number of users. Therefore, the rank reduction

algorithm suggested in [HP10b,HP10a] cannot be applied and the suboptimal randomization technique has to be employed. This is the main motivation for suggesting an alternative approach to reduce the obtained solutions rank.

## 4.2 Rank Reduction Approach

The rank of a matrix is a non-convex function, for which the nuclear norm is a convex approximation [CR08]. In the case of a positive semidefinite matrix  $\mathbf{X}$  the nuclear norm of matrix  $\mathbf{X}$  corresponds to its trace, i.e.  $\text{tr}(\mathbf{X})$ . A better approximation of the rank function can be obtained using the function  $\text{logdet}$  [Faz02]. In this section, an alternative optimization approach compared to problem (2.24) is proposed. This can be achieved by minimizing the function  $\text{logdet}(\mathbf{X} + \alpha\mathbf{I})$ , where  $\alpha$  is a small regularization variable as in [Faz02, FHB04]. The value of  $\alpha$  is chosen to balance the transmit power and the convergence time of the rank regularization algorithm as will be shown later. The optimization problem is given by

$$\min_{\mathbf{X}} \quad \text{logdet}(\mathbf{X} + \alpha\mathbf{I}) \quad (4.1a)$$

$$\text{s.t.} \quad \mathbf{X} \succeq \mathbf{0}, \quad (4.1b)$$

$$\text{tr}(\mathbf{X}\mathbf{H}_j) \geq \gamma_j \sigma_j^2, \quad j = 1, \dots, M, \quad (4.1c)$$

where the definition of  $\mathbf{X} \triangleq \mathbf{W}\mathbf{W}^H$  is used as in Section 2.4.1, the SDR technique is employed to drop the non-convex rank condition and the assumption in (2.35) to obtain the positive semi-definite constraint of (4.1b),  $\frac{\text{tr}(\mathbf{X}\mathbf{H}_j)}{\sigma_j^2}$  is the SNR of the  $j$ th user as in (2.32), where  $\mathbf{H}_j = \mathbf{h}_j\mathbf{h}_j^H$ ,  $\mathbf{h}_j$  is the  $j$ th user channel,  $\sigma_j^2$  is the  $j$ th user's noise and  $\gamma_j$  is the SNR threshold at the  $j$ th users as in (2.32).

In the following, the approximate of the non-convex optimization problem of (4.1) is presented. Furthermore, an iterative algorithm to approximately solve problem (4.1) sequentially is employed. Remark that the  $\text{logdet}$  function is concave. Hence the minimization over a convex set results in a non-convex optimization problem. Notice that the concave  $\text{logdet}$  function is differentiable, thus it can be approximated using the first order Taylor expansion of the  $\text{logdet}$  in the vicinity of the current point  $\mathbf{X}^{(k)}$  in iteration  $k$  [Faz02, SBP17].

The first order Taylor expansion is given by

$$\begin{aligned} \text{logdet}(\mathbf{X} + \alpha\mathbf{I}) &\approx \text{logdet}(\mathbf{X}^{(k)} + \alpha\mathbf{I}) + \text{tr}(\nabla \text{logdet}(\mathbf{X}^{(k)} + \alpha\mathbf{I})(\mathbf{X} - \mathbf{X}^{(k)})) \\ &= \text{logdet}(\mathbf{X}^{(k)} + \alpha\mathbf{I}) + \text{tr}((\mathbf{X}^{(k)} + \alpha\mathbf{I})^{-1}(\mathbf{X} - \mathbf{X}^{(k)})), \end{aligned} \quad (4.2)$$

where  $\nabla \log \det \mathbf{A} = \mathbf{A}^{-1}$ , for  $\mathbf{A} \succeq \mathbf{0}$  denotes the matrix of partial derivative with respect to  $\mathbf{A}$  of the logdet function [Faz02, FHB04]. Inserting (4.2) in (4.1) and ignoring constant terms yields the optimization problem at the  $(k+1)$ -th iteration.

$$\min_{\mathbf{X}_\alpha^{(k+1)}} \operatorname{tr} \left( (\mathbf{X}_\alpha^{(k)} + \alpha \mathbf{I})^{-1} \mathbf{X}_\alpha^{(k+1)} \right) \quad (4.3a)$$

$$\text{s.t. } \mathbf{X}_\alpha^{(k+1)} \succeq \mathbf{0}, \quad (4.3b)$$

$$\operatorname{tr} (\mathbf{X}_\alpha^{(k+1)} \mathbf{H}_j) \geq \gamma_j \sigma_j^2, \quad j = 1, \dots, M, \quad (4.3c)$$

where  $\mathbf{X}_\alpha^{(k+1)}$  denotes the optimal solution at the  $(k+1)$ -th iteration. By setting  $\mathbf{X}_\alpha^{(1)} = \mathbf{I}$  for every value  $\alpha$ , the problem (4.3) is equivalent to the QoS problem (2.24) at the first iteration. Furthermore, for arbitrary points  $\mathbf{X}_\alpha^{(k)}$  problem (4.3) is approximately equal to the QoS problem of (2.24) for large values of  $\alpha$ . Problem (4.3) belongs to the class of semidefinite programs (SDP). Thus, it can be solved efficiently using interior point solvers and general purpose solvers such as cvx [GBY08, BV04]. Problem (4.3) has an appealing interpretation. It is an iteratively weighted version of the power minimization problem in (2.24). The power weighting reduces the costs of large eigenvalue components and increases the cost for low eigenvalue components of  $\mathbf{X}_\alpha^{(k+1)}$ , hence it encourages lower rank solutions. In order to compute a stationary point of (4.1) for a given value of  $\alpha$ , the upper bound of problem (4.3) is iteratively solved. The stationary point computation algorithm is outlined in Algorithm 3. The algorithm runs until the convergence criterion is met, i.e.,  $E^{(k)} = \frac{\|\mathbf{X}_\alpha^{(k+1)} - \mathbf{X}_\alpha^{(k)}\|_F}{\|\mathbf{X}_\alpha^{(k)}\|_F} \leq \epsilon$ , where  $\epsilon$  is a small precision value. At iteration  $k$ , the beamforming solution  $\mathbf{X}_\alpha^{(k+1)}$  and its corresponding rank  $R^{(k+1)}$  are updated accordingly.

Based on the results of the majorization-minimization approach [HP10b, p. 796], the following lemma can be presented.

**Lemma 2.** *Iteratively solving (4.3) using Algorithm 3 converges to a stationary point of (4.1).*

*Proof.* Consider the function

$$f(\mathbf{X}_\alpha) = \log \det (\mathbf{X}_\alpha + \alpha \mathbf{I}), \quad (4.4)$$

and its approximate function about  $\mathbf{X}_\alpha^{(k)}$  given by

$$\begin{aligned} g(\mathbf{X}_\alpha | \mathbf{X}_\alpha^{(k)}) = & \log \det (\mathbf{X}_\alpha^{(k)} + \alpha \mathbf{I}) \\ & + \operatorname{tr} \left( (\mathbf{X}_\alpha^{(k)} + \alpha \mathbf{I})^{-1} (\mathbf{X}_\alpha - \mathbf{X}_\alpha^{(k)}) \right). \end{aligned} \quad (4.5)$$

We have

$$f(\mathbf{X}_\alpha) \leq g(\mathbf{X}_\alpha | \mathbf{X}_\alpha^{(k)}). \quad (4.6)$$

Assume that  $\mathbf{X}_\alpha^{(k+1)}$  is a solution of the approximate problem at iteration  $k$ , then

$$f(\mathbf{X}_\alpha^{(k+1)}) \leq g(\mathbf{X}_\alpha^{(k+1)}|\mathbf{X}_\alpha^{(k)}) \leq g(\mathbf{X}_\alpha^{(k)}|\mathbf{X}_\alpha^{(k)}) = f(\mathbf{X}_\alpha^{(k)}). \quad (4.7)$$

Assume  $\Xi$  is the nonempty closed convex set defined by the problem constraints in (4.1b) to (4.1c) and the domain constraints of (4.1a). From (4.7), it can be concluded that the subset of the optimization solutions  $\{\mathbf{X}_\alpha \in \Xi | f(\mathbf{X}_\alpha) \leq f(\mathbf{X}_\alpha^{(1)})\}$  is compact since  $f(\mathbf{X}_\alpha^{(1)}) < \infty$ . Furthermore the functions  $f(\mathbf{X}_\alpha)$  and  $g(\mathbf{X}_\alpha|\mathbf{X}_\alpha^{(k)})$  are continuously differentiable and  $g(\mathbf{X}_\alpha|\mathbf{X}_\alpha^{(k)})$  is continuous in  $\mathbf{X}_\alpha$  and  $\mathbf{X}_\alpha^{(k)}$ . From the inequality in (4.7), it follows that

$$f(\mathbf{X}_\alpha^{(k+1)}) \leq g(\mathbf{X}_\alpha^{(k+1)}|\mathbf{X}_\alpha^{(k)}) \leq g(\mathbf{Y}|\mathbf{X}_\alpha^{(k)}) \quad \forall \mathbf{Y} \in \Xi. \quad (4.8)$$

Let  $k \rightarrow \infty$  and assume that the limit point of the iterative algorithm is  $\mathbf{Z}$ . The inequality (4.8) leads to

$$f(\mathbf{Z}) \leq g(\mathbf{Y}|\mathbf{Z}), \quad \forall \mathbf{Y} \in \Xi, \quad (4.9)$$

which can equivalently be expressed as

$$g(\mathbf{Y}|\mathbf{Z}) - f(\mathbf{Z}) \geq 0, \quad \forall \mathbf{Y} \in \Xi. \quad (4.10)$$

Substituting equations (4.5) and (4.4) in equation (4.10), results in

$$\text{tr}((\mathbf{Z} + \alpha\mathbf{I})^{-1}(\mathbf{Y} - \mathbf{Z})) \geq 0, \quad \forall \mathbf{Y} \in \Xi. \quad (4.11)$$

The set of stationary points is defined by [SBP17]

$$\Xi^* = \{\mathbf{X}_\alpha | \text{tr}(\nabla f(\mathbf{X}_\alpha)^H(\mathbf{Y} - \mathbf{X}_\alpha)) \geq 0, \forall \mathbf{Y} \in \Xi\}, \quad (4.12)$$

which is equivalent to

$$\Xi^* = \{\mathbf{X}_\alpha | \text{tr}((\mathbf{X}_\alpha + \alpha\mathbf{I})^{-1}(\mathbf{Y} - \mathbf{X}_\alpha)) \geq 0, \forall \mathbf{Y} \in \Xi\}. \quad (4.13)$$

From (4.11), it can be concluded that the limit point  $\mathbf{Z}$  is also a stationary point to the iterative Algorithm 3 [SBP17].  $\square$

In the following, two algorithms to iteratively determine suitable values for  $\alpha$  are proposed, one two scale algorithm and one single scale algorithm.



**Algorithm 3:** Stationary point computation algorithm

```

Input:  $E, \epsilon, \alpha, \mathbf{X}_\alpha^{(1)}, \mathbf{H}_j, \sigma_j, \gamma_j, j = 1, \dots, M$ 
Set  $k = 1$ .
begin
  while  $E \geq \epsilon$  do
    Solve the rank regularized beamforming problem in (4.3) to obtain  $\mathbf{X}_\alpha^{(k+1)}$ .
    Compute  $R^{(k+1)}$  and  $E = \frac{\|\mathbf{X}_\alpha^{(k+1)} - \mathbf{X}_\alpha^{(k)}\|_F}{\|\mathbf{X}_\alpha^{(k)}\|_F}$ .
    Set  $k = k + 1$ .
  end
end
return  $\mathbf{X}_\alpha^{(k)}, R^{(k)}$ .

```

## Two Scale Rank Reduction Algorithm

In this section a two scale algorithm is presented to compute a rank  $R$  beamforming solution for the QoS based beamforming single group multicasting problem in (4.1). The stationary points of problem (4.1) are computed sequentially for a sequence of decreasing regularization values  $\alpha^{(1)} \geq \alpha^{(2)} \geq \dots$  of  $\alpha$ .

The goal is to find a value of  $\alpha$  that yields stationary points that exhibit the desired rank  $R$  with reasonable transmit power.

In the  $\ell$ -th iteration, problem (4.3) is solved for a value of  $\alpha = \alpha^{(\ell)}$  using Algorithm 3. The value of the regularization variable  $\alpha^{(\ell)}$  is decreased at each iteration  $\ell$  using  $\alpha^{(\ell)} = \alpha^{(1)}/\ell$ . The algorithm runs until the rank of the solution is reduced to the desired value of  $R$ , i.e., until the number of eigenvalues that are larger than a predetermined small threshold is equal or less than  $R$ . The proposed algorithm is outlined in Algorithm 4.

Simulations show that the two scale rank regularized algorithm is successful in reducing the rank of the beamforming solutions in different network scenarios. However, this comes along with the high computational complexity. In the following, the one scale rank regularized algorithm will be provided to reduce the computational cost.

## One Scale Rank Reduction Algorithm

In this subsection, the one scale rank regularized beamforming problem is employed. The regularization parameter that yields the desired rank is sought. Simultaneously,

**Algorithm 4:** The two scale rank regularized algorithm

**Input:**  $\alpha^{(1)}$ ,  $R$ ,  $N$ ,  $\epsilon$ ,  $\mathbf{H}_j$ ,  $\sigma_j$ ,  $\gamma_j$ ,  $j = 1, \dots, M$   
 Set  $\ell = 1$  and  $R^{(1)} = N$  .  
**begin**  
   **while**  $R^{(\ell)} > R$  **do**  
     Set  $\mathbf{X}_{\alpha^{(\ell)}}^{(1)} = \mathbf{I}$ ,  $\alpha^{(\ell)} = \alpha^{(1)}/\ell$ ,  $k = 1$  and  $E = 1$ .  
     Call Algorithm 3 using  $E$ ,  $\epsilon$ ,  $\mathbf{H}_j$ ,  $\sigma_j$ ,  $\gamma_j$ ,  $j = 1, \dots, M$ ,  $\alpha^{(\ell)}$ ,  $\mathbf{X}_{\alpha^{(\ell)}}^{(1)}$ .  
     Set  $\mathbf{X}_{\alpha^{(\ell)}}^{(\ell+1)} = \mathbf{X}_{\alpha^{(\ell)}}^{(k)}$ ,  $R^{(\ell+1)} = R^{(k)}$  and  $\ell = \ell + 1$  .  
   **end**  
**end**  
**return**  $\mathbf{X}_{\alpha^{(\ell)}}^{(k)}$ ,  $R^{(k)}$ .

the beamforming problem in (4.3) is solved. The purpose of the algorithm is to reduce the high computational demand of Algorithm 4, where the optimization problem is solved for each value of  $\alpha$  until convergence to a stationary point, which is an unnecessary overhead. The value of  $\alpha^{(k+1)}$  at the  $(k+1)$ -th iteration is decreased smoothly with  $\alpha^{(k)}$  using the eigenvalues of the beamforming solutions of indexes larger than the desired rank  $R$ . This can be expressed by

$$\alpha^{(k+1)} = (1 - q^{(k+1)})^\beta \alpha^{(k)}, \quad (4.14)$$

where  $q^{(k+1)} = \sum_{j=R+1}^{R^{(k+1)}} \lambda_j^{(k)} / \text{tr}(\mathbf{X}_{\alpha^{(k)}}^{(k)})$ ,  $R^{(k+1)} > R$  and  $\lambda_j^{(k)}$  is the  $j$ th eigenvalue of the beamforming solution for  $\mathbf{X}_{\alpha^{(k)}}^{(k)}$  at the  $k$ th iteration.

Notice that the value of  $\beta$  can be chosen to control the speed of decreasing  $\alpha^{(k+1)}$ . Choosing a small value of  $\beta$  means a small decrease of  $\alpha^{(k+1)}$  proportional to the decrease of the rank at iteration  $(k+1)$  denoted by  $1 - q^{(k+1)}$ , where  $\text{tr}(\mathbf{X}_{\alpha^{(k)}}^{(k)})$  is employed as a rank approximation. This can also be useful to ensure small, however non-zero values of  $\alpha^{(k)}$ , due to  $1 - q^{(k+1)} < 1$  and  $q^{(k+1)} > 0$  for  $R^{(k+1)} > R$ . The value of  $\beta$  can be chosen to balance the performance in terms of transmit power and the execution time that is required to solve the iterative algorithm. The value of  $\beta$  is chosen to be smaller or equal to one. As in Algorithm 4, the iterative one scale Algorithm 5 starts by solving the conventional optimization problem (2.24) by setting  $\mathbf{X}_{\alpha^{(1)}}^{(1)} = \mathbf{I}$  and an initial value of the regularization variable  $\alpha^{(1)}$ , then the optimization problem in (4.3) is solved and the values of  $\mathbf{X}_{\alpha^{(k+1)}}^{(k+1)}$  and  $\alpha^{(k+1)}$  are updated at the  $(k+1)$ -th iteration. The algorithm stops when the desired rank is achieved.

**Algorithm 5:** The one scale rank regularized algorithm

**Input:**  $\alpha^{(1)}, R, N, \epsilon, \mathbf{H}_j, \sigma_j, \gamma_j, j = 1, \dots, M$   
Set  $k = 1, \mathbf{X}_{\alpha^{(1)}}^{(1)} = \mathbf{I}$  and  $R^{(1)} = N$ .  
**begin**  
  **while**  $R^{(k)} > R$  **do**  
    Solve the rank regularized beamforming problem in (4.3) to obtain  $\mathbf{X}_{\alpha^{(k)}}^{(k+1)}$ .  
    Update  $\alpha^{(k+1)}$  using (4.14).  
    Compute  $R^{(k+1)}$ .  
    Set  $k = k + 1$ .  
  **end**  
**end**  
**return**  $\mathbf{X}_{\alpha^{(k)}}^{(k)}, R^{(k)}$ .

### 4.3 Computational Complexity of Algorithm 5

Interior point methods are used by the existing SDP solvers such as SeDuMi to provide solutions of the optimization problems as in (2.24) [KSL08b, HRVW96]. The worst case computational complexity problem of (4.3) using a single iteration is  $O(\sqrt{N}(N^6 + MN^2)\log(1/\xi))$ , where  $\xi$  represents the solutions' precision achieved at the interior iterative method [KSL08b, WSC<sup>+</sup>14]. Assuming that Algorithm 5 is solved in  $K$  iterations at the maximum, then the worst case complexity of Algorithm 5 is given by  $O(K\sqrt{N}(N^6 + MN^2)\log(1/\xi))$ . This means that the complexity of the proposed approach scales with the number of iterations. It is worth noting that this complexity is for the worst case scenario, thus in real scenarios these values are much smaller.

## 4.4 Simulation Results

In the following, several rank reduction algorithms, namely MU, Consensus-alternating Direction Method of Multipliers (ADMM) and Successive Linear Approximation (SLA), are generalized to produced general rank  $R$  solutions rather than the rank one beamforming vectors, for the purpose of performance evaluation of Algorithms 4 and 5.

### 4.4.1 A Generalization of the MU Algorithm

As mentioned in Chapter 2, the MMF (max-min fair) optimization problem maximizes the minimum user SNR subject to the transmit power constraint. The conventional

iterative MU algorithm proposed by [GS15] solves the MMF problem in (2.28), by updating the beamformer vector using the inverse of the weighted SNR gradient vectors of all users. A generalization of the MU algorithm is presented in Algorithm 6, where  $e$  denotes a small positive scalar used for numerical stability.

<b>Algorithm 6:</b> The MU algorithm	
<b>Input:</b>	$e, \epsilon, \mathbf{H}_j, j = 1, \dots, M$
1	Choose $\mathbf{W}^{(1)}$ randomly.
2	Scale the Frobenius norm of $\mathbf{W}^{(1)}$ to one .
3	Set $E = 1$ and $k = 1$ .
	<b>begin</b>
4	<b>while</b> $E > \epsilon$ <b>do</b>
5	Set $\mathbf{W}_{\text{MU}} = \sum_{j=1}^M \frac{\mathbf{H}_j \mathbf{W}^{(k)}}{\ \mathbf{W}^{(k)}\mathbf{H}_j \mathbf{W}^{(k)}\ _{F+e}}$ .
6	Set $\mathbf{W}_{\text{MU}} = \frac{\mathbf{W}_{\text{MU}}}{\ \mathbf{W}_{\text{MU}}\ _F}$ .
7	Set $E = \ \mathbf{W}_{\text{MU}} - \mathbf{W}^{(n)}\ _F$ .
8	Set $\mathbf{W}^{(k+1)} = \mathbf{W}_{\text{MU}}$ .
9	Set $k = k + 1$ .
	<b>end</b>
	<b>end</b>
10	<b>return</b> $\mathbf{W}_{\text{MU}}$ .

#### 4.4.2 A Generalization of the ADMM Algorithm

A generalization of consensus-ADMM algorithm for single-group multicast beamforming is presented in this section [HS16]. The iterative algorithm starts with a randomly generated beamformer. A scaling is necessary to satisfy the SNR constraints as in the conventional QoS problem in (2.21). The non-convex quadratically constrained quadratic problem (QCQP) is solved using multiple sub-problems, each one is a QCQP with a single constraint. A small value of  $\rho$  provides better performance in terms of convergence. Similar to [HS16],  $\rho$  is chosen to be  $\rho = 2\sqrt{M}$ . Furthermore, the ADMM algorithm is initialized by the beamformer  $\mathbf{W}_{\text{MU}}$ , as it provides faster convergence and better performance. Assuming  $\mathbf{W}_{\text{ADMM}}$  is  $R \times N$  and  $\mathbf{H}_s$  is the matrix of all channel vectors, the ADMM is introduced in Algorithm 7.

#### 4.4.3 A Generalization of the SLA procedure

An idea very close to the inner approximation procedure is proposed in [THJ14]. Taylor series expansion is used to linearize the non-convex term of the optimization problem

of (2.24) for a general rank  $R$ . A generalization of the SLA procedure leads to

$$\min_{\mathbf{W}_{\text{SLA}}} \|\mathbf{W}_{\text{SLA}}\|_F^2 \quad (4.15\text{a})$$

$$\text{s.t.} \quad \text{tr}\left(\mathbf{W}^{(k)}\mathbf{W}^{(k)\text{H}}\mathbf{H}_j\right)+2\text{tr}\left(\text{Re}\left(\mathbf{W}^{(k)}\left(\mathbf{W}_{\text{SLA}}-\mathbf{W}^{(k)}\right)^{\text{H}}\mathbf{H}_j\right)\right)\geq\gamma_j \quad j=1,\dots,M. \quad (4.15\text{b})$$

Similar to the inner approximation algorithm in Chapter 3.6, the SLA procedure is randomly initialized and iterates until the difference  $\|\mathbf{W}_{\text{SLA}} - \mathbf{W}^{(k)}\|_F \leq \epsilon$ . The authors of [GS15], use the SLA procedure initialized with  $\mathbf{W}_{\text{MU}}$  to boost the performance in the MU-SLA procedure and iterate the SLA algorithm just once. Similar approach is followed in this work to produce the generalized MU-SLA (G-MU-SLA).

In the simulations, the number of transmit antennas at BS is assumed to be  $N = 12$ , the SNR at each user  $\text{SNR}_j = 10$  dB and SNR threshold  $\gamma_j = 10$  dB. Moreover, we assume independent flat Rayleigh fading channel with circularly symmetric unit-variance channel coefficients. The simulation results are averaged over 100 Monte-Carlo runs.

For the first set of simulation results, the BS applies OSTBC to send the  $T \times R$  code matrix  $\mathbf{S}$ , where  $T = 4$ ,  $R = 4$  and the channel coefficients are known both at the BS and the users.

Moreover, the simulations are performed in Matlab on a Linux desktop using 8 x Intel i7-4790K cores and 32 GB of RAM.

Figure 4.1 shows the rank of the beamforming solutions for multicasting scenario of a group of 400 users for QoS problem using the SDR relaxation technique (2.24) and the proposed Algorithms of 4 and 5. It can be seen from Figure 4.1 that the rank of most of the SDR solutions is 8. The simulations depict that both proposed algorithms are successful in reducing the rank of the SDR solutions for a system of large number of users to a value equal or less than  $R$ . All the solutions of Algorithms 4 and 5 are of rank 4.

The precision value is set to  $\epsilon = 10^{-2}$  for SLA, MU-SLA, Algorithm 4 and the inner approximation algorithms. For the ADMM Algorithm 7 and MU Algorithm 6 the value is set  $\epsilon = 10^{-4}$ . The ADMM and SLA are initialized with the beamforming matrix  $\mathbf{W}_{\text{MU}}$  and the number of iterations is set to one in the SLA as in [THJ14]. Furthermore,  $\alpha^{(0)} = 2$  for both Algorithm 4 and Algorithm 5 and  $\beta = 1$  for Algorithm 5. The number of iterations is  $K = 10^3$  for the randomization procedure.

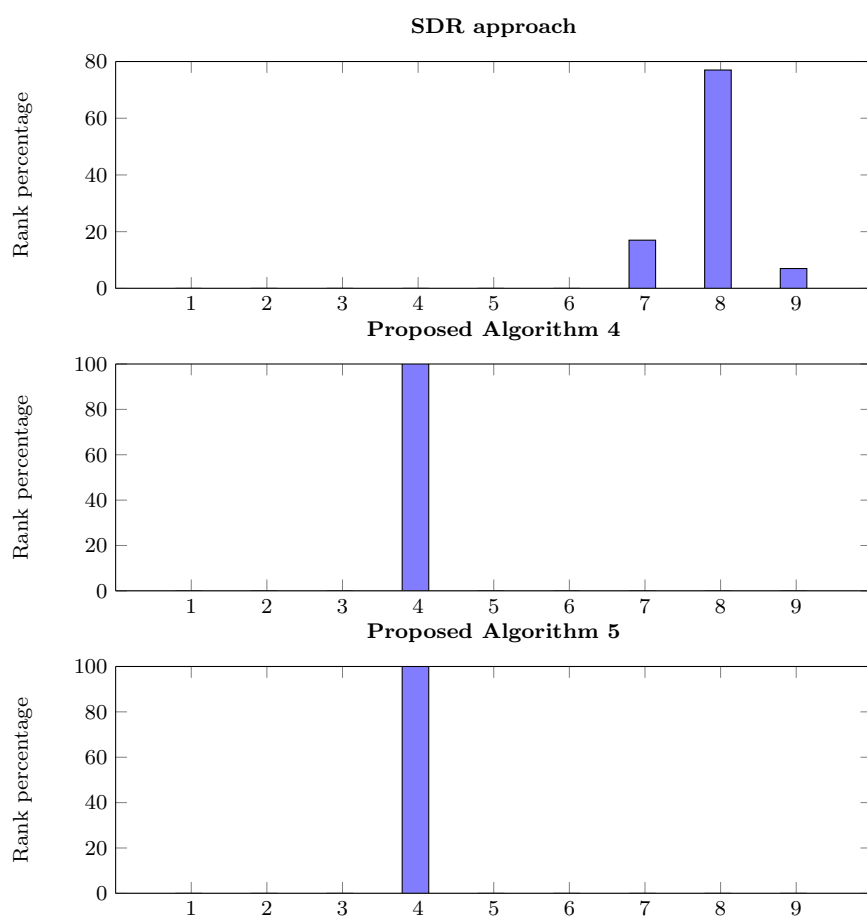


Figure 4.1. The rank percentage for a system with  $M = 400$  users

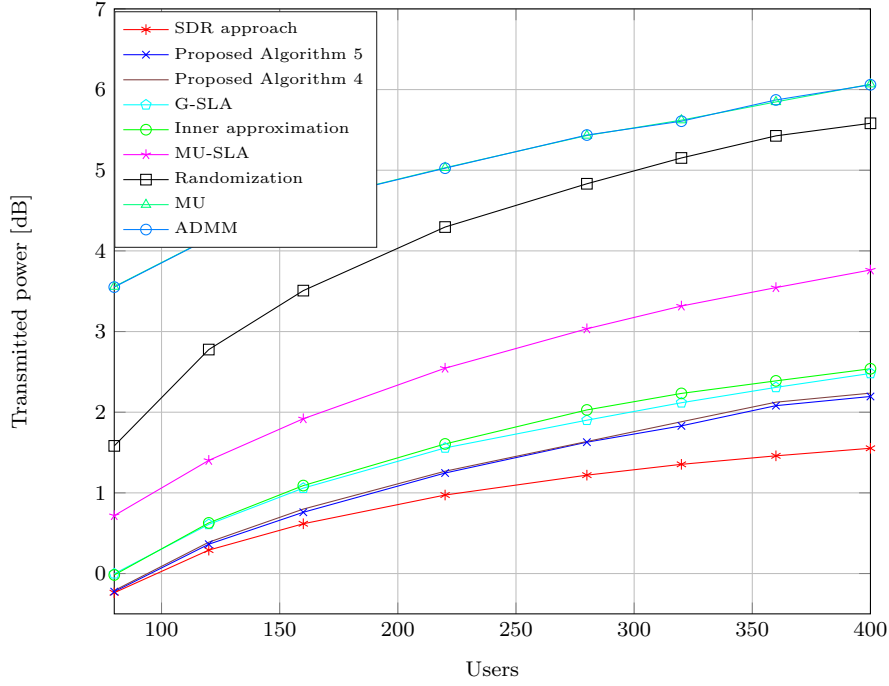


Figure 4.2. The transmit power in dB with varying number of users for  $\alpha^{(0)} = 2$  and  $\beta = 1$

In Figure 4.2 the transmit power is displayed versus the number of users for the proposed approaches, the QoS SDR design, the randomization procedure of Algorithm 1 using the solutions of the SDR technique, MU Algorithm 6, SLA algorithm, MU-SLA, ADMM Algorithm 7 and the inner approximation algorithm. We assume  $\gamma_j = 10$  dB for each user and each compared algorithm. As seen from Figure 4.2 both SLA and the inner approximation algorithms perform almost the same. Both proposed Algorithms 4 and 5 perform equally and outperform both G-SLA and inner approximation designs by approximately 0.3 dB for a group of 400 users. Moreover, the proposed Algorithms 4 and 5 have approximately 1.6 dB less transmit power compared with the MU-SLA algorithm.

Both MU and the ADMM procedure have the worst transmit power compared to the other approaches. The performance of the ADMM can be improved by choosing a smaller value of  $\epsilon$  or more simulation runs.

In Figure 4.3, the transmit power is normalized for each approach to one and the average minimum SNR for different number of users is displayed. Both proposed designs outperform all the state-of-the-art approaches and have approximately equal performance gap of 0.6 dB compared with the optimal SDR approach.

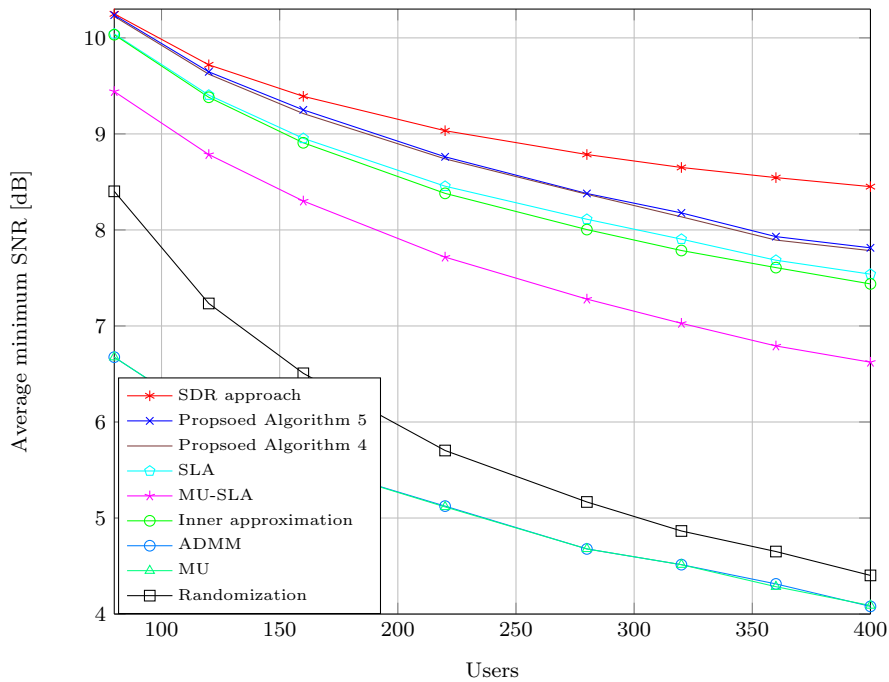


Figure 4.3. System performance of average minimum SNR with varying number of users for SNR threshold  $\gamma_j = 10$  dB,  $\alpha^{(0)} = 2$  and  $\beta = 1$

In Figure 4.4, the execution time is shown for each approach assuming different number of users. It is clear that the execution time for the proposed designs increases with increasing the number of users and Algorithm 4 is more time consuming as it has two nested loops, one for decreasing the  $\alpha$  and the other is for solving the optimization problem until reaching the required precision value  $\epsilon$ . Thus, the number of iterations for Algorithm 4 is relatively larger compared to Algorithm 5. Algorithm 5 has high time complexity compared with the SLA and inner approximation algorithms. However, choosing a smaller value of  $\alpha^{(0)}$  leads to better convergence time for Algorithm 5 with approximately the same transmit power as in Figure 4.2 as will be shown in the following simulation results in more details.

In Figure 4.5, the transmit power is shown for different number of users for our approaches and the state-of-the-art- approaches assuming  $\alpha^{(0)} = 1$  and  $\beta = 1$ . It can be noticed that the transmit power for Algorithm 5 is the same compared with the transmit power in Figure 4.2. However, the transmit power for Algorithm 4 is slightly increased compared with the scenario of  $\alpha^{(0)} = 2$ .

The same observation can be concluded regarding the minimum user SNR as in Figure 4.6



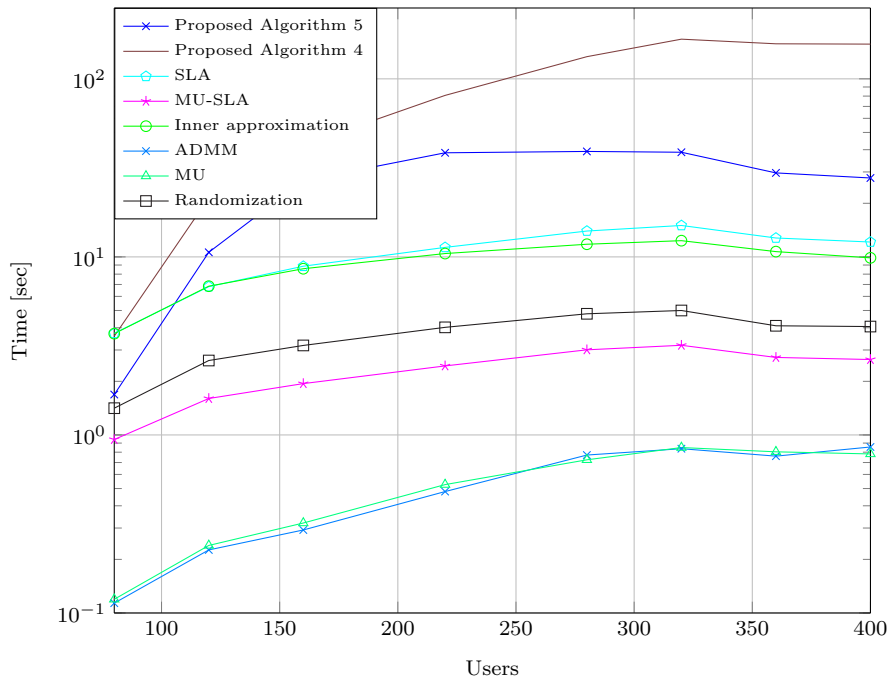


Figure 4.4. Execution time in sec with varying number of users for  $\sigma_j^2 = 0.1$ ,  $\alpha^{(0)} = 2$  and  $\beta = 1$

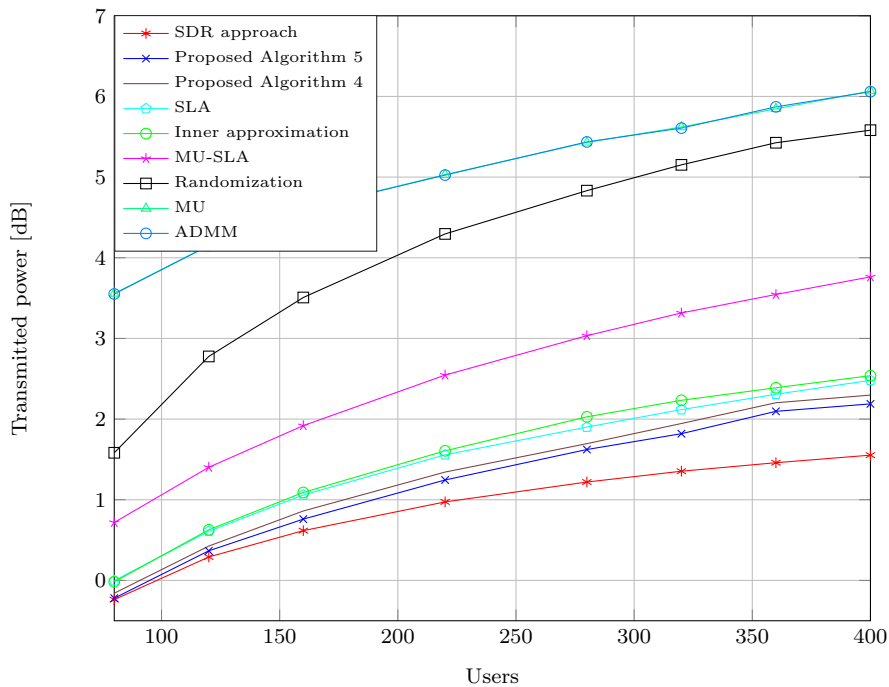


Figure 4.5. The transmit power in dB with varying number of users for  $\alpha^{(0)} = 1$  and  $\beta = 1$

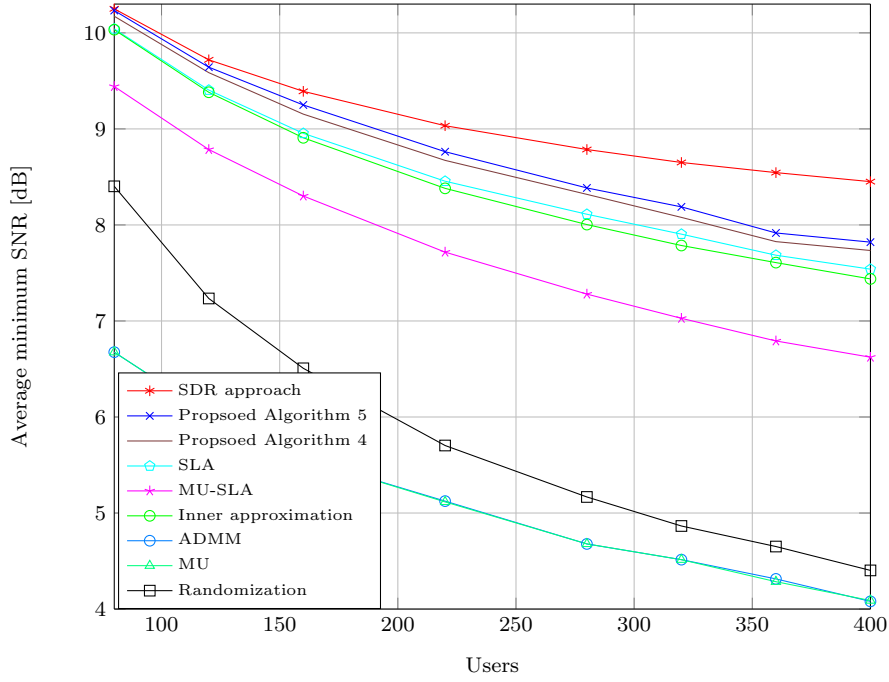


Figure 4.6. System performance of average minimum SNR with varying number of users for SNR threshold  $\gamma_j = 10$  dB,  $\alpha^{(0)} = 1$  and  $\beta = 1$

In Figure 4.7 the execution time of the proposed designs is compared with the state-of-the-art approaches. It can be noticed that the time complexity for Algorithm 5 is reduced and the transmit power is reserved compared with the scenario of  $\alpha^{(0)} = 2$ , thus a smaller initial value of the regularization variable is used in the next simulation results.

In Figure 4.8, Figure 4.9 and Figure 4.10 it is assumed that  $\alpha^{(0)} = 0.4$  and  $\beta = 1$ . Compared with the previous simulation results for  $\alpha^{(0)} = 2$  the transmit power for a group of 400 users has slightly increased by approximately 0.04 dB for Algorithm 5. However, a power increase of 0.3 dB for Algorithm 4 can be noticed in Figure 4.8, the average minimum SNR in Figure 4.9 has decreased by 0.04 dB and 0.3 dB for Algorithm 5 and Algorithm 4, respectively. However, the time complexity is improved for both approaches, where a convergence is achieved in 20.75 and 88.31 seconds in average for Algorithm 5 and Algorithm 4, respectively, for a group of 400 users as in Figure 4.10.

In the next example the values  $\alpha^{(0)} = 1/R^{(0)}$  and  $\beta = 0.1$  are chosen such that the initial value of  $\alpha^{(0)}$  is proportional to the rank of the QoS solutions and a small value of  $\beta$  decreases the value of  $\alpha(k)$  at the  $k$ th iteration smoothly. The transmit power, the average minimum SNR and the average time are depicted in Figure 4.11, Figure 4.12

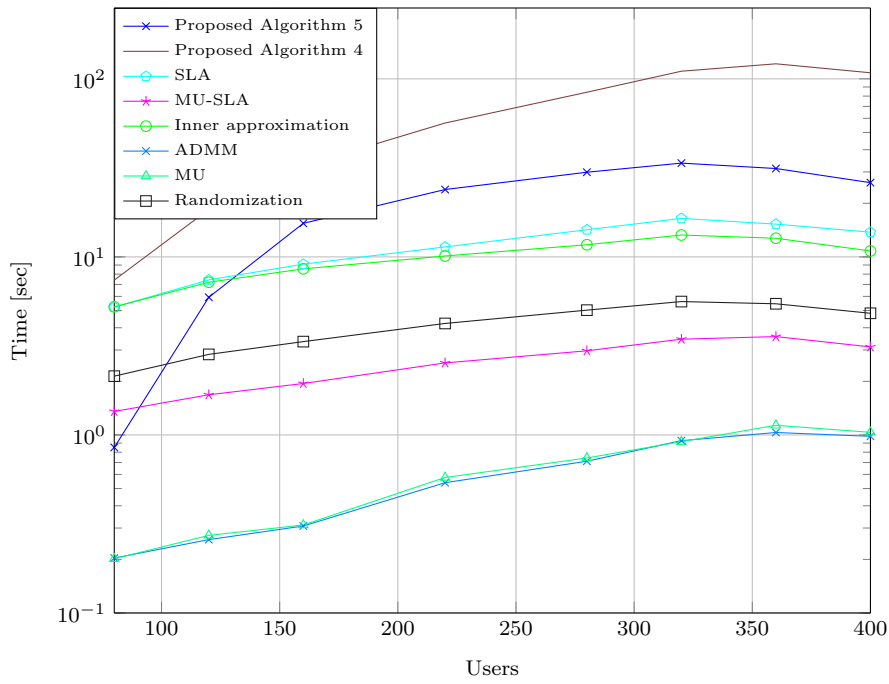


Figure 4.7. Execution time in sec with varying number of users for  $\sigma_j^2 = 0.1$ ,  $\alpha^{(0)} = 1$  and  $\beta = 1$

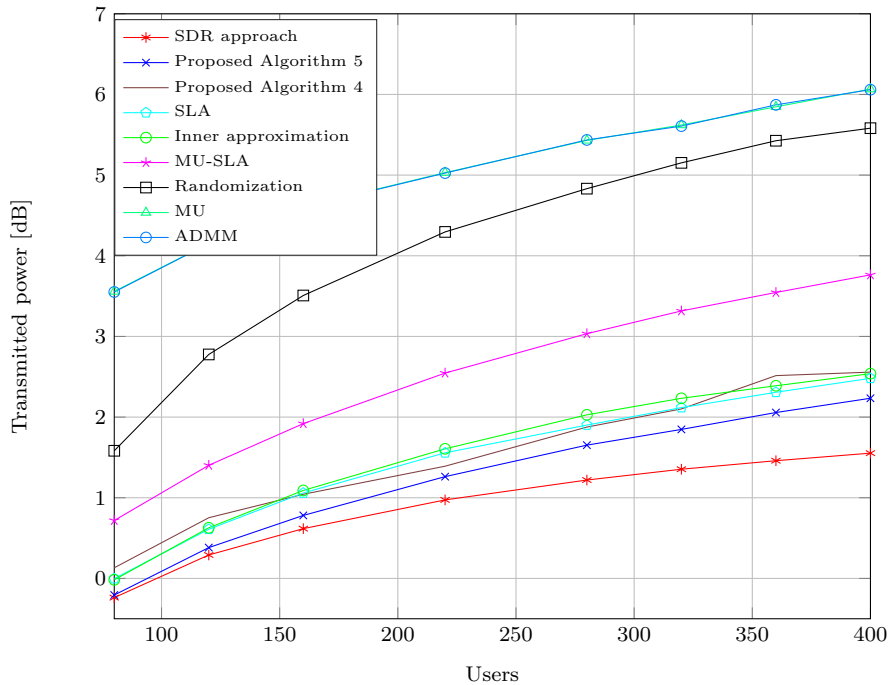


Figure 4.8. The transmit power in dB with varying number of users for  $\alpha^{(0)} = 0.4$  and  $\beta = 1$

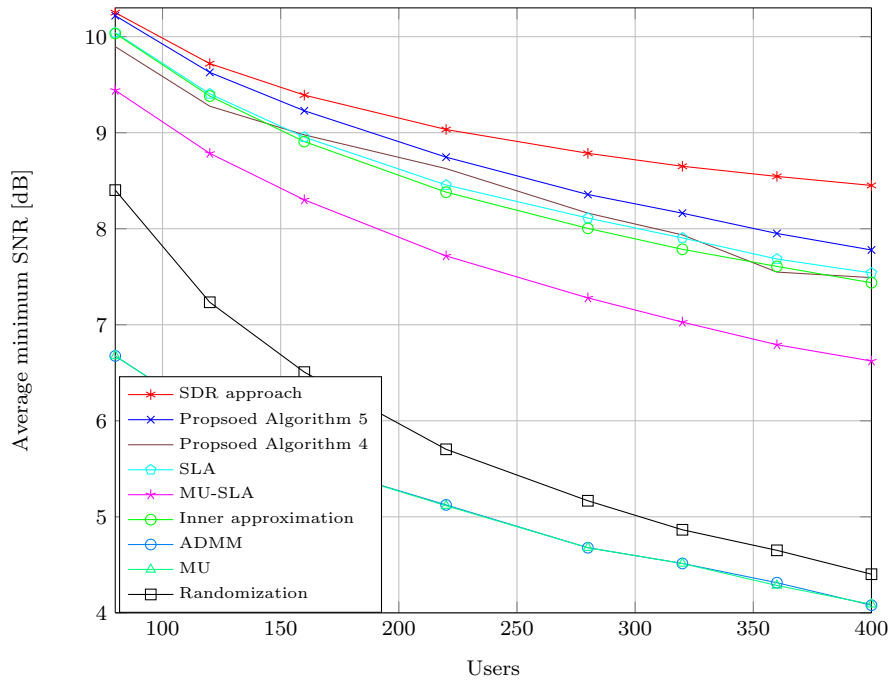


Figure 4.9. System performance of average minimum SNR with varying number of users for SNR threshold  $\gamma_j = 10$  dB,  $\alpha^{(0)} = 0.4$  and  $\beta = 1$

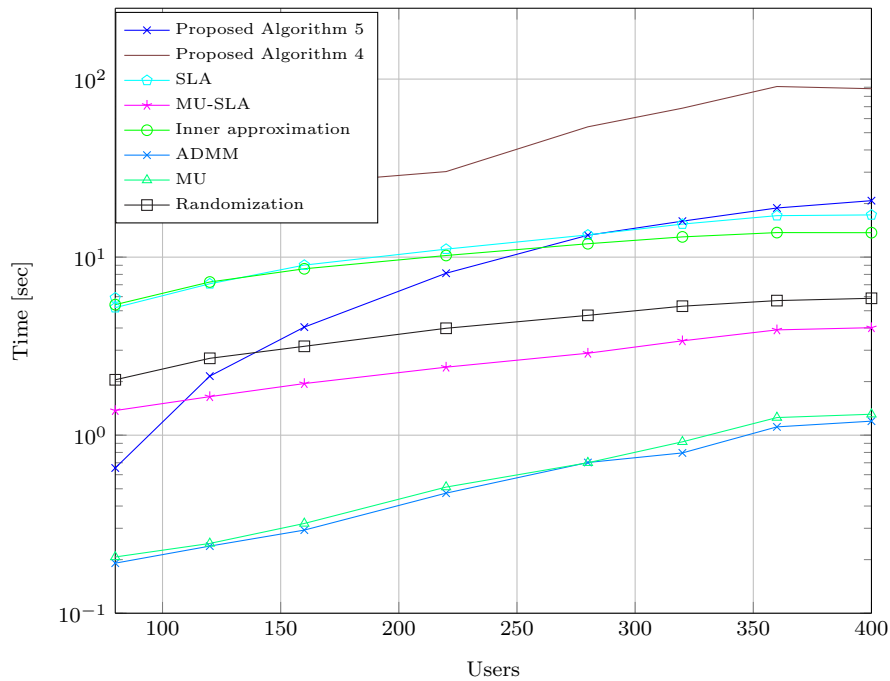


Figure 4.10. Computational time in sec with varying number of users for  $\sigma_j^2 = 0.1$ ,  $\alpha^{(0)} = 0.4$  and  $\beta = 1$

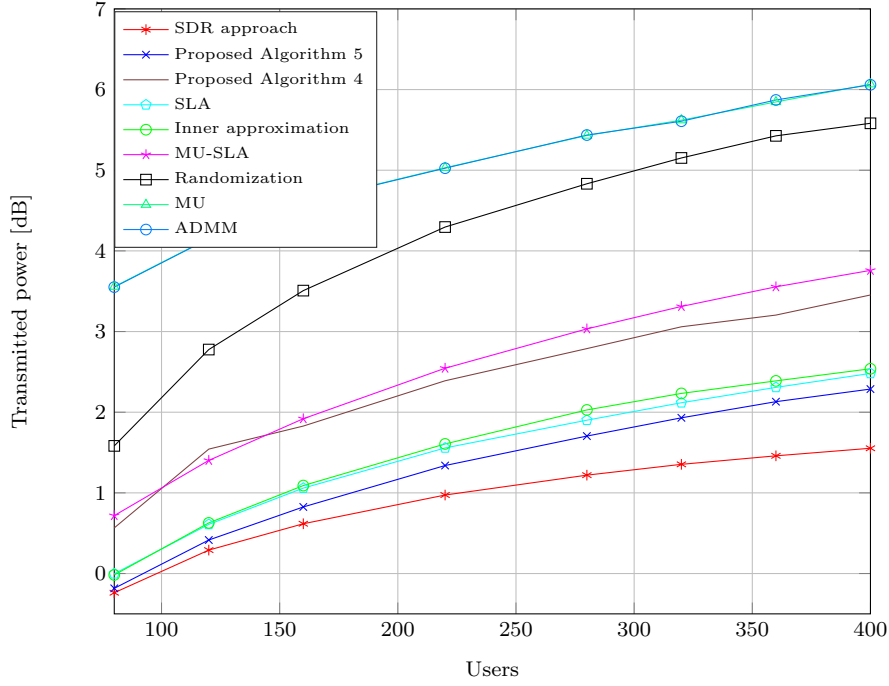


Figure 4.11. The transmit power in dB with varying number of users for  $\alpha^{(0)} = 1/R^{(0)}$  and  $\beta = 0.1$

and Figure 4.13, respectively. The performance of Algorithm 5 in terms of transmit power and average minimum SNR outperforms the competing approaches. However, the performance of Algorithm 4 is worse than both inner approximation and G-SLA approaches. Moreover, the time complexity of Algorithm 5 has improved significantly and outperforms both G-SLA and inner approximation methods. The time complexity of Algorithm 4 has improved. However, due to the nested loops based design, Algorithm 4 has a larger execution time compared with all the other approaches as shown in Figure 4.13. It can be concluded that Algorithm 5 is less sensitive to the initial value of  $\alpha$  compared to Algorithm 4 in terms of transmit power. However, the time complexity decreases significantly by choosing a small value of  $\alpha^{(0)}$ .

Figure 4.14 displays the average symbol-error rate (SER) versus  $\frac{1}{\sigma_j^2}$  for  $10^6$  different Monte-Carlo runs assuming OSTBC code at the BS and a group of 300 users as in [STPS17]. Assuming  $\alpha^{(0)} = 0.4$  and  $\beta = 1$ , the proposed approach in Algorithm 5 outperforms all the state-of-the-art designs in terms of the SER. For  $\text{SER} = 3 \cdot 10^{-6}$  Algorithm 5 performs approximately 0.5 dB better than both G-SLAs and, for  $\text{SER} = 1 \cdot 10^{-5}$ , 1 dB better than Algorithm 4.

The value of the desired rank  $R$  is changed for the following simulation results. The simulation results of Algorithm 4 are excluded due to the high computational complex-

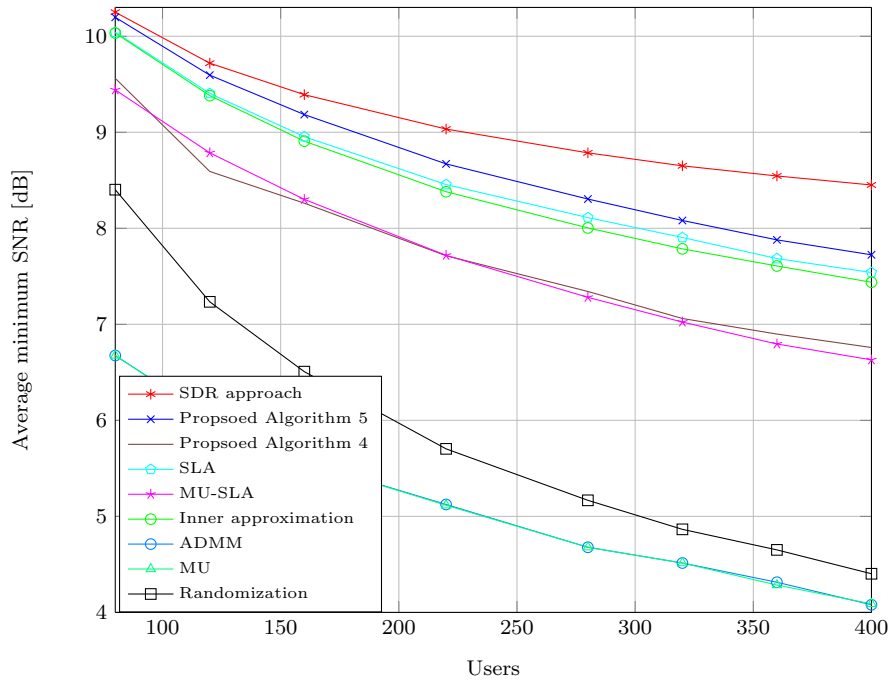


Figure 4.12. System performance of average minimum SNR with varying number of users for SNR threshold  $\gamma_j = 10$  dB,  $\alpha^{(0)} = 1/R^{(0)}$  and  $\beta = 0.1$

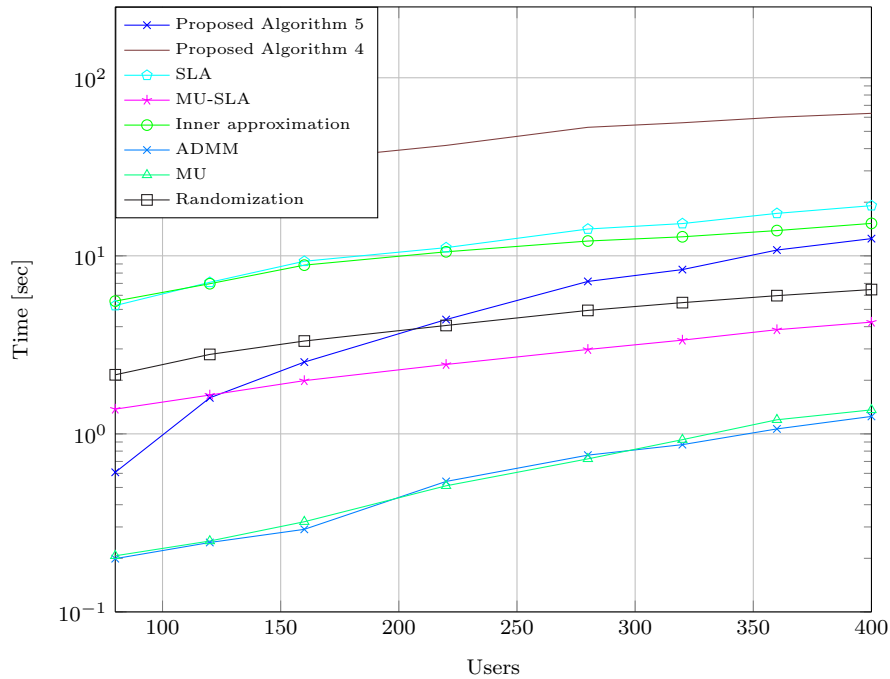


Figure 4.13. Computational time in sec with varying number of users for  $\sigma_j^2 = 0.1$ ,  $\alpha^{(0)} = 1/R^{(0)}$  and  $\beta = 0.1$

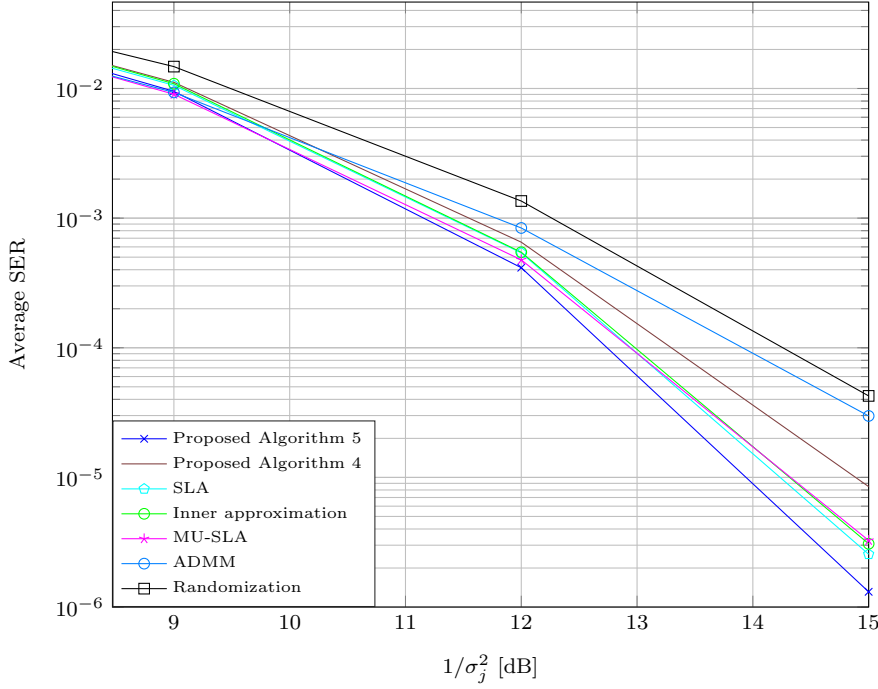


Figure 4.14. System performance of SER plotted against SNR in dB for  $M = 300$  users,  $\alpha^{(0)} = 0.4$  and  $\beta = 1$

ity. Algorithm 5 is capable of reducing the rank to  $R$  in each simulation scenario and each Monte-Carlo run, assuming  $\alpha^{(0)} = 1/R^{(0)}$  and  $\beta = 0.1$

It is easy to convey that reducing the value of  $R$  to 3 increases the transmit power for each simulated design. However, the proposed Algorithm 5 outperforms all the compared designs in terms of the transmit power shown in Figure 4.15 and minimum SNR shown in Figure 4.16.

A further reducing  $R$  to 2 leads to similar simulation results as in the previous scenarios. The transmit power versus the number of user is depicted in Figure 4.17. The minimum SNR versus the number of users is displayed in Figure 4.18.

## 4.5 Summary

In this chapter, a new rank regularized beamforming technique for multicasting transmit general rank beamforming networks is introduced, where the rank reduction proposed in [HP10b, HP10a] cannot be applied, as the rank is larger than the threshold

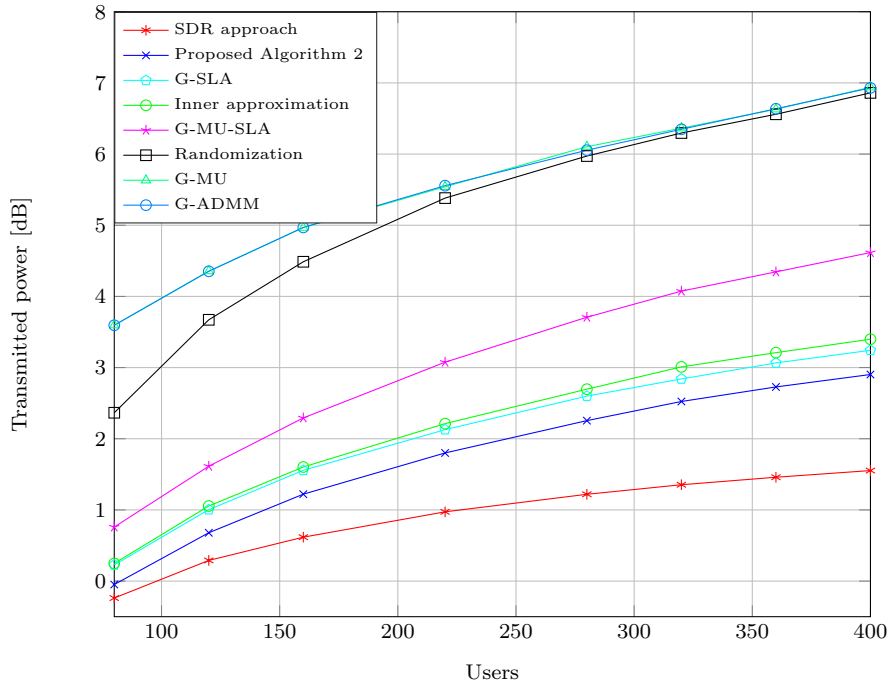


Figure 4.15. The transmit power in dB with varying number of users for  $R = 3$ ,  $\alpha^{(0)} = 1/R^{(0)}$  and  $\beta = 0.1$

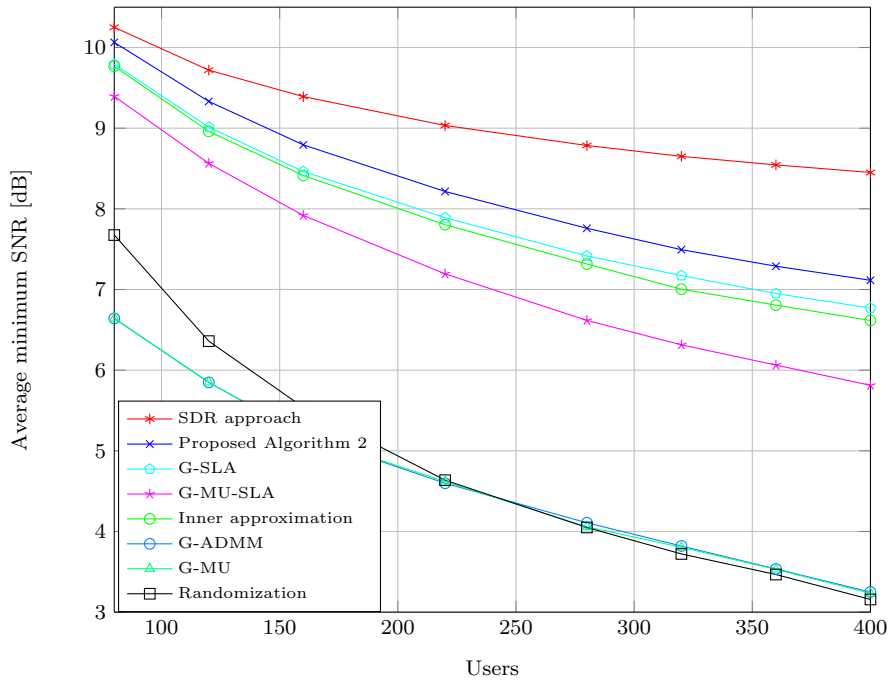


Figure 4.16. System performance of average minimum SNR with varying number of users for SNR threshold  $\gamma_j = 10$  dB,  $R = 3$ ,  $\alpha^{(0)} = 1/R^{(0)}$  and  $\beta = 0.1$



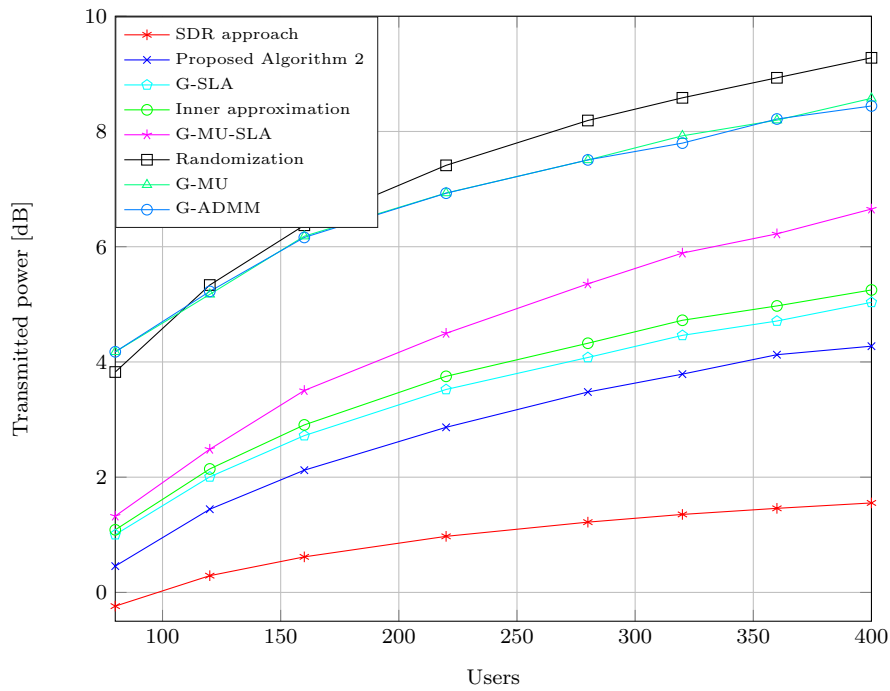


Figure 4.17. The transmit power in dB with varying number of users for  $R = 2$ ,  $\alpha^{(0)} = 1/R^{(0)}$  and  $\beta = 0.1$

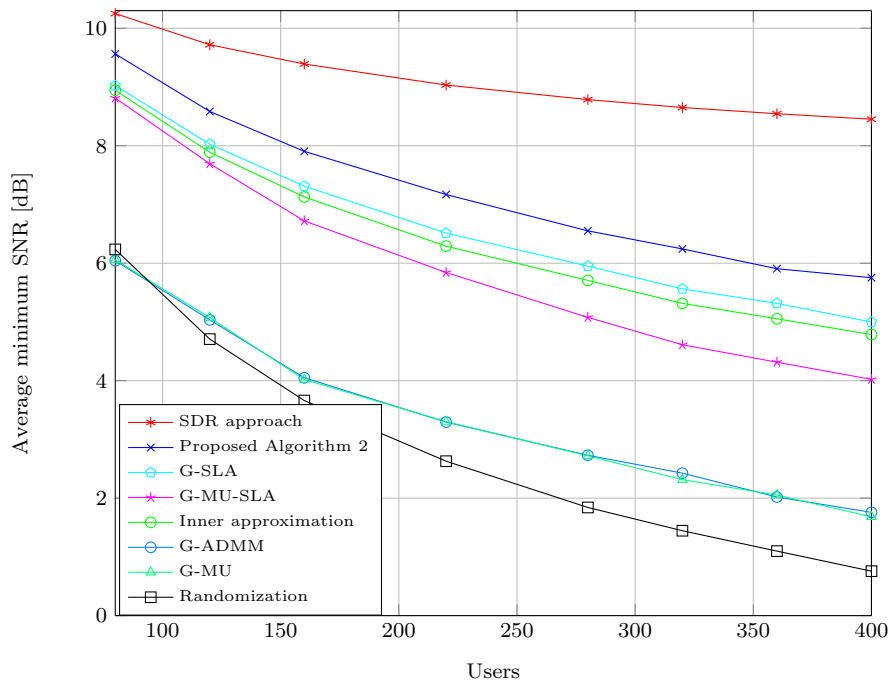


Figure 4.18. System performance of average minimum SNR in dB with varying number of users for SNR threshold  $\gamma_j = 10$  dB,  $R = 2$ ,  $\alpha^{(0)} = 1/R^{(0)}$  and  $\beta = 0.1$

given by  $\sqrt{M}$ . Two algorithms are proposed to regularize the rank of the beamforming problem assuming a network of single group of users. The two scale iterative algorithm utilizes two nested loops to reduce the rank sequentially using decreasing values of the regularization variable. A smooth regularization of the rank function is employed, where a Taylor approximation is used to linearize the surrogate function and obtain a convex optimization problem. On the other hand, the one scale algorithm solves the problem iteratively, however, the value of the regularization variable is degraded proportionally to the reduced rank. The Generalization of many beamforming designs, namely SLA, MU-SLA, MU and ADMM were provided to reduce the rank of the transmit beamforming problem to the desired value. It has been shown that the rank can be reduced efficiently using the iterative Algorithm 4 and Algorithm 5, even for systems with large number of users. The proposed approaches enjoy the best performance in terms of the transmit power, minimum SNR, SER compared with the state-of-the-art approaches. Additionally, it has been shown that the one scale algorithm has an efficient average computational time compared with the best state-of-the-art methods.

**Algorithm 7:** The generalized ADMM algorithm

**Input:**  $M, \epsilon, \mathbf{H}_j, \sigma_j, \gamma_j, j = 1, \dots, M$

- 1 Choose  $\mathbf{W}_{\text{ADMM}}$  randomly and scale it to satisfy the most violated constraint.
- 2 Set  $\mathbf{Z}_s = M\mathbf{W}_{\text{ADMM}}, \mathbf{U}_s = \mathbf{0}, \rho = 2\sqrt{M}, E = 1$  and  $\mathbf{g}_j = \mathbf{0}, j = 1, \dots, M$ .

**begin**

- 3 **while**  $E > \epsilon$  **do**
- 4   Set  $\mathbf{W}_s = \frac{1}{M+\rho^{-1}} (\mathbf{Z}_s + \mathbf{U}_s)$ .
- 5   **for**  $j \in \{1, \dots, M\}$  **do**
- 6     Set  $\mathbf{q}_j = \mathbf{h}_j^H \mathbf{W}$ .
- 7     **if**  $\{\|\mathbf{q}_j - \mathbf{g}_j\|_F < 1\}$  **then**
- 8       Set  $\mathbf{v}_j = \frac{(\mathbf{q}_j - \mathbf{g}_j)}{\|\mathbf{q}_j - \mathbf{g}_j\|_F} \frac{(1 - \|\mathbf{q}_j - \mathbf{g}_j\|_F)}{\|\mathbf{h}_j\|_F}$ .
- 9       **else**
- 9       Set  $\mathbf{v}_j = \mathbf{0}$ .
- 9       **end**
- 9     **end**
- 10    Set  $\mathbf{Z}_s = M\mathbf{W}_s - \mathbf{U}_s + \mathbf{H}_s \mathbf{V}_s$ .
- 11    Set  $\mathbf{U}_s = \mathbf{U}_s + \mathbf{Z}_s - M\mathbf{W}_s$ .
- 12    **for**  $j \in \{1, \dots, M\}$  **do**
- 13     Set  $\mathbf{q}_j = \mathbf{h}_j^H \mathbf{W}_s$ .
- 14     **if**  $\|\mathbf{q}_j - \mathbf{g}_j\|_F < 1$  **then**
- 15       Set  $\mathbf{g}_j = \frac{(\mathbf{q}_j - \mathbf{g}_j)}{\|\mathbf{q}_j - \mathbf{g}_j\|_F} (1 - \|\mathbf{q}_j - \mathbf{g}_j\|_F)$ .
- 16       **else**
- 16       Set  $\mathbf{g}_j = \mathbf{0}$ .
- 16       **end**
- 16     **end**
- 16    **end**
- 17    Set  $E = \|\mathbf{W}_s - \mathbf{W}_{\text{ADMM}}\|_F$ .
- 18    Set  $\mathbf{W}_{\text{ADMM}} = \mathbf{W}_s$ .
- 18    **end**
- 18    **end**
- 19 **return**  $\mathbf{W}_{\text{ADMM}}$ .



---

## Chapter 5

# Conclusion and Outlook

Transmit beamforming techniques are used in multicasting networks to steer the information in the desired directions of the users. Two famous designs, namely QoS and MMF problems, are employed to obtain the beamforming vectors. Both optimization problems are NP-hard, thus the SDR technique is used to relax the non-convex problem and obtain the beamforming solutions. In this thesis, we considered the scenario of single group multicasting, where a single group of users receives the same information transmitted by the BS. For single group multicasting networks with a large number of users, the beamforming solutions of the state-of-the-art rank one and rank two based beamforming designs are non-optimal in terms of the design metrics. Due to this fact, the performance of the whole multicasting network degrades severely as the number of the network users grows. As part of this thesis, general rank transmit beamforming designs are developed for the scenario of multicasting networks, where the BS transmits the same information to a single group of users. Various methods are provided, to increase the degrees of freedom and improve the overall system performance in order to enable the BS to serve an increased number of users with optimal beamformers compared with the rank one and rank two transmit beamforming designs. Moreover, a rank regularization algorithm is provided to reduce the rank of the obtained beamforming solutions to the desired value.

In Chapter 3, various novel general rank beamforming approaches are presented to overcome the performance degradation issue of the state-of-the-art designs using unique methods.

A general rank beamforming method based on STTCs is provided. Using the studied STTC, more users ( $> 8$ ) can be served optimally. The error correcting properties of the STTCs combined with the diversity and coding gain enable this approach to outperform the rank one and the Alamouti based beamforming methods. To solve the beamforming optimization problem, the SDR technique is employed to relax the MMF problem. The rank of the beamforming solutions of the relaxed problem is used to choose the appropriate STTC matrix order. The main disadvantage of the STTCs based beamforming approach is the high decoding complexity at the users' side, which has motivated the investigation of other STBCs based beamforming methods in Chapter 3 to overcome this problem.

Furthermore, in Chapter 3 the higher order ( $> 2$ ) OSTBCs based transmit beamforming approach is presented. Despite the fact that the OSTBCs based beamforming

approach increases the degrees of freedom, which in turn improves the system reliability compared with the Alamouti based beamforming approach, higher order ( $> 2$ ) OSTBCs do not enjoy full transmission rate. Thus, higher modulation schemes or channel codes with higher rates than the state-of-the-art designs are used to compensate the rate loss. The increased degrees of freedom enhances the overall system performance. For this design, the choice of the employed modulation scheme or the channel code depends on the utilized OSTBC code, which represents the main disadvantage of this approach.

In addition, the real-valued OSTBCs with higher order ( $> 2$ ) based transmit beamforming design is provided. The proposed approach offers a simple symbol-to-symbol decoding method at the receivers' side and enjoys full transmission rate. The increased degrees of freedom improve the overall system performance compared with the other state-of-the-art rank one and rank two beamforming designs. Nevertheless, the real-valued modulated symbols have less performance gains in terms of BER compared to the complex-modulated symbols.

Moreover, another approach is presented in the same chapter, where the STBC is employed and combined with the beamforming problem. Although the orthogonality of the OSTBCs is sacrificed, yet STBCs enjoy full rate. A novel design criterion is provided, where the worst user PEP is minimized under the transmit power constraint. The obtained new optimization problem is non-convex, thus a first order Taylor approximation is used to reformulate the originally non-convex problem into a linear program, which is solved in an iterative fashion to obtain the beamforming solutions. QOSTBC is employed as an example of the STBCs. Simulation results show that the QOSTBC based beamforming approach outperforms real-valued OSTBCs, OSTBCs based beamforming and the state-of-the-art designs. Moreover, for higher values of SNR ( $> 10$  dB), the real-valued OSTBC based beamforming approach outperforms the general complex-valued OSTBCs based beamforming design. This is because the error correcting properties of the convolutional code combined with the real-valued OSTBC are superior to those implemented to compensate the code rate of the complex-valued OSTBC.

In Chapter 4 the rank of the beamforming solutions is regularized using log-det function, which represents a smooth surrogate of the rank function. The non-convex surrogate function is linearized using a first order Taylor approximation. To obtain the reduced rank beamforming solutions, two different iterative algorithms are provided. In the first algorithm, two nested loops are employed. The implementation of two loops guarantees the convergence of the iterative algorithm to the desired rank using a convergence criterion in combination with decreasing a regularization variable to push the

---

rank of the beamforming solutions to a lower value. However, the proposed two scale algorithm exhibits a high computational complexity that results in a long processing time. An alternative approach is proposed to simultaneously scale the regularization variable using the eigenvalue of the beamforming solutions. Several state-of-the-art procedures were generalized to produce general rank beamforming solutions of the desired rank, namely randomization, inner approximation, MU, ADMM, SLA and MU-SLA. The simulation results demonstrate that the proposed rank regularization approach outperforms the generalized state-of-the-art procedures.

The general rank-based beamforming designs have tremendous advantages, however the decoding latency at the receiver and the assumption of perfect CSI are the main drawbacks. In FDD systems, the channel estimation is quantized and sent by the receiver to the BS using pilots signals and a dedicated feedback channel. In TDD systems, the CSI can be obtained at the BS using the channel reciprocity. General beamforming designs assume the availability of CSI and the beamforming vectors at the BS and the receivers' side, which increase the signaling overhead over the rank one beamforming design. Quantization errors and the limited capacity of feedback channels lead to CSI estimation errors, which make the assumption of perfect CSI impractical in real communication systems. The covariance based CSI methods can be used to overcome the problem of imperfect CSI, see [WPEC13]. Furthermore, to reduce the computational complexity of the iterative algorithms proposed in this thesis, see, e.g., Algorithm 4 in Section 4.2, deep unfolding can be used by mapping the iterative algorithm into the architecture of a deep network as in [NML<sup>+</sup>23], such that each layer corresponds to one iteration of the algorithm. These observations provide insights into future research follow-up work.





---

## List of Acronyms

<b>1G</b>	First generation mobile networks
<b>2G</b>	Second generation mobile networks
<b>3G</b>	Third generation mobile networks
<b>3GPP</b>	Third generation partnership project
<b>4G</b>	Fourth generation mobile networks
<b>5G</b>	Fifth generation mobile networks
<b>6G</b>	Sixth generation mobile networks
<b>ADMM</b>	Alternating direction method of multipliers
<b>BER</b>	Bit-error rate
<b>BS</b>	Base station
<b>CCK</b>	Complementary code key
<b>CDMA</b>	Code division multiple access
<b>CSI</b>	Channel state information
<b>DC</b>	Difference of convex
<b>EDGE</b>	Enhanced data rate for GSM evolution
<b>FER</b>	Frame-error rate
<b>FDD</b>	Frequency division duplex
<b>GSM</b>	Global systems for mobile communications
<b>GPS</b>	Global positioning system
<b>GPSR</b>	General packet radio service
<b>HD</b>	High definition
<b>IEEE</b>	Electrical and electronic engineers
<b>IoT</b>	Internet of things
<b>LTE</b>	Long-term evolution

<b>M2M</b>	Machine-to-machine
<b>MAC</b>	Media access control
<b>MFG</b>	Moment generating function
<b>MIMO</b>	Multiple-input multiple-output
<b>MISO</b>	Multiple-input single-output
<b>ML</b>	Maximum likelihood
<b>MMF</b>	Max-min fair
<b>MMMF</b>	Modified max-min fair
<b>mmWave</b>	Millimeter wave
<b>MU</b>	Multiplicative update
<b>MU-MIMO</b>	Multi-user MIMO
<b>OFDM</b>	Orthogonal frequency-division multiplexing
<b>OSTBC</b>	Orthogonal space-time block codes
<b>PEP</b>	Pairwise error probability
<b>PSK</b>	Phase-shift keying
<b>QAM</b>	Quadrature amplitude modulation
<b>QoS</b>	Quality-of-service
<b>QOSTBC</b>	Quasi-orthogonal STBC
<b>QPSK</b>	Quadrature phase-shift keying
<b>SDR</b>	Semi-definite relaxation
<b>SDM</b>	Spatial-division multiplexing
<b>SER</b>	Symbol-error rate
<b>SINR</b>	Signal-to-interference-plus-noise ratio
<b>SLA</b>	Successive linear approximation
<b>SNR</b>	Signal-to-noise ratio

<b>STBC</b>	Space-time block codes
<b>STC</b>	Space-time codes
<b>STTC</b>	Space-time trellis codes
<b>TDD</b>	Time division duplex
<b>TDMA</b>	Time division multiple access
<b>V2X</b>	Vehicle to everything
<b>WCDMA</b>	Wide code division multiple access
<b>WiMax</b>	Worldwide interoperability for microwave access
<b>WLAN</b>	Wireless local area networks



## List of Symbols

$N$	Number of transmit antennas at BS
$M$	Number of users
$s$	Information symbol
$\mathbf{w}$	$N_t \times 1$ beamforming vector
$y_j$	Received signal at the $j$ th user
$\mathbf{h}_j$	Channel of the $j$ th user
$\mathbf{n}_j$	Noise of the $j$ th user
$\sigma_j^2$	Noise variance at the $j$ th user
$P$	Total transmitted power
$\gamma_j$	SNR threshold at the $j$ th user
$P_{\max}$	Maximum transmitted power
$\mathbf{s}$	Information vector
$\mathcal{S}$	Transmission matrix
$\mathbf{W}$	Transmit beamforming matrix
$\mathbf{y}_j$	Received signal vector at the $j$ th user
$\mathbf{n}_j$	Noise vector of the $j$ th user
$\tilde{\mathbf{h}}_j$	Virtual channel of the $j$ th user
$R$	Rank of $\mathbf{W}$
$T$	Number of time slots
$\mathbf{I}_T$	$T \times T$ identity matrix
$\mathbf{c}$	Binary input stream
$m$	Number of information bits at each time slot
$\mathbf{g}^{(k)}$	Generator matrix of $k$ th branch
$L$	Bit rate
$P_t$	Transmitted power per time slot
$K$	Number of iteration of Randomization procedure
$\mathbf{D}_{mn}$	Code difference matrix
$\tilde{\mathbf{D}}_{mn}$	Code distance matrix



# List of Notations

$(\cdot)^H$	Hermitian transpose
$\triangleq$	Defined as
$\text{tr}(\cdot)$	Trace of a matrix
$\cdot \succeq \mathbf{0}$	A matrix is positive semidefinite
$\text{rank}(\cdot)$	Rank of a matrix
$(\cdot)^T$	Transpose of a matrix
$(\cdot)^*$	Complex conjugate
$ \cdot $	Absolute value
$\ \cdot\ _F$	Frobenius norm
$\mathcal{CN}(\cdot, \cdot)$	Gaussian noise variable
$E\{\cdot\}$	Statistical expectation
$\text{Pr}(\cdot \rightarrow \cdot   \cdot)$	Conditional probability
$Q(\cdot)$	Gaussian Q-function
$\exp$	Exponential function
$M(\cdot)$	Moment generating function
$\det(\cdot)$	Determinant of a matrix
$\text{Re}(\cdot)$	Real value of a matrix
$\text{Im}(\cdot)$	Imaginary value of a matrix
$\text{vec}(\cdot)$	Vectorization of a matrix
$\cdot \otimes \cdot$	Kronecker product of two matrices
$\langle \cdot, \cdot \rangle$	Inner product of two matrices
$\overline{\text{diag}}(\cdot)$	Anti-diagonal matrix





# List of Figures

1.1	Illustration of the transmit diversity technique using multiple antennas at the transmitter. . . . .	4
1.2	Illustration of transmit beamforming networks. . . . .	7
2.1	STTC encoder with $m$ binary input bits and $N$ transmit antennas. . .	18
2.2	Example of a STTC encoder with 3 transmit antennas. . . . .	18
2.3	Trellis diagram for the encoder example. . . . .	20
2.4	System model for rank one transmit beamforming. . . . .	21
2.5	System model. . . . .	26
2.6	System illustration using the virtual channels. . . . .	27
3.1	System performance of FER with varying number of users for $N = 3$ transmit antennas and SNR= 20 dB . . . . .	35
3.2	System performance of capacity plotted against SNR in dB for $N = 4$ transmit antennas and $M = 32$ users . . . . .	36
3.3	Rank percentage of the matrix $\mathbf{X}$ with varying number of users . . . .	37
3.4	System performance of BER plotted against SNR in dB for bit rate of $L = 3$ bpcu, $N = 6$ transmit antennas and $M = 64$ users . . . . .	43
3.5	System performance of BER with varying number of Users for $N = 6$ transmit antennas and SNR = 13 dB . . . . .	44
3.6	Rank percentage of $\mathbf{X}$ vs. number of users . . . . .	45
3.7	System performance of BER plotted against SNR in dB for $N = 6$ transmit antennas and $M = 64$ users . . . . .	49

3.8	System performance of BER with varying number of users for $N = 6$ transmit antennas and SNR= 12 dB . . . . .	51
3.9	Lower and upper bounds on $\gamma_{\text{BF-STBC}}$ at the worst user plotted against SNR in dB for $N = 4$ transmit antenna . . . . .	62
3.10	A histogram of the number of iterations for a system of 64 users and $N = 4$ transmit antennas . . . . .	62
3.11	System performance of the worst user FER plotted against SNR in dB for a system of 64 users and $N = 4$ transmit antennas . . . . .	63
3.12	System performance of the worst user FER with varying number of users for SNR= 10 dB and $N = 4$ transmit antennas . . . . .	64
3.13	System performance of BER plotted against SNR in dB for transmission rate $L = 1$ bpcu and $M = 64$ users . . . . .	66
4.1	The rank percentage for a system with $M = 400$ users . . . . .	80
4.2	The transmit power in dB with varying number of users for $\alpha^{(0)} = 2$ and $\beta = 1$ . . . . .	81
4.3	System performance of average minimum SNR with varying number of users for SNR threshold $\gamma_j = 10$ dB, $\alpha^{(0)} = 2$ and $\beta = 1$ . . . . .	82
4.4	Execution time in sec with varying number of users for $\sigma_j^2 = 0.1$ , $\alpha^{(0)} = 2$ and $\beta = 1$ . . . . .	83
4.5	The transmit power in dB with varying number of users for $\alpha^{(0)} = 1$ and $\beta = 1$ . . . . .	83
4.6	System performance of average minimum SNR with varying number of users for SNR threshold $\gamma_j = 10$ dB, $\alpha^{(0)} = 1$ and $\beta = 1$ . . . . .	84
4.7	Execution time in sec with varying number of users for $\sigma_j^2 = 0.1$ , $\alpha^{(0)} = 1$ and $\beta = 1$ . . . . .	85
4.8	The transmit power in dB with varying number of users for $\alpha^{(0)} = 0.4$ and $\beta = 1$ . . . . .	85

4.9	System performance of average minimum SNR with varying number of users for SNR threshold $\gamma_j = 10$ dB, $\alpha^{(0)} = 0.4$ and $\beta = 1$ . . . . .	86
4.10	Computational time in sec with varying number of users for $\sigma_j^2 = 0.1$ , $\alpha^{(0)} = 0.4$ and $\beta = 1$ . . . . .	86
4.11	The transmit power in dB with varying number of users for $\alpha^{(0)} = 1/R^{(0)}$ and $\beta = 0.1$ . . . . .	87
4.12	System performance of average minimum SNR with varying number of users for SNR threshold $\gamma_j = 10$ dB, $\alpha^{(0)} = 1/R^{(0)}$ and $\beta = 0.1$ . . . . .	88
4.13	Computational time in sec with varying number of users for $\sigma_j^2 = 0.1$ , $\alpha^{(0)} = 1/R^{(0)}$ and $\beta = 0.1$ . . . . .	88
4.14	System performance of SER plotted against SNR in dB for $M = 300$ users, $\alpha^{(0)} = 0.4$ and $\beta = 1$ . . . . .	89
4.15	The transmit power in dB with varying number of users for $R = 3$ , $\alpha^{(0)} = 1/R^{(0)}$ and $\beta = 0.1$ . . . . .	90
4.16	System performance of average minimum SNR with varying number of users for SNR threshold $\gamma_j = 10$ dB, $R = 3$ , $\alpha^{(0)} = 1/R^{(0)}$ and $\beta = 0.1$ . . . . .	90
4.17	The transmit power in dB with varying number of users for $R = 2$ , $\alpha^{(0)} = 1/R^{(0)}$ and $\beta = 0.1$ . . . . .	91
4.18	System performance of average minimum SNR in dB with varying number of users for SNR threshold $\gamma_j = 10$ dB, $R = 2$ , $\alpha^{(0)} = 1/R^{(0)}$ and $\beta = 0.1$ . . . . .	91

## List of Tables

3.1	The rank percentage obtained from QoS problem for $N = 6$ transmit antennas and $M = 64$ users . . . . .	50
3.2	The rank percentage obtained from QoS problem for $N = 6$ transmit antennas and SNR= 12 dB . . . . .	52
4.1	Rank upper bound comparison between theoretical values and QoS problem . . . . .	71

---

## Bibliography

- [AGS10] A. Abdelkader, A. Gershman, and N. D. Sidiropoulos, “Multiple-antenna multicasting using channel orthogonalization and local refinement,” *IEEE Transactions on Signal Processing*, vol. 58, no. 7, pp. 3922–3927, Jul. 2010.
- [Ala98] S. M. Alamouti, “A simple transmit diversity technique for wireless communications,” *IEEE Journal on Selected Areas in Communications*, vol. 16, no. 8, pp. 1451–1458, Oct. 1998.
- [AMH22] M. Z. Asghar, S. A. Memon, and J. Hámáláinen, “Evolution of wireless communication to 6G: Potential applications and research directions,” *Sustainability 2022*, vol. 14, pp. 1–26, 23 May 2022.
- [ASK<sup>+</sup>17] M. Alodeh, D. Spano, A. Kalantari, C. T. G., D. Christopoulos, S. Chatzinotas, and B. Ottersten, “Symbol-level and multicast precoding for multiuser multiantenna downlink: A state-of-the-art, classification, and challenges,” *IEEE Communications Surveys & Tutorials*, vol. abs/1703.03617, pp. 1–21, Mar. 2017.
- [AT05] L. T. H. An and P. D. Tao, “The DC difference of convex functions programming and DCA revisited with DC models of real world non-convex optimization problems,” *133. Annals of Operations Research*, vol. 133, pp. 23–46, Jan. 2005.
- [ATP98] S. Alamouti, V. Tarokh, and P. Poon, “Trellis-coded modulation and transmit diversity: design criteria and performance evaluation,” *IEEE International Conference on Universal Personal Communications (ICUPC '98)*, vol. 1, pp. 703–707, 5-9 Oct. 1998.
- [AZ11] D. P. Agrawal and Q.-A. Zeng, *Introduction to Wireless and Mobile Systems*. CENGAGE Learning, 2011.
- [BC17] C. O. B. Clerckx, *MIMO Wireless Networks: Channels, Techniques and Standards for Multi-Antenna, multi-User and multi-cell systems, 2nd Ed.* Elsevier Science, 2017.
- [BDFS22] R. Behrends, L. K. Dillon, S. D. Fleming, and R. E. K. Stirewalt, “Whitepaper: Green G: The path towards sustainable 6G,” *Alliance for Telecommunications Industry Solutions*, pp. 1–38, 1 Jun. 2022.

- [BO99] M. Bengtsson and B. Ottersten, “Optimal downlink beamforming using semidefinite optimization,” *Annual Allerton Conference on Communication, Control and Computing*, vol. 37, pp. 987–996, 1999.
- [BO01] —, “Optimal and suboptimal transmit beamforming,” *Handbook of Antennas in Wireless Communications*, 2001.
- [BV98] S. Boyd and L. Vandenberghe, *Convex Analysis and Global Optimization*. Boston: Kluwer Academic Publishers, 1998.
- [BV04] —, *Convex Optimization*. Cambridge, 2004.
- [CIS20] CISCO, “Cisco annual internet report, 2018-2023,” CISCO public, Tech. Rep., 9 Mar. 2020.
- [CP12] Y. Cheng and M. Pesavento, “Joint optimization of source power allocation and distributed relay beamforming in multiuser peer-to-peer relay networks,” *IEEE Transactions on Signal Processing*, vol. 60, no. 6, pp. 2395–2404, Jun. 2012.
- [CR08] E. J. Candès and B. Recht, “Exact matrix completion via convex optimization,” *IEEE Communications Surveys & Tutorials*, vol. abs/0805.4471, pp. 1–49, May 2008.
- [CY05] L. Chu and J. Yuan, “A trellis coded beamforming scheme over mimo fading channels,” *IEEE International Conference on Communications (ICC)*, vol. 3, pp. 2031–2035, 16–20 May 2005.
- [Dik22] B. C. Dike, “5G Emancipation: A review of the panacea for an efficient communication growth in the evolution of cellular networks,” *Proceedings of the 2022 ASEE Gulf-Southwest Annual Conference*, pp. 1–8, Mar. 2022.
- [DPS01] E. Dahlman, S. Parkvall, and J. Skold, *4G: LTE/LTE-Advanced for Mobile Broadband: LTE/LTE-Advanced for Mobile Broadband*. Elsevier Science, 2001.
- [Faz02] M. Fazel, *Matrix rank minimization with applications*. PhD thesis, Stanford University, 2002.
- [FHB04] M. Fazel, H. Hindi, and S. Boyd, “Rank minimization and applications in system theory,” *Proceeding of the 2004 American Control Conference Boston*, vol. 4, pp. 3273–3278, 30 June-02 July 2004.

- [GBY08] M. Grant, S. Boyd, and Y. Ye, *CVX: Matlab Software for Disciplined Convex Programming*, 2008. [Online]. Available: <http://www.stanford.edu/boyd/cvx/>
- [GS05] A. Gershman and N. D. Sidiropoulos, *Space-Time Processing for MIMO Communications*. John Wiley and Sons, Ltd, 2005.
- [GS15] B. Gopalakrishnan and N. D. Sidiropoulos, “High performance adaptive Algorithm for single-group multicast beamforming,” *IEEE Transactions on Signal Processing*, vol. 63, no. 16, pp. 5297–5310, Aug. 2015.
- [GSS<sup>+</sup>10] A. Gershman, N. D. Sidiropoulos, S. Shahbazpanahi, M. Bengtsson, and B. Ottersten, “Convex optimization-based beamforming: From receive to transmit and network design,” *IEEE Transactions on Signal Processing Magazine*, vol. 27, no. 3, pp. 62–75, May 2010.
- [GZCVCV10] A. G.-Zambrana, C.C.-Vázquez, and B. C.-Vázquez, “Space-time trellis coding with transmit laser selection for FSO links over strong atmospheric turbulence channels,” *Opt. Express*, vol. 18, no. 6, pp. 5356–5366, Mar 2010.
- [HP10a] Y. Huang and D. Palomar, “A dual perspective on separable semidefinite programming with applications to optimal beamforming,” *IEEE Transactions on Signal Processing*, vol. 58, no. 8, pp. 4254–4271, Aug. 2010.
- [HP10b] —, “Rank-constrained separable semidefinite programming with applications to optimal beamformings,” *IEEE Transactions on Signal Processing*, vol. 58, no. 2, pp. 664–678, Feb. 2010.
- [HRVW96] C. Helmberg, F. Rendl, R. J. Vanderbei, and H. Wolkowicz, “An interior-point method for semidefinite programming,” *Society for Industrial and Applied Mathematics*, vol. 6, no. 2, pp. 342–361, May 1996.
- [HS16] K. H. Huang and N. D. Sidiropoulos, “Consensus-ADMM for general quadratically constrained quadratic programming,” *IEEE Transactions on Signal Processing*, vol. 64, no. 20, pp. 5297–5310, Oct. 2016.
- [HT99] R. Horst and N. V. Thoai, “DC programming: Overview,” *Optim. Theory Appl.*, vol. 103, no. 1, pp. 1–43, Oct. 1999.

- [HT04] H. Holma and A. Toskala, *WCDMA for UMTS: Radio Access for Third Generation Mobile Communication, 3rd ed.* John Wiley and Sons, Ltd, 2004.
- [Jaf01] H. Jafarkhani, “A quasi-orthogonal space-time block code,” *IEEE Transactions on Communications*, vol. 49, no. 1, pp. 1–4, Jan. 2001.
- [Jaf05] ———, *Space-Time Coding: Theory and Practice.* U.K. Cambridge Univ. Press, 2005.
- [Jan04] M. Jankiraman, *Space-time codes and MIMO systems.* Artech House, 2004.
- [JSB02] G. Jongern, M. Skoglund, and B. Ottersten, “combining beamforming and orthogonal space-time block coding,” *IEEE Transactions on Information Theory*, vol. 48, no. 3, pp. 611–627, Mar. 2002.
- [KC08] D. Kim and H.-W. Choi, “Advanced constant multiplier for multipath pipelined FFT processor,” *IET Electronics Letters*, vol. 44, no. 8, pp. 518–519, 10 Apr. 2008.
- [KG10] F. Kienle and C. Gimpler, “Space-time bit trellis codes,” *International Conference on Source and Channel Coding (SCC)*, pp. 1–6, 18-21 Jan. 2010.
- [KL15] J. Kim and I. Lee, “802.11 WLAN: history and new enabling mimo techniques for next generation standards,” *IEEE Communications Magazine*, vol. 53, no. 3, pp. 134–140, March 2015.
- [Kor03] J. Korhonen, *Introduction to 3G Mobile Communications, 2nd Ed.* Artech House, 2003.
- [KSL08a] E. Karipidis, N. D. Sidiropoulos, and Z. Q. Luo, “Quality of service and max-min fair transmit beamforming to multiple cochannel multicast groups,” *IEEE Transactions on Signal Processing*, vol. 56, no. 3, pp. 1268–1279, Mar. 2008.
- [KSL08b] E. Karipidis, N. D. Sidiropoulos, and Z.-Q. Luo, “Quality of service and max-min fair transmit beamforming to multiple cochannel multicast groups,” *IEEE Transactions on Signal Processing*, vol. 56, no. 3, pp. 1268–1279, Mar. 2008.
- [LJ05] L. Liu and H. Jafarkhani, “Application of quasi-orthogonal space-time block codes in beamforming,” *IEEE Transactions on Information Theory*, vol. 53, no. 1, pp. 54–63, Jan. 2005.



- [LLLS21] R. Liu, M. Li, Q. Liu, and A. L. Swindlehurst, “Joint symbol-level precoding and reflecting designs for IRS-enhanced MU-MISO systems,” *IEEE Transactions on Wireless Communications*, vol. 23, no. 2, pp. 798–811, Feb. 2021.
- [LMS<sup>+</sup>10] Z.-Q. Luo, W.-K. Ma, A.-C. So, Y. Ye, and S. Zhang, “Semidefinite relaxation of quadratic optimization problems: From its practical deployments and scope of applicability to key theoretical results,” *IEEE Transaction on Signal Processing Magazine (Special Issue on Convex Optimization Signal Processing)*, vol. 27, no. 3, pp. 20–34, May 2010.
- [Loz07] A. Lozano, “Long-term transmit beamforming for wireless multicasting,” *IEEE International Conference on Acoustics, Speech, and Signal Processing (ICASSP 2007)*, vol. 3, no. 6, pp. 417–420, 15–20 Apr. 2007.
- [LSTZ07] Z.-Q. Luo, N. D. Sidiropoulos, P. Tseng, and S. Zhang, “Approximation bounds for quadratic optimization with homogeneous quadratic constraints,” *SIAM Journal on Optimization*, vol. 18, pp. 1–28, Feb. 2007.
- [LTPD03] H. A. L-Thi and T. P-Dinh, “Large-scale molecular optimization from distance matrix by a D.C. optimization approach,” *SIAM Journal on Optimization*, vol. 14, pp. 77–117, Jan. 2003.
- [LV06] Y. Li and B. Vucetic, “Code design for combined space time trellis codes and beamforming on slow fading channels,” *Processing of IEEE Information Theory Workshop (ITW 2006)*, pp. 473–477, 13–17 Mar. 2006.
- [LWTP15] K. L. Law, X. Wen, M. Thanh, and M. Pesavento, “General rank multiuser downlink beamforming with shaping constraints using real-valued OSTBC,” *IEEE Transactions on Signal Processing*, vol. 63, no. 21, pp. 5758–5771, Nov. 2015.
- [Mol11] A. F. Molisch, *Wireless communications, 2nd Ed.* John Wiley and Sons, Ltd, 2011.
- [MP92] M. Mouly and M.-B. Pautet, *The GSM System for Mobile Communications.* Telecom, 1992.
- [MSG13] O. Mehanna, N. D. Sidiropoulos, and G. B. Giannakis, “Joint multicast beamforming and antenna selection,” *IEEE Transactions on Signal Processing*, vol. 61, no. 10, pp. 2660–2674, 2013.

- [NC00] H. T. Nguyen and A. Chattejee, “Number-splitting with shift-and-add decomposition for power and hardware optimization in linear dsp synthesis,” *IEEE Transactions on Very Large Scale Integration (VLSI) Systems*, vol. 8, pp. 419–424, Aug. 2000.
- [NML<sup>+</sup>23] N. T. Nguyen, M. Ma, O. Lavi, N. Shlezinger, Y. C. Eldar, A. L. Swindlehurst, and M. Juntti, “Deep unfolding hybrid beamforming designs for THz massive MIMO systems,” *IEEE Transactions on Vehicular Technology*, pp. 1–15, Feb 2023.
- [Ode79] J. P. Odenwalder, *Optimal Decoding of Convolutional Codes*. University Microfilms International, 1979.
- [OP05] B. O’Hara and A. Petrick, *IEEE 802.11 Handbook: A Designer’s Companion, 2nd Ed.* Standard Information Network IEEE Press, 2005.
- [Pat98] G. Pataki, “On the rank of extreme matrices in semidefinite programs and the multiplicity of optimal eigenvalues,” *Mathematics of Operations Research*, vol. 23, no. 2, pp. 339–358, May 1998.
- [PP12] K. B. Petersen and M. S. Pedersen, *The Matrix Cookbook*. Technical University of Denmark, 2012. [Online]. Available: <http://www.math.uwaterloo.ca/~hwolkowi/matrixcookbook.pdf>
- [Rod15] J. Rodriguez, *Fundamentals of 5G mobile networks*. Wiley, 2015.
- [SBP17] Y. Sun, P. Babu, and D. Palomar, “Majorization-Minimization Algorithms in signal processing, communications, and machine learning,” *IEEE Transactions on Signal Processing*, vol. 65, no. 3, pp. 794–816, Feb. 2017.
- [SCH10] K.-T. Shr, H.-D. Chen, and Y.-H. Huang, “A low-complexity viterbi decoder for space-time trellis codes,” *IEEE Transactions on Circuits and Systems*, vol. 57, no. 4, pp. 873–885, Apr. 2010.
- [SDL06] N. D. Sidiropoulos, T. Davidson, and Z.-Q. Luo, “Transmit beamforming for physical-layer multicasting,” *IEEE Transactions on Signal Processing*, vol. 54, no. 6, pp. 2239–2251, Jun. 2006.
- [SL01] Z. Safar and K. R. Liu, “Systematic space-time trellis code design for an arbitrary number of transmit antennas,” *IEEE 54th Vehicular Technology Conference. VTC Fall 2001. Proceedings (Cat. No.01CH37211)*, vol. 1, pp. 8–12 vol.1, 2001.

- [SL09] B. K. Sriperumbudur and G. R. G. Lanckriet, “On the convergence of concave-convex procedure,” in *In NIPS Workshop on Optimization for Machine Learning*, 2009.
- [SLP15] A. Schad, K. L. Law, and M. Pesavento, “Rank-two beamforming and power allocation in multicasting relay networks,” *IEEE Transactions on Signal Processing*, vol. 63, no. 13, pp. 3435–3447, Jul. 2015.
- [SP03] N. Sharma and C. Papadias, “Improved quasi-orthogonal codes through constellation rotation,” *IEEE Transactions on Communications*, vol. 51, no. 3, p. 332–335, Mar. 2003.
- [SS10] A. Sharma and P. Sinha, “Performance analysis of space time trellis codes over Nakagami fading and Rayleigh fading channels: With comparative analysis,” *International Journal of Computer Applications*, vol. 7, no. 7, pp. 19–26, October 2010.
- [STC98] N. Seshadri, V. Tarokh, and A. Calderbank, “Space-time codes for high data rate wireless communication: performance criterion and code construction,” *IEEE Transactions on Information Theory*, vol. 44, no. 2, pp. 744–765, Mar. 1998.
- [STC99a] —, “Space-time block codes from orthogonal designs,” *IEEE Transactions on Information Theory*, vol. 45, no. 5, pp. 1456–1467, Jul. 1999.
- [STC99b] —, “Space-time block coding for wireless communications: Performance results,” *IEEE Journal on Selected Areas in Communications*, vol. 17, no. 2, pp. 451–460, Mar. 1999.
- [STPS17] D. Schenck, D. Taleb, M. Pesavento, and A. Sezgin, “General rank beamforming using high order OSTBC for multicasting networks,” *21th International ITG Workshop on Smart Antennas. (WSA 2017)*, pp. 175–181, 15-17 Mar. 2017.
- [SX04] W. Su and X. Xia, “Signal constellations for quasi-orthogonal space-time block codes with full diversity,” *IEEE Transactions on Information Theory*, vol. 50, no. 10, p. 2331–2347, Oct. 2004.
- [TAP15] D. Taleb, S. Alabed, and M. Pesavento, “Optimal general-rank transmit beamforming technique for single-group multicasting service in modern wireless networks using STTC,” *9th International ITG Workshop on Smart Antennas. (WSA 2015)*, pp. 1–7, 3-5 Mar. 2015.

- [THJ14] L. N. Tran, M. Hanif, and M. Juntti, "A conic quadratic programming approach to physical layer multicasting for large-scale antenna arrays," *IEEE Signal Processing Letters*, vol. 21, no. 1, pp. 114–117, Jan. 2014.
- [TLP16] D. Taleb, Y. Liu, and M. Pesavento, "Full-rate general rank beamforming in single-group multicasting networks using non-orthogonal STBC," *Signal Processing Conference (EUSIPCO 2016)*, pp. 2365–2369, 29 Aug.–2 Sep. 2016.
- [TSS05] A. Tarighat, M. Sadek, and A. Sayed, "A multi user beamforming scheme for downlink MIMO channels based on maximizing signal-to-leakage ratios," *IEEE International Conference on Acoustics, Speech, and Signal Processing (ICASSP 2005)*, vol. 3, pp. 1129–1132, 18–23 Mar. 2005.
- [TU07] P. Tejera and W. Utschick, "Feedback of channel state information in wireless systems," *IEEE International Conference on Communications*, pp. 908–913, Aug. 2007.
- [Vit71] A. J. Viterbi, "Convolutional codes and their performance in communication systems," *IEEE Transactions on Circuits and Systems*, vol. 19, no. 5, pp. 751 – 772, oct. 1971.
- [VT17] R. Vannithamby and S. Talwar, *Towards 5G: Applications, Requirements and Candidate Technologies*. John Wiley and Sons, Ltd, 2017.
- [VY03] B. Vucetic and J. Yuan, *Space-Time Coding*. Wiley, 2003.
- [WLAP12] X. Wen, K. Law, S. Alabed, and M. Pesavento, "Rank-two beamforming for single-group multicasting networks using OSTBC," *7th IEEE Sensor Array and Multichannel Signal Processing Workshop (SAM 2012)*, pp. 65–68, 17–20 Jun. 2012.
- [WM11] S. X. Wu and W.-K. Ma, "Multicast transmit beamforming using a randomize-in-time strategy," *IEEE International Conference on Acoustics, Speech, and Signal Processing (ICASSP 2011)*, pp. 3376–3379, 22–27 May 2011.
- [WMB06] B. H. Walke, S. Mangold, and L. Berlemann, *IEEE 802 Wireless Systems: Protocols, Multi-Hop Mesh/Relaying, Performance and Spectrum Coexistence*. John Wiley and sons, Ltd, 2006.
- [WMS13] S. X. Wu, W.-K. Ma, and A. M.-C. So, "Physical-layer multicasting by stochastic transmit beamforming and Alamouti space-time coding,"

- IEEE Transactions on Signal Processing*, vol. 61, no. 17, pp. 4230–4245, Sep. 2013.
- [WPEC13] I. Wajid, M. Pesavento, Y. C. Eldar, and D. Ciochina, “Robust downlink beamforming with partial channel state information for conventional and cognitive radio networks,” *IEEE Transactions on Signal Processing*, vol. 61, no. 14, pp. 3656–3670, July 2013.
- [WSC<sup>+</sup>14] K.-Y. Wang, A. M.-C. So, T.-H. Chang, W.-K. Ma, and C.-Y. Chi, “Outage constrained robust transmit optimization for multiuser MISO downlink: Tractable approximations by conic optimization,” *IEEE Transactions on Signal Processing*, vol. 62, no. 21, pp. 5690–5705, Nov. 2014.
- [WSM12] S. X. Wu, A. M.-C. So, and W.-K. Ma, “Rank-two transmit beamformed Alamouti space-time coding for physical-layer multicasting,” *IEEE International Conference on Acoustics, Speech, and Signal Processing (ICASSP 2012)*, pp. 2793–2796, 25–30 Mar. 2012.
- [WXH<sup>+</sup>17] F. Weng, C. Xu, Y. Huang, X. Wang, and X. Gao, “REEL-BF design: Achieving the SDP bound for downlink beamforming with arbitrary shaping constraints,” *IEEE Transactions on Signal Processing*, vol. 65, no. 10, pp. 2672–2685, May 2017.
- [YLV05] Y. T. Y. Li and B. Vucetic, “Space-time trellis codes with linear precoding for transmit beamforming,” *16th International Symposium on Personal Indoor and Mobile Radio Communications (PIMRC)*, vol. 4, pp. 2461–2465, 11–14 Sep. 2005.
- [ZBRCVCV15] A. Zambrana, R. B.-Ruiz, C. C.-Vázquez, and B. C.-Vázquez, “Novel space-time trellis codes for free-space optical communications using transmit laser selection,” *Opt. Express*, vol. 23, no. 19, pp. 24 195–24 211, Sep 2015.
- [ZG02] S. Zhou and G. Giannakis, “Optimal transmitter eigen-beamforming and space-time block coding based on channel mean feedback,” *IEEE Transactions on Signal Processing*, vol. 50, no. 10, pp. 2599–2613, Oct. 2002.
- [ZG03] —, “Optimal transmitter eigen-beamforming and space-time block coding based on channel correlations,” *IEEE Transactions on Information Theory*, vol. 49, no. 7, pp. 1673–1690, Jul. 2003.



---

# Lebenslauf

Name: Dima Taleb

## Schulausbildung

1988-1994 Grundschule in Damaskus

1994-2000 Gymnasium in Damaskus

## Studium

2000-2005 Studium der Elektrotechnik an der  
HIAST ,  
Studienabschluß: Diplom of Engineering

2010-2012 Studium der Elektrotechnik an der  
TU Darmstadt ,  
Studienabschluß: Master of Science

## Berufstätigkeit

2005-2010 Research Assintance an der  
HIAST, Damaskus

November 2013 bis April 2018 Wissenschaftlicher Mitarbeiter am  
Fachgebiet Kommunikationstechnik,  
Institut für Nachrichtentechnik,  
Technische Universität Darmstadt

Januar 2019 bis April 2022 Radar und Software Inginuerin an der  
Mobis Hyundai, Frankfurt

Seit Mai 2022 ADAS Expertin an der  
TÜV Rheinland , Wiesbaden





## Erklärung laut §9 der Promotionsordnung

Ich versichere hiermit, dass ich die vorliegende Dissertation allein und nur unter Verwendung der angegebenen Literatur verfasst habe. Die Arbeit hat bisher noch nicht zu Prüfungszwecken gedient.

Darmstadt, 19. 03. 2023,

